Role of Undecaprenyl Phosphokinase in mycobacteria: impact on biofilm formation, growth properties, persistence, and virulence

DISSERTATION

zur Erlangung des akademischen Grades doctor rerum naturalium (Dr. rer. nat.) im Fach Biologie

eingereicht an der Mathematisch-Naturwissenschaftlichen Fakultät I der Humboldt-Universität zu Berlin

von Dipl.-Biol. Lars Röse (geb. 27.08.1974, Geesthacht)

Dekan der Mathematisch-Naturwissenschaftlichen Fakultät I Prof. Dr. Michael Linscheid

Gutachter:

1. Prof. Dr. Erwin Schneider

2. Prof. Dr. Stefan Kaufmann

3. PD Dr. Ulrich Schaible

Tag der Einreichung: 03.03.04

Tag der mündlichen Prüfung: 09.06.04

Zusammenfassung

Die Familie der Mykobakterien setzt sich aus pathogenen und apathogenen Vertretern zusammen. In dieser Arbeit wurden 3 Mitglieder dieser Familie für Untersuchungen herangezogen: ihr prominentester pathogener Vertreter *Mycobacterium tuberculosis*, der Erreger der Tuberkulose, das als Impfstoff eingesetzte *Mycobacterium bovis* BCG, das durch Attenuierung aus dem Rindertuberkulose-Erreger *Mycobacterium bovis* hervorging und das apathogene Bodenbakterium *Mycobacterium smegmatis*.

Ein Schlüssel zum Verständnis der Mykobakterien und speziell ihrer Widerstandsfähigkeit ist die Kenntnis ihrer komplexen Zellwand. Peptidoglycan als deren Bestandteil und insbesondere der mittels Undecaprenyl-Monophosphat bewerkstelligte Transport von Peptidoglycan-Vorläufern aus dem Cytoplasma an die Zelloberfläche steht dabei im Zentrum der Zellwandbildung. In *M. tuberculosis, M. bovis* BCG und *M. smegmatis* wurden Deletionsmutanten für die Undecaprenyl-Phosphokinase (Upk) hergestellt.

Für *M. smegmatis* wurde gezeigt, daß die Δ*upk* Deletionsmutante, in Übereinstimmung mit Deletionsmutanten homologer Gene in anderen Bakterien, eine erhöhte Sensitivität gegenüber dem die Zellwandsynthese hemmenden Antibiotikum Bacitracin aufwies. Überraschenderweise zeigte *M. tuberculosis* Δ*upk* diesen Phänotyp nicht. Weiterhin ließ sich für *M. smegmatis* Δ*upk* im Vergleich zum *M. smegmatis* Wildtyp Peptidoglycan an der Zelloberfläche in geringerem Maße nachweisen. Eindrucksvoll zeigte sich die Bedeutung der Undecaprenyl Phosphokinase in der gestörten Entwicklung von Biofilmen im Falle der *M. smegmatis* Δ*upk* Mutante. Dies galt sowohl für *in vitro* Bedingungen als auch für ein, im Rahmen dieser Arbeit, neu entwickeltes *in vivo* Modell.

Vergleiche von *M. tuberculosis* Wildtyp und *M. tuberculosis* Mutante auf der Ebene von Proteom- und Transkriptom-Analysen führten zur Identifikation eines zum mykobakteriellen Fettsäure-Synthese II (FASII) System gehörenden Operons, das im Falle der *upk*-Deletion verstärkt exprimiert wurde und damit möglicherweise einen Kompensationsmechanismus für die fehlende Phosphokinase darstellt.

Eine reduzierte Persistenz von *M. smegmatis* Δ*upk* in infizierten Makrophagen legte nahe, daß Upk bei mykobakteriellen Infektionen eine entscheidende Rolle für das Überleben der Bakterien und ihre Virulenz spielt. Dies konnte erstmals für *M. tuberculosis* im Rahmen von Maus-Infektionsversuchen gezeigt werden. *M. tuberculosis* Δ*upk* ließ sich als neues Mitglied in eine Reihe von als *growth in vivo (giv)* klassifizierten Mutanten einreihen.

Die Herstellung von Deletionsmutanten wird als Möglichkeit betrachtet, verbesserte Impfstoffe herzustellen. Die physiologische Konsequenz der Deletion sollte bestenfalls neben einer Attenuierung des Ausgangsbakteriums (gilt besonders für *M. tuberculosis*) eine Überexpression protektionsrelevanter Antigene zur Folge haben. Im Vergleich zum bestehenden Impfstoff *M. bovis* BCG führte die Impfung von Mäusen mit *M. bovis* BCG Δ*upk* sowohl zu geringerer bakterieller im Anschluß an die Vakzinierung als auch zu einer verbesserten Langzeit-Protektion gegen Tuberkulose.

Schlagworte:

    Biofilm
    Persistenz
    Virulenz
    Mycobacterium tuberculosis
    Mycobacterium smegmatis
    Mycobacterium bovis BCG
    Undecaprenyl-Phosphokinase

Summary

The family of mycobacteria is composed of pathogenic and apathogenic bacteria. This study was performed with 3 members of this family, the most prominent pathogenic member, *Mycobacterium tuberculosis,* the causative agent of tuberculosis, the vaccine strain *Mycobacterium bovis* BCG which was developed by attenuation of the bovine tuberculosis agent *Mycobacterium bovis*, and *Mycobacterium smegmatis* which is apathogenic and widely distributed in soil.

A key to understanding mycobacteria and, especially, their resistance is to understand the complexity of their cell wall. Peptidoglycan is a major component of the cell wall and the transport of peptidoglycan precursors out of the cytoplasm to the bacterial surface by undecaprenyl monophosphate is central to cell wall synthesis. Therefore, deletion mutants of the undecaprenyl phosphokinase gene (*upk*) were generated in *M. tuberculosis*, *M. bovis* BCG, and *M. smegmatis*.

In the case of *M. smegmatis* it was shown that a Δ*upk* deletion mutant, as with deletion mutants of homologous genes in other bacteria, exhibited an increased sensitivity to the antibiotic bacitracin, indicating that cell wall synthesis was hampered. Surprisingly, *M. tuberculosis* Δ*upk* did not exhibit this phenotype. Furthermore, a lower level of peptidoglycan was detected on the cell surface of an *M. smegmatis* Δ*upk* mutant compared to *M. smegmatis* wildtype. Relevance of the undecaprenyl phosphokinase was demonstrated by impaired biofilm development in the case of the *M. smegmatis* Δ*upk* mutant. This was observed *in vitro* as well as *in vivo* using an animal model which was newly developed in this thesis.

A fatty acid synthase II (FASII) system related operon revealed by comparative proteome- and transcriptome-analyses comparing *M. tuberculosis* wildtype and *M. tuberculosis* Δ*upk* mutant, and may reflect a compensatory mechanism for the loss of *upk*.

Reduced persistence of *M. smegmatis* in infected macrophages suggested a decisive role of Upk in mycobacterial infection concerning survival and virulence of bacteria. This was later demonstrated to be true for *M. tuberculosis* in a mouse model. *M. tuberculosis* Δ*upk* was, therefore, classified as a new member of the group of *growth in vivo (giv)* mutants.

Construction of deletion mutants is a strategy to identify improved vaccines. Ideally, the physiologic consequences of a gene deletion would result in attenuation of the modified bacterium (especially in the case of *M. tuberculosis*) and overexpression of antigens relevant for protection. Compared to the existing vaccine *M. bovis* BCG, vaccination of mice with *M. bovis* BCG Δ*upk* exhibited a lower bacterial load upon vaccination as well as an improved long-lasting protection against *M. tuberculosis* infection.

Keywords:

    biofilm
    persistence
    virulence
    Mycobacterium tuberculosis
    Mycobacterium smegmatis
    Mycobacterium bovis BCG
    undecaprenyl phosphokinase

Table of contents

Table of abbreviations

Ab	antibody
ADS	albumin-dextrose-saline
AG	arabinogalactan
amp	ampicillin
BCG	Bacille Calmette et Guérin
bp	base pair
BSA	bovine serum albumin
BSL3	biosafety level 3
C57BL/6	C57BL/6 is one of the most widely used inbred mouse strains
cfu	colony forming unit
Ct	threshold cycle
2-DE	2 dimensional electrophoresis
DIG	digoxigenin
DNA	deoxyribonucleic acid
DMSO	dimethyl sulfoxid
DTT	dithiothreitol
EDTA	ethylenediaminetetraacetic acid
ELISA	enzyme-linked immunosorbent assay
FAS	fatty acid synthase
FCS	fetal calf serum
Fig.	Figure
GTE	glucose-Tris-EDTA
H&E	Hematoxalin and Eosin
HIV	human immunodeficiency virus
hyg	hygromycin
IFNγ	interferon γ
IPTG	isopropyl beta-D-thiogalactopyranoside
i.v.	intravenous
kan	kanamycin
LB	Luria Bertani medium
MHC	major histocompatibility complex

MAPc	mycolyl-AG-peptidoglycan complex
MDR	multiple drug resistance
MOI	multiplicity of infection
MP-buffer	mycobacteriophage buffer
mRNA	messenger RNA
OADC	oleic acid-dextrose-catalase
OD	optical density
ori	origin of replication
PBS	phosphate buffered saline
PCR	polymerase chain reaction
PFA	paraformaldehyde
pfu	plaque forming unit
p.i.	post infection
PVA	polyvinyl alcohol
rag	recombination activation gene
RNA	ribonucleic acid
rpm	rotations per minute
RPMI	Roswell Park Memorial Institute (culture medium)
RLT-Buffer	RNeasy lysis buffer
RT	room temperature
SDS	sodium dodecyl sulfate
SSC	saline sodium citrate
TAE	Tris-acetate-EDTA buffer
TE	Tris EDTA
Tris	hydroxymethyl aminomethan
TNFα	tumor necrosis factor α
Upk	undecaprenyl phosphokinase
uv	ultra violet
WHO	world health organization

1. Introduction

The family of mycobacteria comprises pathogens and apathogenic environmental bacteria [1,2]. Mycobacteria are unusual among bacteria since they have an enormously thick, hydrophobic cell wall which e.g. prevents desiccation. Numerous mycobacteria are harmless and useful because they degrade organic matter in soil. Better known are, however, the few human pathogenic mycobacteria which cause tuberculosis (*Mycobacterium tuberculosis, Mycobacterium africanum, Mycobacterium bovis*) and leprosy (*Mycobacterium leprae*). Discovery of *M. tuberculosis* as an etiologic agent was reported to the "Physiologische Gesellschaft" in Berlin on March 24th, 1882 by Robert Koch. During his lecture on the "Ätiologie der Tuberkulose" Koch pointed out that it was a specific staining procedure that visualized characteristic, so far unknown bacteria in tuberculous affected organs [3]. The staining was performed with alkaline methylene blue and bismarck brown. Hence, *M. tuberculosis* as causal agent of tuberculosis was identified. At about the same time of Robert Koch's discovery, Paul Clemens von Baumgarten brightened bacilli with caustic soda in caesous tissue and saw the bacteria under the microscope. Baumgarten's publication came out a few weeks after Robert Koch's lecture in the Charité in Berlin [4]. The staining procedures were modified first, by Paul Ehrlich, and subsequently by Franz Ziehl and Adolf Neelsen, to the use of a mixture of acids and aniline dye, today known as "Ziehl-Neelsen-staining" [5,6,7]. Therefore, the mycobacterial cell wall and its staining attributes were of notable importance right from the beginning.

From a public health standpoint, *M. tuberculosis* is of utmost importance because it kills more human beings than any other bacterial species

(www.who.int/mediacentre/factsheets/who104/en/print.html). The World Health Organization (WHO) declares that approximately 2 million people die of tuberculosis each year. It is estimated that between 2002 and 2020, approximately 1000 million people will be newly infected, over 150 million people will develop disease, and 36 million will die of tuberculosis, if control is not improved. HIV and tuberculosis form a lethal combination, each speeding up the other's progression. Because HIV weakens the immune system, an HIV-positive individual who is infected with *M. tuberculosis* is many times more likely to develop disease than someone infected with *M. tuberculosis* who is HIV-negative. Tuberculosis is the leading cause of death among people who are HIV-positive with about 11% of AIDS deaths worldwide. In Africa, HIV is the single most important factor determining the increased incidence of tuberculosis in the past 10 years. By inconsistent or partial treatment, drug resistant bacilli have emerged. A particularly dangerous form of drug-resistant tuberculosis are the multidrug-resistant (MDR) strains causing MDR-tuberculosis, which is defined as the disease caused by bacilli resistant to at least Isoniazid and rifampicin, the two most powerful anti-tuberculosis drugs.

1.1.   Koch's postulate and Koch's molecular postulate

Robert Koch's lecture on the " Ätiologie der Tuberkulose " provided an experimental methodology and an intellectual basis for acquiring knowledge about the cause of tuberculosis. Koch's postulate was of great importance:

To prove that tuberculosis was caused by the invasion, growth and multiplication of the bacilli, it was necessary to:

1. solate the bacilli from the body,

2. grow them in pure culture, and

3. by administering the isolated bacilli to animals, reproduce similar moribund
    conditions.

Similarly, the knowledge of the molecular bases (the genotypes) for the phenotypes which allow *M. tuberculosis* to cause disease and escape therapies is essential in developing new effective treatment strategies. The conceptual methodology by which we acquire knowledge about what genotype is responsible for a particular phenotype is called Koch's molecular postulate [8]:

To prove that a phenotype in a mutant bacterium, such as drug resistance or virulence, is caused by a specific genotype, it is necessary to:

1. Isolate a mutant with a defined altered phenotype,

2. clone the genotype from the mutant, and

3. by introducing the cloned genotype into a wildtype bacterium, reproduce the
    same phenotype of the mutant bacterium.

Based on this principle, a large number of genetic functional analyses regarding a variety of virulence and other factors in different bacteria have been achieved. Technological progress paved the way for the generation of mutant libraries and targeted gene deletions, as well as overproduction of selected genes. *M. tuberculosis* has been one of the most challenging and refractory organisms in this process. Nevertheless, there exists a set of tools to manipulate these bacilli [9], e.g. the

sophisticated TM4-phage based knockout technology [9].

1.2 *Mycobacterium bovis* BCG

Soon after Robert Koch's discovery of *M. tuberculosis*, innumerable attempts toward vaccine development began. On December 28th, 1908, the French bacteriologists Albert C. Calmette and Guérin notified a loss of virulence of *M. bovis* when cultured in bile containing media. These scientists passaged *M. bovis* over a period of 13 years in a bile-glycerin-medium thereby developing an attenuated strain that, when used as a vaccine, provided protection to high risk groups, especially newborns of tuberculous mothers. This vaccine strain was called *Mycobacterium bovis* BCG. It was introduced into the clinic in 1921 and is one of the oldest applications of vaccination. Nevertheless, there were severe complications [10] and later it was proven that *M. bovis* BCG fails to provide satisfying protection in adults against reactivated pulmonary tuberculosis [11,12]. In the Federal Republic of Germany the routine vaccination was discontinued in 1985 and has been offered since 1987 only upon request. Since there is no better anti-tuberculous vaccine than *M. bovis* BCG available so far, it still is the golden standard to which new candidates have to be compared in animal models.

1.3 Immune response to *M. tuberculosis*

The immune system is divided into two categories: innate and adaptive. Innate immunity refers to nonspecific defense mechanisms that come into play immediately or within hours of an antigen's appearance in the body. These mechanisms include physical barriers such as skin, effector molecules in body fluids such as mucosal

secretions and blood, and immune cells of the myeloid lineage. The innate immune response is activated by chemical properties of the antigen. Adaptive immunity, on the other hand, refers to antigen-specific immune responses. The adaptive immune response is more complex than the innate. The antigen first must be processed and presented. Once an antigen has been recognized, the adaptive immune system creates a set of immune cells specifically designed to attack that antigen or the antigen bearing pathogen within days or weeks. The adaptive immunity includes a "memory" that renders future responses against a specific antigen more efficient. Innate and adaptive immunity are closely inter-connected. Macrophages and dendritic cells, the primary cell types involved in the innate immune response to mycobacteria, play a crucial role in the initiation of adaptive immunity. For example, infected macrophages are recognized by T lymphocytes through their major histocompatibility complex (MHC) presentation of mycobacterial antigens. Tuberculosis is caused by airborne infection. Inhaled droplets containing low numbers of bacteria are taken up by alveolar macrophages. Spontaneous healing cannot be measured nor excluded but is unlikely to occur to a significant degree. The vast majority, about 90 % of infected individuals, does not develop acute disease and stays latently infected. Patients with a compromised immune system, for example in the case of HIV infection, develop acute disease directly after primary infection [13]. Within 1 year more than 10 % of infected individuals develop disease. M. tuberculosis resides in early phagosomes and blocks phagosome maturation including phagolysosome formation [14,15,16,17]. However, the maturation arrest is incomplete and some bacteria are killed or at least impaired in replication through antibacterial effectors including reactive oxygen and nitrogen intermediates [18]. In addition, iron restriction is an important mechanism of innate immunity to control the infection [19].

Bacterial containment is focused on the granulomatous lesion, where different T cell populations participate in the protective immune response. These include i) CD4+ T cells recognizing antigenic peptides in the context of gene products encoded by MHC class II, ii) CD8 T cells recognizing antigenic peptides in the context of MHC class I, iii) $\gamma\delta$ T cells recognizing unusual antigenic ligands independent of specialized presentation molecules – notably phospholigands, and iv) CD1 restricted T cells recognizing glycolipids abundant in the mycobacterial cell walls presented by the CD1 molecules [20,21]. Upon infection/reactivation antigen specific T cells produce interferon γ (IFNγ) which synergizes with tumor necrosis factor α (TNFα) in activating macrophages. At least some of the CD8 T cells, $\gamma\delta$ T cells, and CD1 restricted T cells secrete perforin and granulysin, thereby directly killing mycobacteria within macrophages (Fig. 1) [22]. Most of this knowledge was obtained from experiments with mice. The immune response of the mouse is well understood, and a large variety of mouse mutants with defined immunodeficiencies are available. Furthermore, the function of IFNγ, IL12, TNFα, or CD4 T cells is similar in mouse and human [23]. Although, there are significant differences between the human and murine immune system, experimental animals are critical to gain insight into general mechanisms underlying natural resistance, and acquisition of a protective immune response.
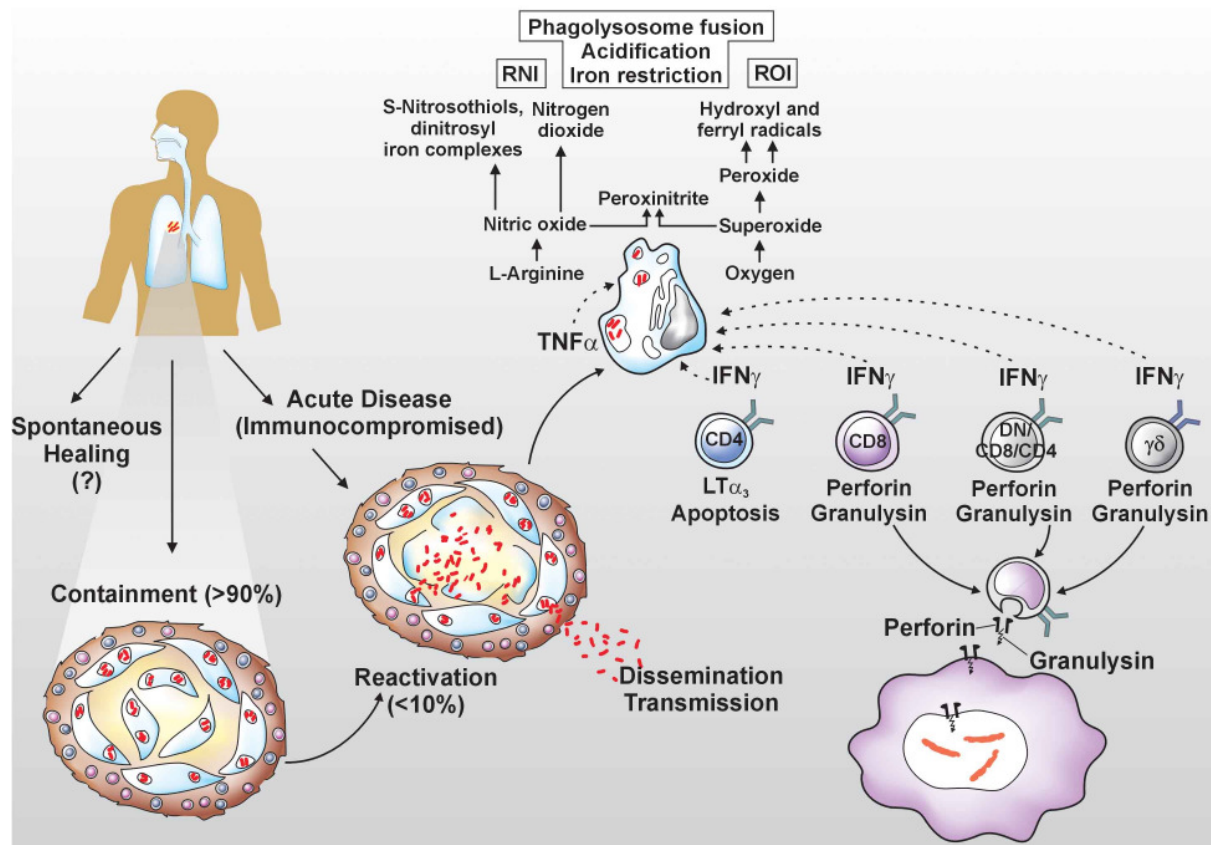
Fig. 1 Scheme of the course of events following contagion with *M. tuberculosis*. Acute disease does only develop for a relatively small subset of immunocompromised individuals. Depicted are the major effector mechanisms of macrophages and the most important T cell populations. (Reprinted from Nature Reviews Immunology [20]).

1.4 The mycobacterial cell wall

The mycobacterial cell wall is impressively thick and unique in its complex composition [24]. Among the strategies by which *M. tuberculosis* has adapted to the environmental conditions in macrophages, the resistance imparted by its cell wall is one of the most striking. The cell envelope is extremely hydrophobic and forms an exceptionally strong permeability barrier, rendering mycobacteria naturally resistant to a wide variety of antimicrobial agents. This is due to the unique structure of the mycobacterial cell wall and the presence of long fatty acids, the mycolic acids [24]. Channel forming proteins which are functionally similar to the well known porins of gram negative bacteria have been demonstrated in *Mycobacterium chelonae* [25]

and *M. smegmatis* [26,27,28], revealing how hydrophilic molecules can pass through the hydrophobic cell wall. The core unit of the envelope consists of peptidoglycan connected to arabinogalactan (AG) which is covalently linked to mycolic acids, thus forming the mycolyl-AG-peptidoglycan complex (MAPc) (Fig. 2). Cell wall synthesis can be divided into 3 separate stages which occur in distinct subcellular compartments:
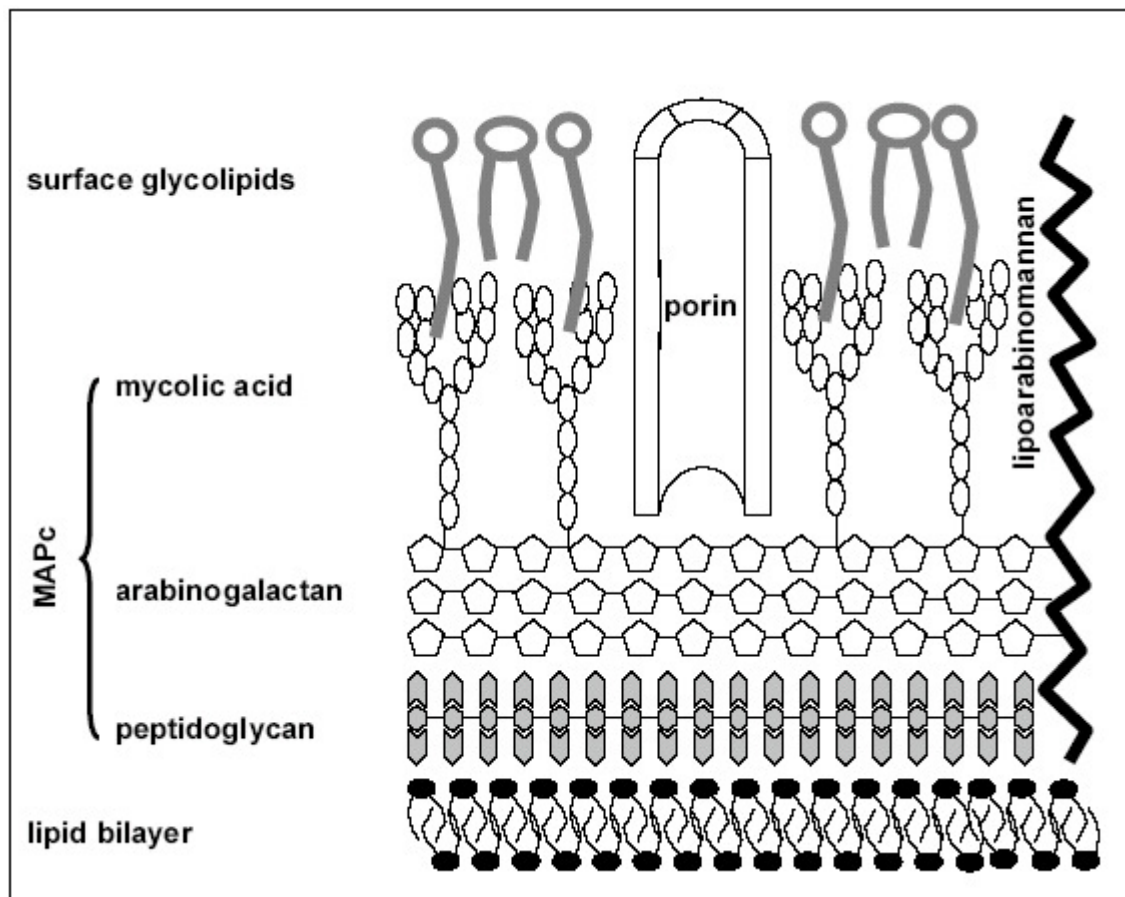
Fig. 2 Scheme of the mycobacterial cell wall structure. The mycolyl-arabinogalactan-peptidoglycan complex forms the core of the robust bacterial envelope.

cytoplasm, membrane, and the cell wall itself (Fig. 3). Peptidoglycan synthesis is initiated with Uridine 5'-Diphospho-*N*-Acetylmuramic Acid (UDP-MurNAc) derived from Uridine 5'-Diphospho-DN-AcetylGlucosamine (UDP-GlcNAc) and phosphoenylpyruvate. Five amino acids are linked to UDP-MurNAc resulting in synthesis of UDP-MurNAc-pentapeptide, also known as Park's nucleotide [29]. UDP-

MurNAc-pentapeptide is linked via a phosphodiester to an undecaprenyl pyrophosphate carrier molecule (C_{55}-PP) constituting C_{55}-PP-MurNAc-pentapeptide, or lipid I. A GlcNAc residue is subsequently added to form lipid II, which is thought to be translocated across the cytoplasmic membrane and serves as substrate for the assembly of peptidoglycan [29]. Generation of undecaprenyl monophosphate (C_{55}-P) from undecaprenyl (C_{55}) by an
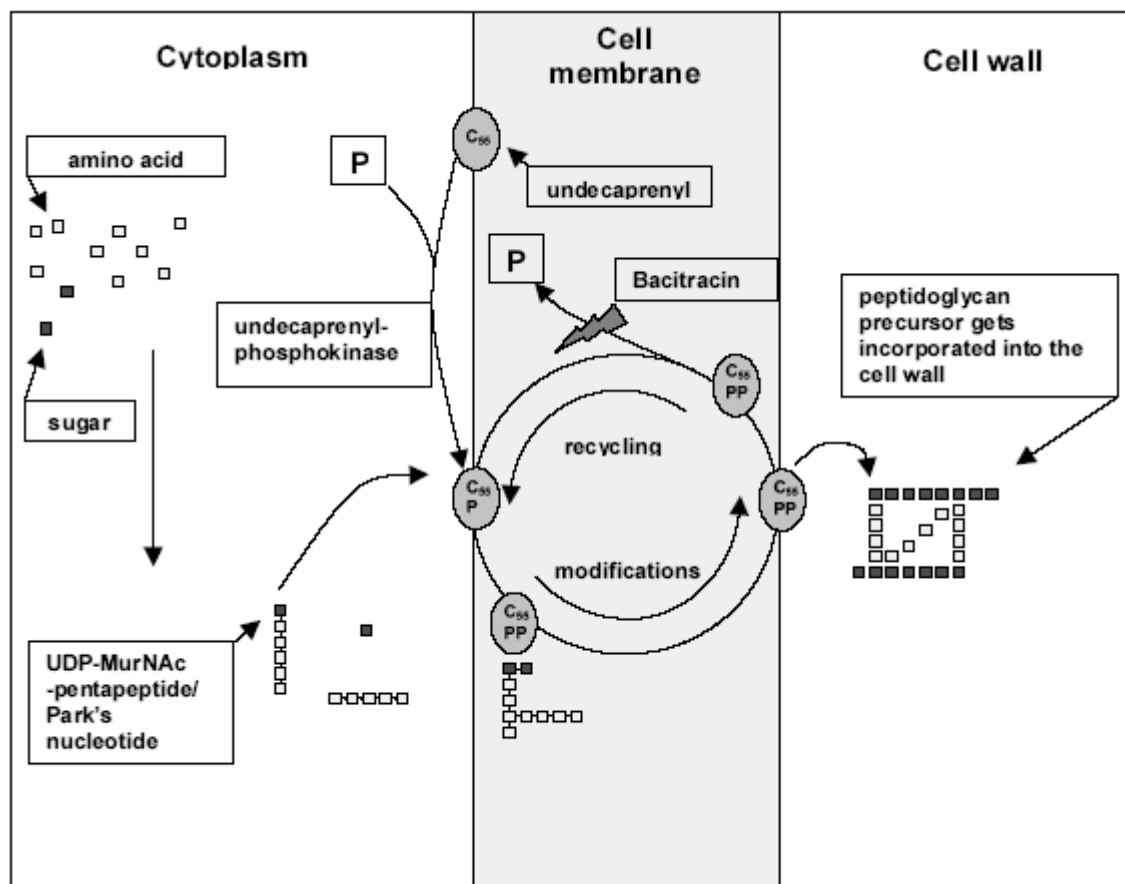
Fig. 3 Model of peptidoglycan synthesis. Precursors are produced in the cytoplasm subsequently coupled to a undecaprenyl monophosphate, the carrier lipid, and modified. After translocation to the outer face, peptidoglycan is assembled and incorporated into the cell wall.

undecaprenyl-phosphokinase (Upk) probably represents a critical step in providing mycobacteria with a sufficient amount of peptidoglycan-precursor carrier molecules. Bacitracin is an antibiotic which binds tightly to C_{55}-PP and blocks C_{55}-P-recycling, in this way also reducing the amount of carrier molecules.

1.5 Mycobacterium smegmatis

To study mycobacterial genetics of tuberculosis, the fast growing, environmental *Mycobacterium smegmatis* is widely used as a model organism. E.g., it was used to understand the effect of single *M. tuberculosis* genes on survival inside human macrophages [30]. Another potential use is to serve as surrogate for *M. tuberculosis* in disinfectant tests. Discovery of *M. smegmatis* was made 2 years after Robert Koch's lecture on the "aetiology of tuberculosis". In November 1884, Lustgarten was first to describe a bacillus with staining appearance of tubercle bacilli in syphilitic chancres and gummae [31]. Soon thereafter Alvarez and Tavel identified microorganisms similar to those in normal genital secretions (smegma) [32]. This kind of growth, as bacterial communities on a surface, is defined as a biofilm. Various gram-negative and gram-positive bacteria as well as fungi show two forms of growth: planktonic and, as a step of microbial development, in biofilms [33]. *M. smegmatis* and other non-tuberculous mycobacteria such as *Mycobacterium fortuitum* and *Mycobacterium marinum* live and grow planktonic or as biofilms [34]. Biofilms support resistance to antimicrobial chemotherapy [35] and play a role in contamination of clinical and industrial settings [36]. *M. smegmatis* has also been described in wound infections, endocarditis, and osteomyelitis [37]. Nevertheless, it is considered as an apathogenic fast growing mycobacterium. Therefore, *M. smegmatis* remains an attractive model organism to study mycobacterial metabolism or, specifically, cell wall synthesis as investigated in this study.

1.6 Aim of the study

As mentioned, the cell envelope is a key to understanding mycobacteria and especially their resistance. Understanding initial processing, transport and assembly

of peptidoglycan precursors, therefore is key to understanding the mycobacterial cell wall. In a first approach, the hypothesis, that gene products which are relevant in this context in other bacterial species, have homologues in mycobacteria with comparable function, was followed. Koch's molecular postulates were used to test this hypothesis as follows:

1.) Isolate a mutant with a defined altered phenotype.

Attention was drawn to undecaprenyl phosphokinase, which is involved in peptidoglycan synthesis, and mediates resistance to the antibiotic bacitracin in the case of *Escherichia coli, Staphylococcus aureus*, and *Streptococcus pneumoniae*. Furthermore, the altered phenotype is characterized by decreased virulence for *Staphylococcus aureus* and *Streptococcus pneumoniae* [38,39].

2.) Clone the genotype from the mutant

The sequences of *E. coli, S. aureus*, and *S. pneumoniae* undecaprenyl phosphokinases are known. The homologous genes of *M. tuberculosis, M. bovis* BCG and *M. smegmatis* had to be identified, and appropriate knockout constructs had to be cloned.

3.) Introduce the cloned genotype into a wildtype bacterium, and reproduce the same phenotype of the mutant bacterium.

Subsequently, the knockout constructs had to be used to introduce the deletions into the selected wildtype mycobacteria, followed by verification that a phenotype

comparable to that of mutants in other species can be reproduced.

An additional aim was the more detailed characterization of Δ*upk* mutants in different mycobacteria. This included determination of influence on peptidoglycan synthesis, bacitracin resistance, biofilm formation in the case of *M. smegmatis*, and virulence and persistence in the case of *M. tuberculosis* and *M. bovis* BCG. This was done in order to:

determine steps in cell wall synthesis which represent potential targets for drug development, and

generate an attenuated new vaccine candidate.

2 Materials and Methods

2.1 Bacterial strains and culture methods

E. coli was transformed by conventional heat shock transformation or electroporation and plated on LB-agar (Invitrogen, Paisley, UK) containing appropriate antibiotics (hygromycin B [Roche, Mannheim, Germany] at 150 µg/ml, kanamycin [Sigma Aldrich, St. Louis, MO, USA] at 35 µg / ml or ampicillin [ICN, Aurora, OH, USA] at 100 µg / ml). For blue-white selection, 1 mM IPTG (Gerbu, Gaiberg, Germany) and 75 µg / ml X-Gal (Roth, Karlsruhe, Germany) were added. All cloning procedures were done in *E. coli* DH5α (Invitrogen) unless stated differently. Liquid *E. coli* cultures were grown in LB-medium (Invitrogen) containing appropriate antibiotics (hygromycin B at 150 µg/ml, kanamycin at 50 µg/ml or ampicillin at 100 µg/ml). *M. smegmatis* mc^{2}155 was electroporated as described [40] and plated on Middlebrook 7H10 agar (BD, Franklin Lakes, NJ, USA) supplemented with 10 % albumin-dextrose saline (ADS: 0.81 % NaCl, 5 % BSA Fraction V [Serva, Heidelberg, Germany], 2 % glucose), 0.5 % glycerol, 0.05 % Tween-80 (Sigma) and either hygromycin B (50 µg/ml) or kanamycin (25 µg/ml). Liquid *M. smegmatis* cultures were grown in Middlebrook 7H9 medium (BD) supplemented with 10 % ADS, 0.05 % Tween-80 (Sigma) and 0.2 % glycerol (further referred to as 7H9 complete medium), containing either hygromycin B (50 µg/ml) or kanamycin (25 µg/ml). If required, sucrose was used at a concentration of 2 % and added after the medium had been autoclaved and cooled to 55 °C. Biofilms were generated in M63 salts minimal medium. One liter M63 medium consisted of 13.6 g KH_2PO_4, 3.8 g $(NH_4)_2SO_4$, 0.5 mg $FeSO_4 \cdot 7\ H_2O$, 0.2 % carbohydrate, 1 mM $MgSO_4$, 0.7 mM $CaCl_2$, 0.5 % casamino acids (BD) adjusted to pH 7.0 (further referred to as biofilm medium).

2.2 Construction of the *M. smegmatis* knockout template

The plasmids used in this study are listed in Table 5. Plasmids were amplified in *E. coli* HB101 or *E. coli* DH5α and purified with Qiagen columns as recommended by the manufacturer (Qiagen, Inc., Chatsworth, CA, USA). DNA fragments used for plasmid construction were purified by agarose gel electrophoresis and recovered by QIAEXII gel extraction kit (Qiagen).

Mycobacterial genomic DNA was prepared from 10 ml cultures. Bacteria were lysed with 1.3 ml of a 3:1 mixture of chloroform-methanol. The lysate was mixed with 1.3 ml of Tris-equilibrated phenol and 2 ml of RLT buffer (Qiagen) supplemented with 0.5% N-lauroylsarcosine (Sigma) and 1% β-mercaptoethanol. The upper phase was collected after centrifugation, and the genomic DNA was precipitated with isopropanol. This DNA preparation method was also scaled down to the use of 1 / 10 of all ingredients and thus was called microprep. For southern blotting, genomic DNA was digested with *BamHI* and transferred to a positively charged nylon membrane (Roche) using a pressure blotter. The probe was labeled and fragments were visualized with DIG DNA Labeling and Detection Kit (Roche) as recommended by the manufacturer.

The in-frame, unmarked deletion template Δupk contains the 2 flanking regions next to upk. Flanking regions (879 bp and 945 bp) and the *M. tuberculosis upk* homologue *rv2136c* were amplified by PCR. Specific primer pairs and chromosomal DNA are listed in Table 5. PCR was carried out for 1 initial cycle of 5 min at 95°C, followed by 25-30 cycles (95 °C for 1 min, 60°C for 1 min, 72 °C for 3 min), and 1 final cycle at 72 °C for 10 min. All PCR products were blunt end cloned into the SrfI site of pPCR-Script SK+ Amp. The respective cloning kit was used (Stratagene, La Jolla, CA, USA). Sequence identity was verified by sequencing. The flanking regions were

cleaved from cloning vectors using *Hind*III and *EcoR*V. In a 2 step ligation, flanking regions 1 and 2 were first dimerized and then inserted into the *EcoR*V predigested and dephosphorylated vector pYUB657.

2.3 Electron microscopy (performed in collaboration by Dr. Volker Brinkmann)

For fine structural analysis, cells were fixed with 2.5 % glutaraldehyde, postfixed with 1 % osmiumtetroxid, contrasted with uranylacetate and tannic acid, dehydrated and embedded in Polybed (Polysciences, Eppelheim, Germany). After polymerization, specimens were cut at 60 nm and contrasted with lead citrate. For immunodetection, cells were fixed with 4 % PFA and embedded in a mixture of 25 % sucrose / 10 % polyvinyl alcohol (PVA). Ultrathin sections were cut at −105 °C, blocked, reacted with primary anti-peptidoglycan-antibodies (Biotrend, Köln, Germany) followed by secondary antibodies coupled to 6 nm gold particles. Specimens were analyzed in a Leo 906E transmission electron microscope.

2.4 Alamar blue assay

Antimicrobial susceptibility testing of bacitracin (Calbiochem, San Diego, CA, USA) and Isoniazid (Sigma) was performed in 96-well microplates. Outer perimeter wells were filled with sterile water to prevent dehydration in experimental wells. Antibiotic dilutions were dissolved in distilled deionized water and subsequent dilutions were performed in 7H9 complete medium. Wildtype, mutant, and the reconstituted strain of *M. smegmatis* mc^2 155 or *M. tuberculosis* H37Rv each were inoculated in 7H9 complete medium and grown at 37 °C until OD_{600} = 1.0 was reached. This culture was diluted 1 : 40 and 100 µl per well were added to a microtiter plate containing titrated

antibiotics. Plates were covered with breathable sealing membrane (Nunc, Naperville, IL, USA) and incubated at 37 °C for 16-20 h in the case of *M. smegmatis* and 4 to 5 days in the case of *M. tuberculosis*. Then 5 µl per well of Alamar Blue (Serotec, Oxford, UK) was added. After further 6-7 h (*M. smegmatis*) incubation at 37°C, extinction at 570 nm was measured in an ELISA-reader. Respectively, after over night (*M. tuberculosis*) incubation pictures were taken to document. Since there was no elisa-reader in the S3 facility, color change was examined visually to determine value of bacterial growth.

2.5 Biofilm formation

Single colonies of *M. smegmatis* mc^2 155 wildtype and *M. smegmatis* Δ*upk* mutant were inoculated in 7H9 complete medium and grown to saturation. Fifty µl from this preculture were inoculated into 1 ml of biofilm medium and cultured in 12 well plates (Nunc) at room temperature (RT) for 4 to 5 days. The medium was removed and 500 µl of 1 % crystal violet (BD) were added. Plates were incubated at RT for 30 min, rinsed with water and examined under the microscope. For microscopy, biofilms were grown on glass cover slips, which had been placed into each cavity of a 12 well plate. Auramine Rhodamine staining was performed with Fluorescent Stain Kit B according to the recommendations of the manufacturer (BD).
Male C57BL/6 mice were used for the *in vivo* biofilm assay. Ten mice per group were anesthetized with 50 µl of a 1:1:3 mixture of Ketavet (Pharmacia, Erlangen, Germany), Rompun (Bayer, Leverkusen, Germany), and PBS. Subsequently 1 x 10^7 bacteria / 5 µl were applied to a penis. Next day, overnight grown smegmata were counted. Mice wore protections manufactured from 50 ml tubes (BD), to avoid cleaning.

2.6 Infection of bone marrow derived mouse macrophages

Bone marrow cells from C57BL/6 mice were flushed out of femura and tibiae using a syringe with a 23G gauge (Braun, Melsungen, Germany). Differentiation and harvesting was performed as described before [41]. Infection was executed in 24 well plates using RPMI medium (Biochrom, Berlin, Germany) supplemented with 10 % FCS (Biochrom), 1 % Hepes (Biochrom), and 1 % L-Glutamine (Biochrom). One million bone-marrow derived macrophages were used per well. *M. smegmatis* was added at a multiplicity of infection (MOI) of 200. Infection lasted for 2 h, followed by 3 washes with RPMI supplemented with 10 % FCS, Hepes, L-Glutamine, and 250 µg Amikacin / ml (Sigma). Subsequently, cells were lysed with 1 ml 0.1 % TritonX100 at different time points and serial dilutions were plated on 7H10 agar plates.

2.7 Construction of a recombinant TM4 knockout phage

Flanking regions to the target gene *upk* were cloned into the vector pJSC284 next to a hygromycin resistance cassette. The sizes of the flanking regions were: flanking region 1 = 810 bp and flanking region 2 = 807 bp amplified by PCR (conditions: see above; Primers: Table 5) and extended with the restriction sites *BamH*I (flanking region 1) and *Age*I (flanking region 2). The PCR products were purified from an agarose gel and ligated in pPCR-Script Amp SK(+) (Stratagene), transformed, amplified, and sequences were verified. Flanking region 2 had an internal *Age*I restriction site which was overlooked in the beginning. To overcome this problem, the fragment was *Not*I-*BamH*I-cut out of pPCR-Script and blunted by Klenow reaction, performed as the manufacturer recommended (NEB). Subsequently fragments were ligated into the *BamH*I blunted *Age*I restriction site of pJSC284. The resulting vector was called pKO-*upk* (Fig. 4). For amplification it had to be transformed into *E. coli*

HB101 as the DH5α strain exhibits resolvase activity which may affect plasmid stability. The pKO-*upk* and the genome of TM4 phage phAE159 were *Pac*I digested in order to fuse the knockout construct to the phage genome. Before, genomic phage DNA had to be self-ligated via internal cos-sites. Because of a very inefficient phAE159-Δ*upk* producing ligation reaction, DNA was *in vitro* packaged into λ-phage-heads using Gigapack III (Stratagene). Transduction-competent *E. coli* HB101 were used, and phasmid containing bacteria were selected on hygromycin containing LB-agar plates. As phasmids are huge molecules, DNA was purified by classical alkaline lysis miniprep. Control for correct insertion of the knockout construct, was performed by *Pac*I digest, which revealed a 5 kb fragment by gel electrophoresis. All positive clones were pooled. One μl of recombinant phasmid DNA was used to transform *M. smegmatis* as a host for phage production. Phages had to maintain temperature sensitivity (t_s) so that they became lytic at 30 °C but not at 37 °C. This was critical because subsequently transduced *M. tuberculosis* was to be grown at 37 °C and should not have succumbed to lysis.

Electroporation conditions for transformation of mycobacteria, in this case *M. smegmatis*, were:

1000 Ω

25 μF

2.5 kV

A cuvette with a 0.2 cm gap was used. This was followed by addition of 1 ml 7H9 complete medium, 30 min incubation at 30 °C and plating in 2 alternative ways:

1. Electroporation of 900 µl *M. smegmatis* solution, mixed with 4 ml top-agar and poured on mycobacteriophage plates. This was working well in the case of inefficient transformation.

2. Electroporation of 100 µl *M. smegmatis* solution, mixed with 100 µl *M. smegmatis* wildtype solution and 4 ml top-agar poured on mycobacteriophage plates. This worked well in the case of a very efficient transformation that was in need of more bacteria for lysis.

mycobacteriophage plates:

19 g 7H10 agar (BD)

1000 ml H_2O

autoclaved, and further enriched with 10 ml 20 % dextrose and 10 ml 50 % glycerin

top agar:

0.235 g 7H9 medium powder (BD)

0.38 g noble agar (BD)

50 ml H_2O

autoclaved, liquefied in a microwave oven before use and enriched with 500 µl 20 % dextrose. Used in 4 ml aliquots that were kept liquid at 50°C in a heat block.

Plates were incubated 3 to 4 days at 30°C. During this time a lawn of *M. smegmatis* was growing in the top-agar, intermitted by plaques, produced by lytic phages. Plaques were picked and patched on 2 top-agars which were subsequently

incubated at 30 °C or 37 °C to assess whether the phages had retained their temperature-sensitivity. One t_s phage was picked and eluted over night at 4 °C in 500 µl of mycobacteriophage-buffer (MP-buffer).

MP-buffer:

25 ml 1 M Tris / HCl, pH 7.5

75 ml 1 M NaCl

5 ml 1 M $MgSO_4$

1 ml 1 M $CaCl_2$

H_2O ad 500 ml

autoclaved, or filter sterilized

This extract was called "phage-lysate". To amplify the phage, 300 µl of serial phage-lysate dilutions (undiluted to 1×10^{-4}) in MP-buffer were mixed with 300 µl of *M. smegmatis* and adsorbed at 30 °C for 30 to 120 min. Out of each dilution-mix, 3 times 200 µl were mixed with 4 ml top-agar, poured on mycobacteriophage plates, and incubated 3 to 4 days. To harvest the phages, plates were chosen in which the phage had lysed almost the entire lawn ("lacy plates"). Top agars were collected with cell scrapers (Sarstedt, Newton, USA) and incubated over night with 2 - 4 ml MP-buffer per top agar at 4 °C. This was followed by 10 min centrifugation at 4000 rpm, and 0.22 µm filter sterilization of supernatants. To determine the titer of the phage lysate, dilutions up to 10^{-9} were prepared in MP-buffer, and 5 µl per dilution were spotted on a mycobacteriophage plate with a top-agar containing 200 to 400 µl *M. smegmatis*. After 3 to 4 days, plaques per spot were counted, and the titers calculated. A last verification of proper orientation of the flanking regions and

possession of the hygromycin resistance cassette was done by PCR using flanking

region- and HygOut- primers and 1×10^{-2} dilutions of the phage lysate.
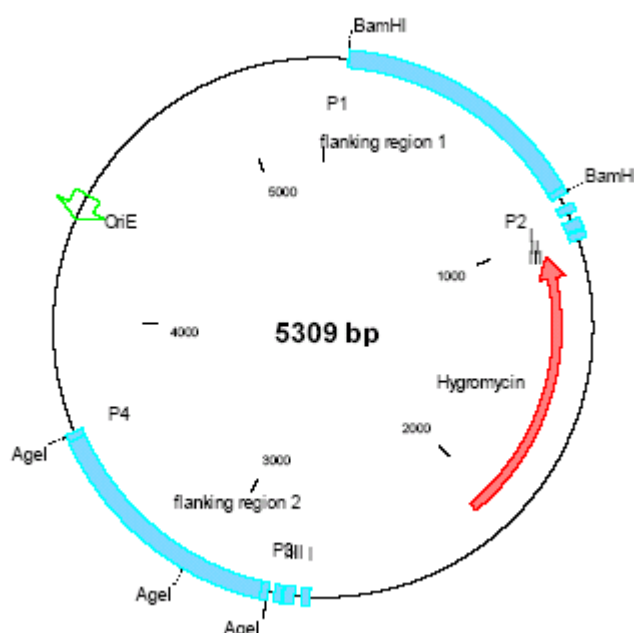
Fig. 4 pKO-*upk*, the vector to be fused to the TM4 phage genome of phAE159. Flanking regions 1 and 2 were cloned next to the hygromycin resistance cassette.

2.8 Transduction of *M. tuberculosis*

A culture of *M. tuberculosis* H37Rv was grown to $OD_{600} = 0.8 - 1.0$. Per transduction,

10 ml culture were centrifuged at 3000 rpm for 10 min and the pellet was

resuspended 1 ml MP-buffer. One ml of a high titer phage lysate (at least 10^{10} pfu/ml)

was pre-warmed at 37°C, mixed with the concentrated bacteria, and incubated for 4

h at 37°C. Subsequently, transduced cells were centrifuged for 10 min at 3000 rpm,

resuspended in 500-1000 µl 7H9 medium, and plated on 4 7H10 plates containing 75

µg hygromycin / ml. After 4 weeks of incubation at 37°C, clones were picked to

inoculate 5 ml liquid cultures in 7H9 complete medium shaking at 90 rpm for 1-2

weeks. Following, medium was added to expand the cultures. Ten ml were used to

prepare chromosomal DNA for southern blot analysis of the clones.

2.9 Reconstitution of the mutants

The *upk* gene was amplified by PCR (Primers: see Table 5), cloned into pPCRScript, sequenced, and cloned into the *E. coli* mycobacteria shuttle vector pMV262 under control of the *M. bovis groEL2* (*hsp60*) promoter as translational fusion. Competent *M. tuberculosis* H37Rv Δ*upk* were electroporated, and plated on 7H10 agar plates containing 75 µg hygromycin per ml and 25 µg kanamycin per ml. After 4 weeks, clones were picked, and 5 ml cultures were inoculated. Out of well-grown cultures, 1 ml was taken to perform DNA microprep and subsequent PCR to check for the kanamycin resistance cassette and the *upk* gene. DNA derived from a positive clone was also taken to transform *E. coli* DH5α. The amplified and purified plasmid was
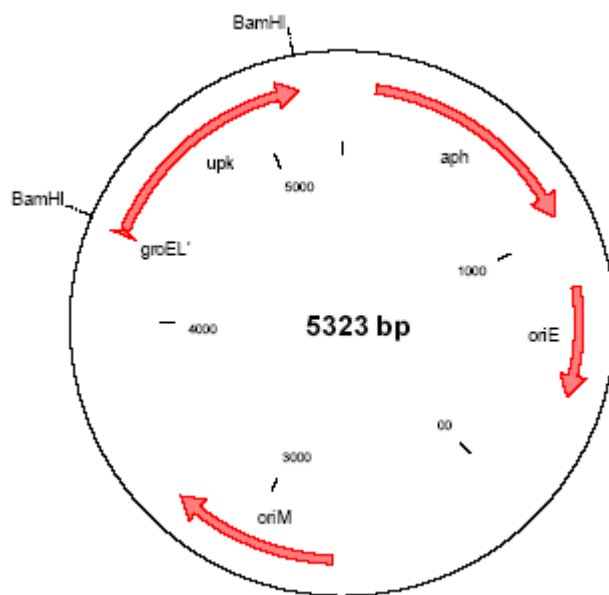
Fig. 5 Reconstitution vector pMV262-*upk*. The *upk* gene was cloned into the *BamH*I restriction site under control of the *groEL2* promoter.

*BamH*I digested and compared by agarose gel electrophoresis to the original plasmid. Transcription of the *upk* gene from the reconstitution vector pMV262-*upk* was quantified by real-time PCR which is based on the measurement of amplified

products after each cycle of the PCR using fluorescent dyes interacting only with double stranded DNA. The more template that is present at the beginning of the reaction, the lower the number of cycles it takes to reach a point in which the fluorescent signal is first recorded as statistically significant above background, which is the definition of the threshold cycle (Ct). Comparison of the threshold cycle for a specific template in each sample leads to semi-quantitative evaluation of original template concentration. For semi-quantitative real-time PCR total RNA was transcribed to cDNA using Superscript[TM] III (Invitrogen) as the manufacturer recommended. All PCRs were run for 40 cylces with 20 sec 94°C and 60 sec 60°C in the ABI Prism 7000 Sequence Detection System (Applied Biosystems, Foster City, CA, USA) using ABI PRISM optical 96-well plates (Applied Biosystems). Primers are listed in Table 5. Reaction mixtures were set up in 30 µl final volume using 15 pmol of each primer, 5 µl template cDNA and 15 µl 2x SYBR-Green PCR Master mix (Applied Biosystems). Data analysis was performed using the ABI Prism 7000 SDS Software and Microsoft Excel.

2.10 Preparation of competent *E. coli*

Five ml of Psi medium was inoculated with one colony and precultured over night at 37°C.

Psi medium:

2.5 g Bacto Yeast Extract (BD)

10 g Bacto Tryptone (BD)

2.5 g $MgSO_4$

500 ml H_2O

adjusted with KOH to pH 7.6 and filter sterilized

One hundred ml of Psi medium were inoculated with 1 ml of the preculture and grown at 37°C to OD_{550} = 0.5. Thereupon the culture was left 15 min on ice, centrifuged for 10 min at 3000 rpm and resuspended in 40 ml cold TfbI solution.

TfbI solution:

30 mM potassium acetate

100 mM rubidium chloride

10 mM calcium chloride

50 mM manganese chloride

15 % v/v glycerol

H_2O ad 200 ml

adjusted to pH 5.8 with diluted acetic acid and filter sterilized

After 15 min on ice, and centrifugation for 10 min at 3000 rpm, the pellet was resuspended in 4ml of cold TfbII solution.

TfbII solution:

10 mM MOPS

75 mM calcium chloride

10 mM rubidium chloride

15 % v/v glycerol

H_2O ad 100 ml

adjusted to pH 6.5 with diluted caustic soda and filter sterilized

After further 15 min on ice, cells were used immediately or were frozen in liquid

nitrogen and stored at −80 °C. For each transformation 40 - 50 µl of the cells were

mixed with up to 1 µg DNA, incubated for 30 min on ice, 45 s at 42 °C, and again 2

min on ice. One ml of SOC medium was added and after 1 h at 37 °C, cells were

plated.

2.11   Purification of chromosomal DNA from mycobacteriophages

Five µl of DNAse (1 mg / ml) and 10 µl RNAse (10 mg / ml) were added to 1 ml of

phage-lysate, incubated for 30 min at 37 °C, and supplemented with 50 µl of freshly

made STEP-buffer.

STEP-buffer:

400 mM EDTA pH 8.0

50 mM Tris pH 8.0

1 % SDS

H_2O

EDTA was pre-warmed to 50 °C, and complete STEP-buffer was kept at 50 °C to

avoid SDS precipitation.

After addition of 20 µl of proteinase K (10 mg / ml) (Merck, Darmstadt, Germany) and

30 min incubation at 56 °C, the sample was split. Each part was 2 times extracted

with 500 µl phenol and 2 times with 500 µl chloroform : iso-amyl-alcohol (24:1).

Supernatants were mixed with 50 µl of sodium acetate and 1 ml of 100 % ethanol. After 2 min at RT, DNA was precipitated by spinning for 20 min at 13,000 rpm. The pellet was washed with 1 ml 70% ethanol, air-dried and resuspended in 50 – 100 µl TE-buffer over night at 4 °C. A few µl on an agarose gel demonstrated a band at 50 kb.

2.12 *In vitro* packaging of phasmid DNA

Two µl of a phasmid ligation were mixed with an aliquot of Gigapack III Gold (Stratagene), briefly centrifuged and incubated at RT for 90-120 min. Afterwards 500 µl of SM-buffer were added. This solution was called packaging mix.

SM-buffer:

0.58 g NaCl

0.2 g $MgSO_4$ x 7 H_2O

5 ml Tris / HCl, pH 7.5

10 mg gelatine or 0.5 ml of a 2 % solution

H_2O ad 100 ml

autoclaved

Fifty µl of the packaging mix were incubated with 200 µl of transduction *competent E. coli* HB101 for 20 min at 37 °C without shaking. After addition of 1 ml LB-medium and 60 min expression at 37 °C, bacteria were plated on LB-plates containing 150 µg of hygromycin and grown over night at 37 °C.

2.13   Preparation of transduction competent *E. coli* HB101

Twenty ml LB-medium which had been enriched with 0.4 % maltose and 10 mM

$MgSO_4$ were inoculated with 500 µl of a well grown *E. coli* HB101 preculture, and

grown to $OD_{600} = 0.5 – 0.7$ at 37°C. Ten ml were centrifuged at 3000 rpm for 10 min,

and the pellet was resuspended in 5 ml of 10 mM $MgSO_4$.

2.14   Classical miniprep

The pellet of a 5 ml *E. coli* culture was resuspended in 100µl of LB-medium. Cells

were lysed in 300 µl TENS-solution and incubated for up to 5 min at RT.

TENS-solution

94 ml sterile TE-buffer

1 ml 10 M NaOH

5 ml 10 % SDS

TE-Buffer

5 ml 1 M Tris/HCl, pH 8.0

1 ml 0.5 M EDTA, pH 8.0

H_2O ad 500 ml

autoclaved

This was mixed with 150 µl sodium acetate (pH 5.2), incubated for 5 – 10 min on ice, and centrifuged for 10 min at 13,000 rpm. The supernatant (about 500 µl) was transferred to a new reaction tube, and mixed with 500 µl phenol : chloroform : iso-amyl-alcohol (25 : 24 : 1). After 5 min centrifugation at 13,000 rpm the supernatant was transferred to a new reaction tube, 900 µl 100 % ethanol was added, followed by 1 min incubation at RT and 15 min centrifugation at 13,000 rpm. The pellet was washed with 1 ml 70 % ethanol, dried, and resuspended in 50 µl TE-buffer enriched with 1 µl RNAse (10 mg / ml).

2.15   Preparation of electro-competent mycobacteria

Fifty ml *M. tuberculosis* respectively *M. smegmatis* was grown in 7H9 complete medium to OD_{600} = 0.6 - 1.0. *M. smegmatis* was cooled for 1-2 h on ice and subsequently washed 3 times with cold 10 % glycerol. The pellet was resuspended in 2 ml cold 10 % glycerol. In case of *M. tuberculosis*, bacteria were washed 3 times with 10 % glycerol at RT and resuspended in 5 ml 10 % glycerol.

2.16   Neutral-red staining

Five ml of a well grown bacterial culture were centrifuged at 3000 rpm for 10 min, supernatant was discarded, 5 ml 50 % aqueous methanol added, followed by incubation for 1 h at 37 °C. Again, the bacteria were washed with 50 % aqueous methanol, and the pellet was resuspended in 5 ml neutral-red (Merck).

neutral red:

1 vial barbital buffer (Sigma)

2 g neutral red

ad 1000 ml

pH 9.8

sterile-filtered

Color change was visible after 1h at RT.

2.17 Pellicle formation

Standing cultures were used to investigate pellicle formation of the *M. tuberculosis* strains. Therefore 20 ml Sauton medium was inoculated with 1 ml of a well grown pre-culture, incubated in 50 ml conical tubes at 37 °C.

Sauton medium:

20 g L-asparagine

10 g sodium-citrate

2.5 g K_2HPO_4

2.5 g $MgSO_4$ x 7 H_2O

250 mg ammonium-iron-III-citrate

300 g glycerin

ad 5 l H_2O

sterile-filtered

2.18 Cording assay

About 3 µl of a well-grown culture were transferred into subdivisions of a 8 chamber-

slide (Nunc), and air dried. Subsequently 1 ml of 7H9 complete medium without

Tween 80 was added, followed by 2 – 3 weeks incubation at 37°C. Then, medium

and chambers were removed, and the slide was soaked in formalin over night.

Staining was performed with the TB Fluorescent Stain Kit B (Auramine O-Rhodamine

B) (BD) as the manufacturer recommended.

2.19 RNA-preparation from mycobacteria and analysis of the gene expression pattern (performed in collaboration with Dr. Helmy Rachman)

RNA-preparation was performed in conformity with isolation of genomic DNA (see

above) as this procedure allows purification of all nucleic acids. Purification of RNA

from the aqueous phase was performed using RNeasy Mini Kit (Qiagen) as the

manufacturer recommended. Labeling, hybridization to a DNA-array, scanning and

evaluation of the signals were done in collaboration with Helmy Rachman and is

described in his thesis "Functional Genome Analysis of *Mycobacterium tuberculosis*",

2003.

2.20 Preparation of *M. tuberculosis* whole cell lysates for two-dimensional electrophoresis (2-DE)

A culture of 100 ml *M. tuberculosis* was grown to OD_{600} = 0.8 – 1, centrifuged at 3000

g and 4°C for 15 min, washed twice with 100 ml cold PBS 0.05 % Tween 80

resuspended in 1 ml cold PBS Tween 80, transferred to a micro-centrifuge screw cab

tube with lid gasket, and centrifuged at 4 °C and 10,000 g for 15 min. To avoid

proteolytic degradation, 1 µl of each of the protease inhibitors TLCK (100 mg / ml),

pepstatin A (50 mg / ml), leupeptin (100 mg / ml) and E64 (25 mg / ml) diluted in

DMSO was added to the cell pellet, which was sonified afterwards. Urea was gradually added to a final concentration of 9 M to the sonicate (108 mg urea / 100 µl sonicate). Furthermore, dithiothreitol (DTT) to a final concentration of 70 mM, ampholytes (Servalytes 2 – 4; 2 %) and Triton X-100 (2 %) were added. The sample was kept at RT for 30 min, stirred occasionally, centrifuged at 10,000 rpm and 16°C for 15 min. The supernatant was removed and 2-DE performed.

2.21   Protein separation by two-dimensional electrophoresis (performed in collaboration with Dr. Jens Mattow)

Protein separation by 2-DE was performed as a combination of carrier ampholyte isoelectric focusing (IEF) and SDS-PAGE using gels with a size of 23 x 30 cm [42]. IEF was performed in rod gels containing 9 M urea, 3.5% acrylamide, 0.3% piperazine diacrylamide and a total of 4% ampholytes pH 2-11 (Servalytes 2-11; Serva, Heidelberg, Germany). Protein samples were applied at the anodic side of the IEF gels and focused under non-equilibrium pH gradient electrophoresis conditions (8,870 Vh). For analytical and preparative investigations 0.75 mm or 1.5 mm thick gels were used, respectively. For analytical investigations, 60 µg of protein sample were applied. For preparative experiments, we applied up to 600 µg of protein sample. SDS-PAGE was performed in gels containing 15% acrylamide using the IEF gels as stacking gels. Following electrophoresis, proteins were visualized by either silver (analytical gels) [43] or Coomassie Brilliant Blue (CBB) G250 staining (preparative gels) [44]. The pI and Mr gradient of the 2-DE gels was determined using an iterative calibration method as described [45].

2.22   Evaluation of differential proteins by PDquest (performed in collaboration with Dr. Jens Mattow)

The 2-DE patterns were first examined visually aimed at the identification of spots of differential relative intensity between whole cell lysates of wild-type *M. tuberculosis* H37Rv on the one hand and the deletion mutant *M. tuberculosis* H37RvΔ*upk* on the other hand. For both strains, 3 different protein samples were prepared, and two 2-DE runs were performed per sample. To elucidate potential variations, two 2-DE gels of independently prepared samples of *M. tuberculosis* H37Rv were compared individually with 2 patterns of the mutant strain. Variants which were detected in both gel comparisons were regarded as potential variants. These were finally checked by analyzing all 2-DE patterns, i.e. 6 patterns per strain, and only stringently confirmed differences were accepted as specific variations. For quantitative analysis, the 2-DE gels were further evaluated using the image analysis software programme PDQuest (Version 7.1, BioRad, Hercules, CA, USA). After scanning the gels (8 bit gray values; 100 dpi), spot detection and quantification were performed automatically by fitting spot intensities with a two-dimensional Gaussian model. Corresponding spots in distinct 2-DE gels were matched using a distortion model that takes into account local gel running differences. Prior to the final quantitative data analysis, spot detection and matching were checked thoroughly and corrected manually in an interactive manner. This time-consuming step was essential to achieve reliable results. For quantitative data analysis of spot intensities, a t-test (significance level $P < 0.05$) was applied.

2.23   Protein identification by mass spectrometry (performed in collaboration with Dr. Jens Mattow)

Identification of gel-separated proteins was performed using matrix assisted laser desorption/ionisation mass spectrometry (MALDI-MS) peptide mass fingerprinting (MALDI-MS PMF) [46,47,48,49], electrospray ionisation tandem mass spectrometry (ESI-MS/MS) [49] and/or capillary liquid chromatography in combination with ESI-MS/MS (CapLC-MS/MS) [50]. MALDI-MS PMF was performed as described [51,52] with minor modifications. In short, spots of interest were excised from preparative CBB G250-stained 2-DE gels and proteins were digested in-gel using trypsin. Resulting peptides were desalted and concentrated prior to mass analysis using ZipTipC$_{18}$ pipette tips (Millipore, Bedford, USA). Masses of the tryptic peptides were determined using a time-of-flight mass spectrometer with delayed extraction. Mass accuracy in the range of 30 ppm was obtained by internal calibration of the spectra. Proteins were identified by PMF using the search algorithm MS-FIT. The applied presettings and criteria for identification have been described previously [53]. In some cases, sequence support was required, to establish protein identity. Sequence support was obtained by either ESI-MS/MS performed as described [54] or CapLC-MS/MS as described below. For ESI-MS/MS analyses the sequence tag method [55] was used to search for the proteins in the NCBI protein database (http://195.41.108.38/PA_PeptidePatternForm.html). If this was not successful, a *de novo* sequencing with the program MassSeq (Micromass, Manchester, UK) and a database search in the *M. tuberculosis* protein database of the Institute for Genomic Research (http://www.tigr.org/tigr-scripts/CMR2/GenomePage3.spl?database=gmt) were performed. The search was carried out for the coding part of the genome and the entire genome. Some peptide mixture samples were chromatographically

separated prior to on-line mass analysis using a capillary liquid chromatography system delivering a gradient to formic acid (0.1%) and acetonitrile (80%). The eluted peptides were ionized by electrospray ionization on a Q-TOF hybrid mass spectrometer. The instrument, in automated switch mode, selects precursor ions based on intensity for peptide sequencing by collision-induced fragmentation tandem MS. The MS/MS analyses were conducted using collision energy profiles that were chosen based on the m/z value of the precursor. The generated mass data were processed into peak lists containing m/z value, charge state of the parent ion, fragment ion masses and intensities, and correlated with proteins and nucleic acid sequence databases using the search algorithm Mascot [56]. Proteins were identified based on matching the MS/MS data with mass values calculated for selected ion series of a peptide. A non-redundant protein database and a nucleotide database (dbEST) were searched without applying any constraints on Mr or species. Results were validated manually.

2.24   Infection procedures

Before intranasal infection, mice were anesthetized according to animal protection law with 10 µl (0.2 mg) Rompun (Bayer), and 10 µl (1.2 mg) Ketavet (Pharmacia). Thirty µl PBS was added, and a total volume of 50 µl / mouse was injected into the femoral muscle. After a few minutes mice were anesthetized, and the appropriate dose of bacteria was given as drops of 20 µl on the nostrils.

Intravenous infections (0.1 ml) were given into the tail vein using a 1 ml Sub-Q syringe (BD).

Aerosol infection was performed as described elsewhere, using a Glas-col aerosol generator (BD) resulting in approximately 100 – 200 cfu of *M. tuberculosis* being

deposited in the lung of each mouse [57].

2.25   Determination of bacterial load

Infected mice were sacrificed at distinct time points by cervical dislocation. The examined organs were transferred to 1 ml PBS, 0.05 % Tween 80, homogenized and after serial dilution in PBS, 0.05 % Tween 80 plated on 7H11 agar plates supplemented with OADC (BD), cycloheximide (Merck), and ampicillin. After 3 – 4 weeks of incubation at 37 °C the cfu were determined.

2.26   Histology

Tissue was fixed in 4 % formalin/PBS, dehydrated and embedded in paraffin, 5 µm sections were cut, and subsequently Hematoxylin and Eosin (H&E) stained. Rehydration was performed at 2 times 10 min Xylene, 2 x 5 min 95% ethanol, 2 x 5 min 80 % ethanol, 1 x 5 min 70 % ethanol, 1 x 5 min deionized H_2O. For hematoxylin staining samples were incubated 1 x 10 min hematoxalin (Sigma), rinsed with water for 10 min, dipped in acid ethanol, rinsed in water, followed by Eosin Y (Sigma) staining for 1 min. Subsequently samples were rinsed in water and dehydrated for 3 min 95 % ethanol and 2 min Xylene. Samples were mounted using coverslip slides and permount.

2.27   Enzyme-Linked Immunosorbent Assay (ELISA)

Coating of 96 well plates was performed with 100 µl / well of monoclonal antibody rat anti-mouse IFNγ (clone R4-6A2, ATCC; 1 µg / ml) for 1 h at 37 °C or over night at 4 °C. Subsequently, 3 x washing with PBS 0.05 % Tween 20, 1 h blocking with 200 µl

of blocking buffer (PBS + 1 % BSA) for 1 h at 37°C and further 3 x washing. Standard (IFNγ [R&D] dilutions) and samples were added and incubated for 3 days. After 3 x washing, 1 h incubation with 100 µl XMG1.2-biotin second monoclonal antibody (1 µg / ml), and further 3 x washing, 100 µl of streptavidine alkaline phosphatase (Dianova, Hamburg, Germany) (diluted 1 : 2000) were added and incubated for 1 h at 37°C. Samples were 3 x washed, and 50 µl of substrate solution (1 tablet p-nitrophenyl-phosphate (Sigma) / 5ml di-ethanolamine-buffer (48.5 ml diethanolamine, 400 mg $MgCl_2$, 100 mg NaN_3 (0.02 %), ad 500 ml H_2O, pH 9.8) per well was added. The reaction was stopped with 50 µl of 0.5 M EDTA, pH 8.0, and samples were measured at 405 nm / 490 nm.

IFNγ containing samples were collected from cells restimulated as follows: Cells were prepared from spleens which were passaged through a mesh, centrifuged for 5 min at 1500 rpm and 4°C. The pellet was resuspended in 1.5 ml erylyse-buffer.

erylyse-buffer:

8.29 g NH_4Cl

1 g $KHCO_3$

0.037 g EDTA

ad 1000 ml H_2O and autoclaved

Subsequently, RPMI was added to a volume of 15 ml, the cells were centrifuged, resuspended in 10 ml RPMI, and adjusted to 1 x 10^6 / ml. One hundred µl were used per well and mixed with 100 µl medium or *M. tuberculosis* protein extract (10 µg / ml), respectively. After 3d of restimulation at 37°C / 5 % CO_2, culture supernatants were collected and measured for IFNγ by ELISA.

3 Results

3.1 *M. smegmatis* Δ*upk*

3.1.1 Sequence comparison of Upk homologues

Protein sequences of *E. coli* undecaprenyl-phosphokinase (BacA), *M. smegmatis* undecaprenyl-phosphokinase (Upk), and *M. tuberculosis* Upk were compared by clustAl analysis (Fig. 6A). Both mycobacterial proteins showed 38 % identity to *E. coli* BacA and about 50 % similarity. ClustAl comparison of *M. smegmatis* and *M. tuberculosis* Upk revealed 73 % identity and 78 % similarity (Fig 6B). Highly conserved features were visible for all three homologues

A

```
                              1                                                    50
        Escherichia_coli      MSDMHSLAIA AILGVVEGLT EFLPVSSTGH MIIVGHLLGF EGDTAKTFEV
   Mycobacterium_smegmatis    ~~~~MSWLQV IVLSIVQGLT EFLPVSSSGH LAITSQVF.F DDDAGASFTA
Mycobacterium_tuberculosis    ~~~~MSWWQV IVLAAAQGLT EFLPVSSSGH LAIVSRIF.F SGDAGASFTA

                              51                                                   100
        Escherichia_coli      VIQLGSILAV VVMFWRRLFG LIGIHFGRPL QHEGESKGRL TLIHILLGMI
   Mycobacterium_smegmatis    VTQLGTEFAV LIYFAKDIGR IIKSWPLGLR APEHRDADYR LGUFVIVGTI
Mycobacterium_tuberculosis    VSQLGTEAAV VIYFARDIVR ILSAWLHGLV VRAHRNTDYR LGWYVIIGTI

                              101                                                  150
        Escherichia_coli      PAVVLGLLFH DTIKS.LFNP INVMYALVVG GLLLIAAECL KPKEPRAPGL
   Mycobacterium_smegmatis    PIGVFGLLFK DEIRTGARNL WLVATALIVF SVVIAAAEYY G.RQVR..QV
Mycobacterium_tuberculosis    PICILGLFFK DDIRSGVRNL WVVVTALVVF SGVIALAEYV G.RQSR..HI

                              151                                                  200
        Escherichia_coli      DDMTYRQAFN IGCFQCLALW PGFSRSGATI SGGMLMGVSR YAASEFSFLL
   Mycobacterium_smegmatis    EQLTWRDSVI VGLAQCLALW PGVSRSGATI SAGLFLGLKR EVAARFGFLL
Mycobacterium_tuberculosis    FRLTWRDAVU VGIAQTLALV PGVSRSGSTI SAGLFLGLDR ELAARFGFLL

                              201                                                  250
        Escherichia_coli      AVPMMMGATA LDLYKSWGFL TSG...DIPM FAVGFITAFV VALIALKTFL
   Mycobacterium_smegmatis    AIPAVLASGL FSLPDAFHPV GEGMSASGPQ LIVATVIAFV VGFAAIAWFL
Mycobacterium_tuberculosis    AIPAVFASGL FSLPDAFHPV TEGMSATGPQ LLVATLIAFV LGLTAVAWLL

                              251                            284
        Escherichia_coli      QLIKRISFIP FAIYRFIVAA AVYVVFF~~~ ~~~~
   Mycobacterium_smegmatis    KFLVSHSMYW FVGYRVVLGV VVLALLGTGV LAAQ
Mycobacterium_tuberculosis    RFLVRHNMYW FVGYRVLVGT GMLVLLATGT VAAT
```

B

```
   Mycobacterium_smegmatis    MSWLQVIVLS IVQGLTEFLP VSSSGHLAIT SQVFFDDDAG ASFTAVTQLG
Mycobacterium_tuberculosis    MSWWQVIVLA AAQGLTEFLP VSSSGHLAIV SRIFFSGDAG ASFTAVSQLG

   Mycobacterium_smegmatis    TEFAVLIYFA KDIGRIIKSW FLGLRAPEHR DADYRLGWFV IVGTIPIGVF
Mycobacterium_tuberculosis    TEAAVVIYFA RDIVRILSAW LHGLVVKAHR NTDYRLGWYV IIGTIPICIL

   Mycobacterium_smegmatis    GLLFKDEIRT GARNLWLVAT ALIVFSVVIA AAEYYGRQVR QVEQLTWRDS
Mycobacterium_tuberculosis    GLFFKDDIRS GVRNLWVVVT ALVVFSGVIA LAEYVGRQSR HIERLTWRDA

   Mycobacterium_smegmatis    VIVGLAQCLA LWPGVSRSGA TISAGLFLGL KREVAARFGF LLAIPAVLAS
Mycobacterium_tuberculosis    VVVGIAQTLA LVPGVSRSGS TISAGLFLGL DRELAARFGF LLAIPAVFAS

   Mycobacterium_smegmatis    GLFSLPDAFH PVGEGMSASG PQLIVATVIA FVVGFAAIAW FLKFLVSHSM
Mycobacterium_tuberculosis    GLFSLPDAFH PVTEGMSATG PQLLVATLIA FVLGLTAVAW LLRFLVRHNM

   Mycobacterium_smegmatis    YWFVGYRVVL GVVVLALLGT GVLAAQ
Mycobacterium_tuberculosis    YWFVGYRVLV GTGMLVLLAT GTVAAT
```

Fig. 6 Protein sequence comparison with clustAl alignment reveals highly conserved features of *E. coli* BacA and mycobacterial Upk. Identity of *E. coli* to *M. smegmatis* and *M. tuberculosis* is 38 % and similarity 50 %(A). Identity of *M. smegmatis* to *M. tuberculosis* is 73 %, and similarity 78 %(B). Color definitions: blue - all amino acids of a column are identical; red - more than half of the amino acids of a column are identical or belong to one of the strong groups (amino acids with strong similarities); orange - more than half of the amino acids of a column belong to one of the weak groups (amino acids with weak similarities), or amino acids that could be grouped into a weak group with every amino acid of the same column belonging to a strong group that is marked red.

3.1.2 Construction of Δ*upk* mutant of *M. smegmatis* mc2 155

An in-frame, unmarked deletion of the *M. smegmatis upk* gene was created by a two-step-method [58]. Regions of 879 bp and 945 bp flanking the *upk* gene in *M. smegmatis* were amplified by PCR and inserted into pYUB657. Thus 96% of the wildtype *upk* gene was deleted. The mutated copy of *upk* was introduced into *M. smegmatis* by electroporation. Hyg^R transformants which displayed a Suc^S phenotype were assayed for recombination by Southern blot. There is the possibility of integration upstream or downstream of the target gene by single crossover. A mutant in which the template plasmid has inserted upstream, resulting in 11,547 bp and 7,337 bp fragments on Southern blot (Fig 7., southern blot a) was chosen for further analysis. A culture of this single crossover strain was grown overnight in complete medium without hygromycin. This period of growth allowed double crossover events to occur, followed by plasmid loss. Deletion or preservation of the wildtype allele occur with equal probability. Two out of 6 analyzed clones displayed the characteristics of a *upk* deletion mutant (Fig. 7, southern blot b). The mutant strain was named *M. smegmatis* Δ*upk*. A complementation strain was constructed, using pMV262-*rv2136c*, a multicopy plasmid expressing the *M. tuberculosis* H37Rv homologue of the *upk* gene under control of the *M. bovis* BCG *groEL*2 (Hsp60) promoter. The parent plasmid, pMV262, is an episomal *E. coli*-mycobacteria shuttle plasmid.
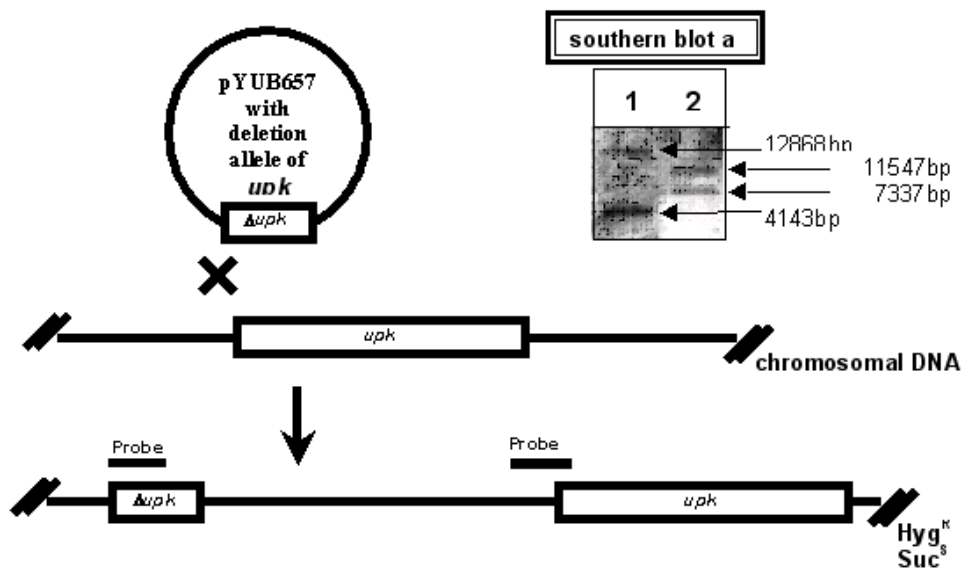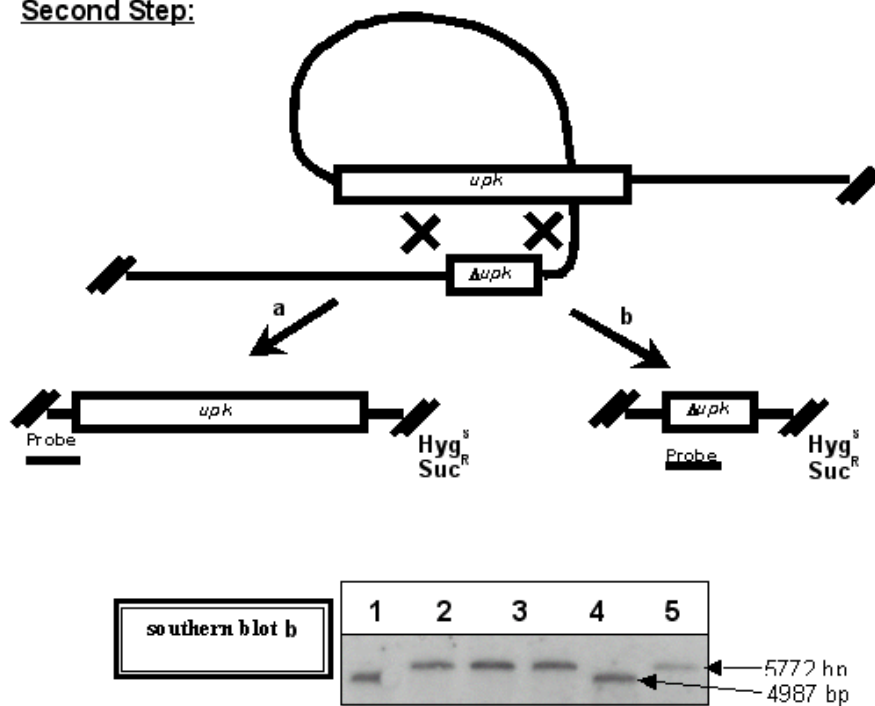
First Step:

Second Step:

Fig. 7 An in-frame, unmarked deletion of *upk* was generated in *M. smegmatis* by a two step approach. In the first step, the counterselectable suicide plasmid pYUB657 carrying the deletion allele of *upk* recombined with the bacterial chromosome. Southern blot analysis confirmed the recombination event. Two orientations are possible (southern blot a: lane 1 and 2). Clone 2 was selected. In the second step the plasmid loops out in the absence of hygromycin selective pressure. The deletion allele or the wildtype copy of *upk* are lost with equal probability. Deletion of *upk* was verified by Southern blot (Southern blot b). Lane 1 and 5 are deletions, the others are wildtype. For the following studies clone number 1 was selected.

3.1.3   Differential abundance of peptidoglycan and colony morphology

Bacteria were grown on 7H10 agar plates. While wildtype *M. smegmatis* showed dome-like morphology, Δ*upk* mutant colonies exhibited caved-in structures (Fig. 8). Although this observation suggests that the cell wall is affected, examination by electron microscopy revealed no differences (Fig. 8). Yet, specific immunogold-staining of peptidoglycan revealed a lower number of gold-particles associated with the cell surface of the Δ*upk* mutant (Table 1). Twenty electron microscopy images of stainings of wildtype and the Δ*upk* mutant were examined. For wildtype, 241 particles were counted of which 27% were surface associated. Of the 225 particles counted on the Δ*upk* mutant bacteria, only 13% were surface associated (Fig. 9).
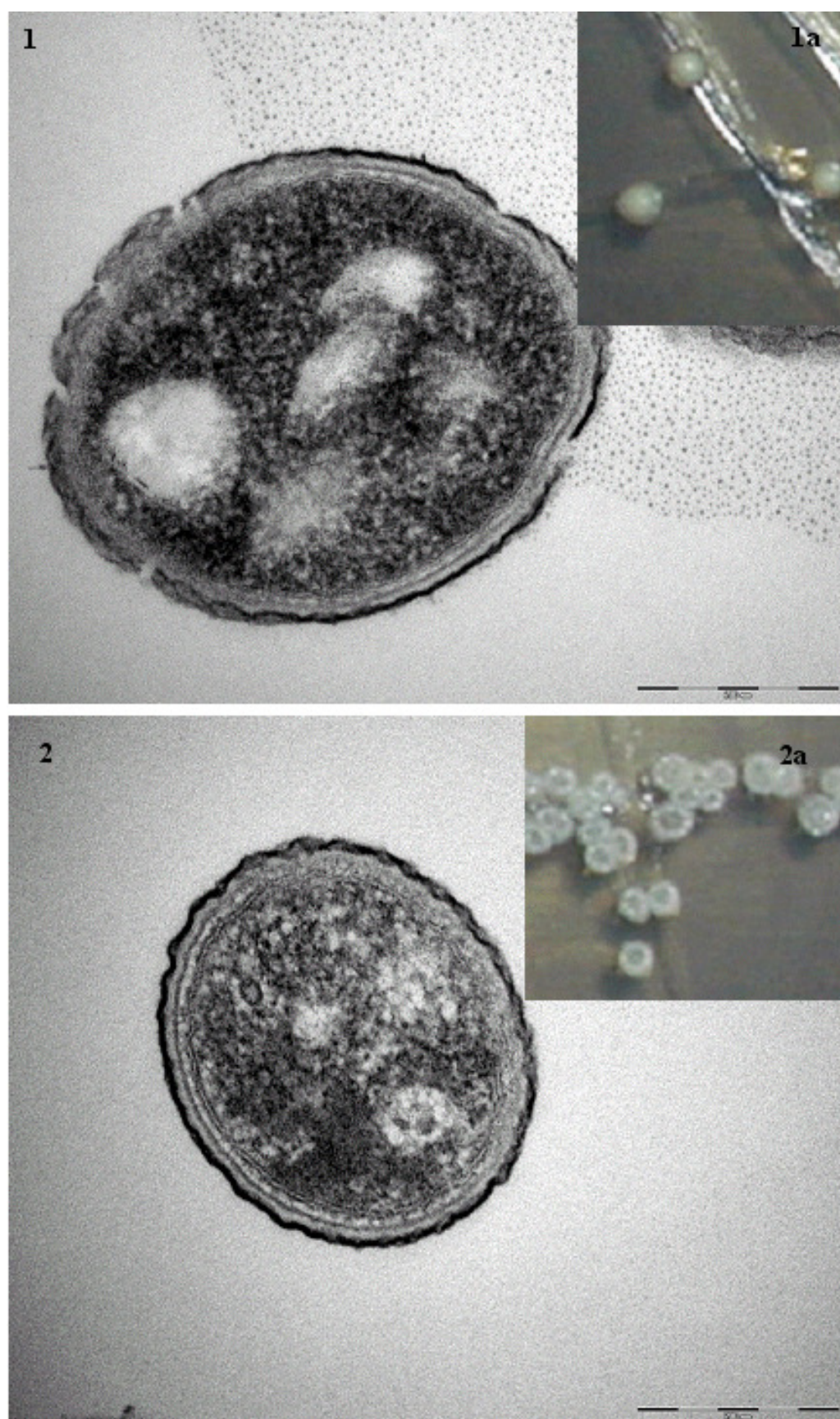
Fig. 8 Differential colony morphology of *M. smegmatis* mc^{2}155 and *M. smegmatis* mc^{2}155Δ*upk*. Mutant colonies have caved-in structures lacking dense cores (1a: wildtype and 2a: Δ*upk* mutant). Using electron microscopy, there is no visible difference in cell wall architecture (1: wildtype and 2: Δ*upk* mutant).
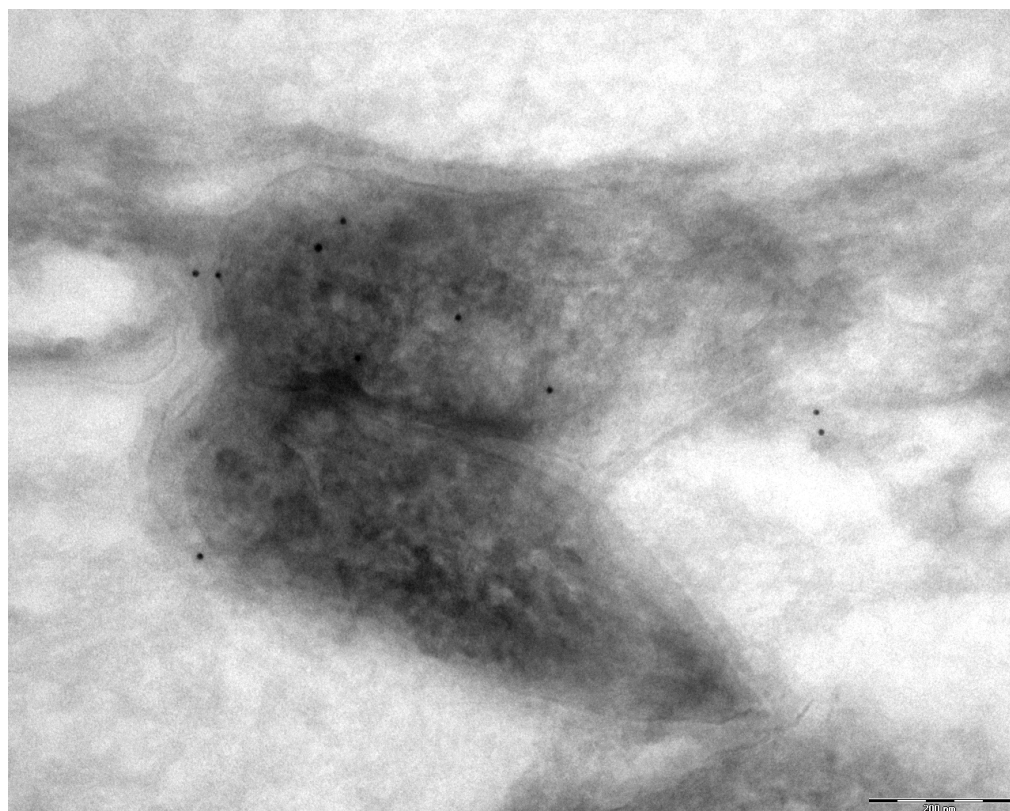
Fig. 9 Distribution of gold particles in an anti-peptidoglycan immuno-gold stain. Twenty electron microscopy images of wildtype and the Δ*upk* mutant were examined. For wildtype, 241 particles were counted of which 27% were surface associated. Of the 225 particles counted on the Δ*upk* mutant bacteria, 13% were surface associated.

Table 1: distribution of gold particles in anti peptidoglycan immuno-gold stain.

	gold particles total	particles in the cytoplasm	particles on the surface
Wildtype	241	176 **73%**	65 **27%**
Δ*upk*	225	195 **86,7%**	30 **13,3%**

3.1.4 Sensitivity to bacitracin

As described above, ∆*upk* mutants are expected to be more sensitive to bacitracin than wildtype *M. smegmatis*. This issue was investigated by the alamar blue assay. Alamar blue is a redox-dye that converts from blue to red upon reduction, reflecting a measure of growth [59]. Bacteria were incubated over night in 7H9 complete medium supplemented with serial dilutions of bacitracin (0 U/ml – 2,500 U/ml). Next day, alamar blue was added and fluorescence at 570 nm was measured. The *M. smegmatis* ∆*upk* mutant showed no growth at a concentration of 500 U/ml bacitracin, whereas wildtype reached 55% of its maximal growth (Fig. 10). The reconstituted strain *M. smegmatis* ∆*upk* + pMV262-*rv2136c* failed to regain wildtype growth but displayed an intermediate phenotype.
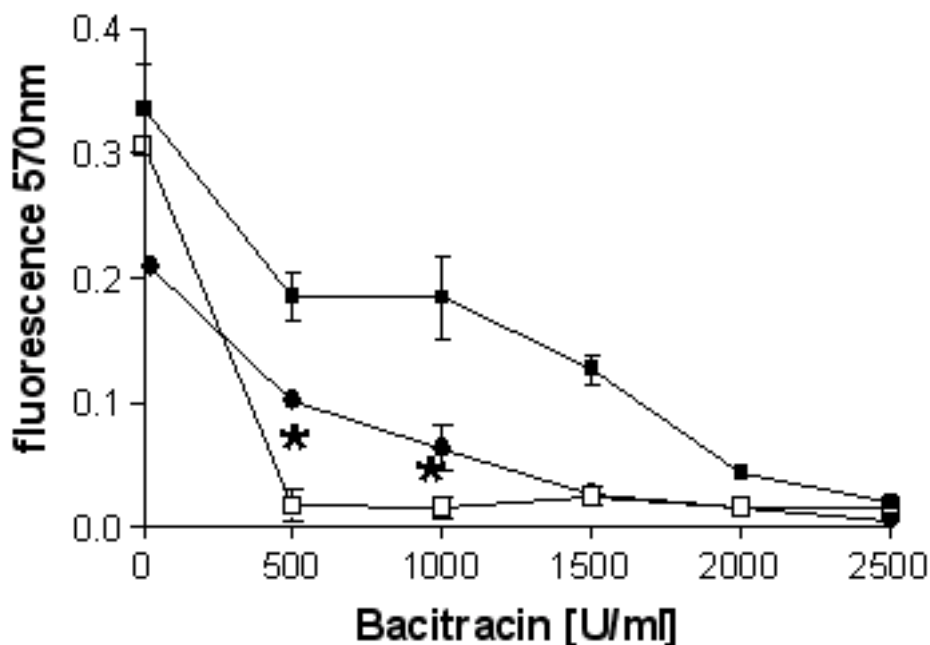

Fig. 10 Sensitivity assay to bacitracin. *M. smegmatis* mc^{2}155 (■), *M. smegmatis* mc^{2}155∆*upk* (□), and *M. smegmatis* mc^{2}155∆*upk* + pMV262-*rv2136c* (●) were incubated with different concentrations of bacitracin over night. Next day alamar blue was added and growth was measured at 570 nm. The Figure shows 1 representative experiment of 3 with similar results.

* Curves were significantly different at 500 and 1000 U bacitracin / ml according to Mann Whitney test (P<0.0001).

3.1.5 Accelerated clearance from infected macrophages

We wanted to find out whether *upk* homologues contribute to virulence of pathogenic

mycobacteria. Therefore we chose the model of macrophage infection. Although, *M.*

smegmatis fails to persist in macrophages it was possible to compare the survival

times of *M. smegmatis* and the Δ*upk* mutant in murine bone marrow derived

macrophages. After infection, bacteria were cleared quickly. The time needed to kill

half of the bacterial number upon infection differed between *M. smegmatis* wildtype

(98 min), *M. smegmatis* Δ*upk* mutant (27 min) and the reconstituted mutant strain
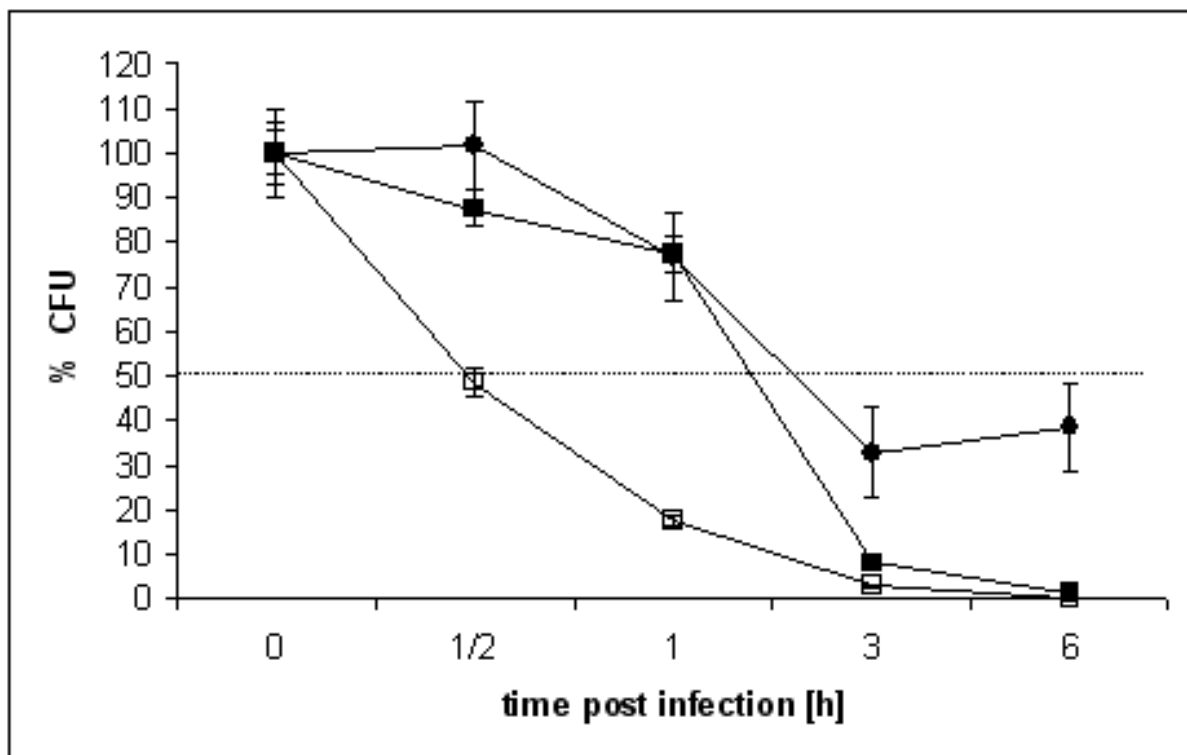
(126 min) (Fig. 11).

Fig. 11 Infection of murine bone marrow derived macrophages. *M. smegmatis* mc^{2}155 (■), *M. smegmatis* mc^{2}155Δ*upk* (□) and *M. smegmatis* mc^{2}155Δ*upk* + pMV262-*rv2136c* (●) were used at a MOI of 200. After 27 min half of *M. smegmatis* Δ*upk* mutants were killed. This was true for wildtype *M. smegmatis* after 98 min and after 126 min for Δ*upk* mutant carrying pMV262-*rv2136c*. The Figure shows 1 representative experiment of 2 with similar results.

3.1.6 Growth properties and biofilm formation

Bacterial growth curves exhibited slightly slower growth of the *M. smegmatis* Δ*upk*

mutant compared to *M. smegmatis* wildtype after 9 h in 7H9 complete medium (Fig.

12A) and after 9 and 24 h in biofilm medium (Fig. 12B). Nevertheless, after 24 h, in

7H9 complete medium and after 72 h in biofilm medium, growth characteristics of all
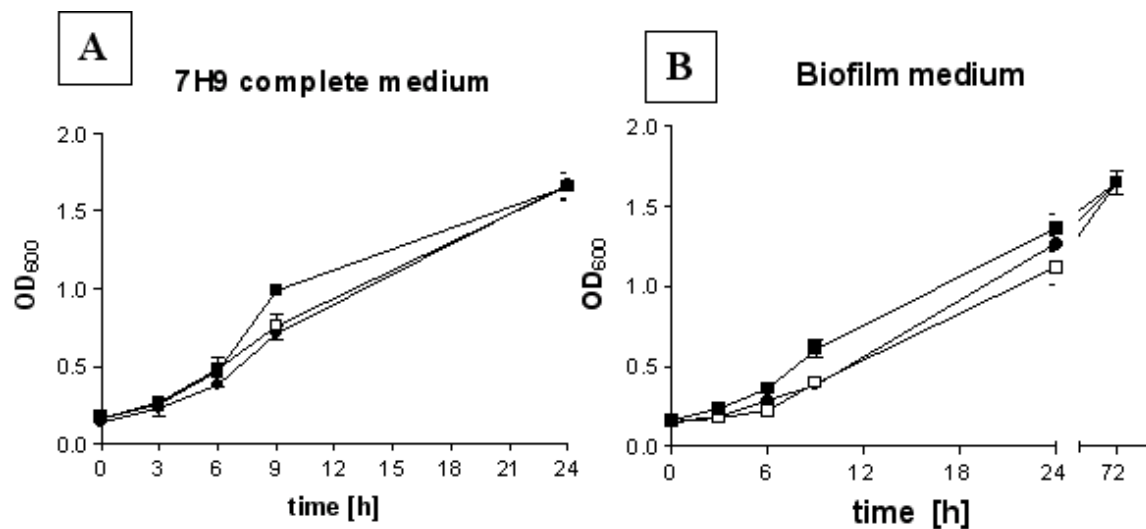
M. smegmatis strains adapted.

Fig. 12 Growth curves. *M. smegmatis* mc²155 (■), *M. smegmatis* mc²155Δ*upk* (□), and *M. smegmatis* mc²155Δ*upk* + pMV262-*rv2136c* (●) grown at 37°C in 7H9 complete medium (A) and biofilm medium (B). The Figure shows 1 representative experiment of 2 with similar results.

According to Mann Whitney test, growth curves in 7H9 complete medium (A) were not different whereas growth of *M. smegmatis* wildtype was significantly different at 9 and 24 h in biofilm medium(B) compared to the *M. smegmatis* Δ*upk* strain and the reconstituted strain (P<0.0001).

M. smegmatis forms biofilms under natural conditions [60]. We determined whether deletion of the *upk* gene affected biofilm formation *in vitro* and *in vivo*. After 4 to 5 days shaking at RT in biofilm medium, biofilms were analyzed. Wildtype bacteria completely covered the surface whereas Δ*upk M. smegmatis* only produced scattered islands of biofilm (Fig. 13).

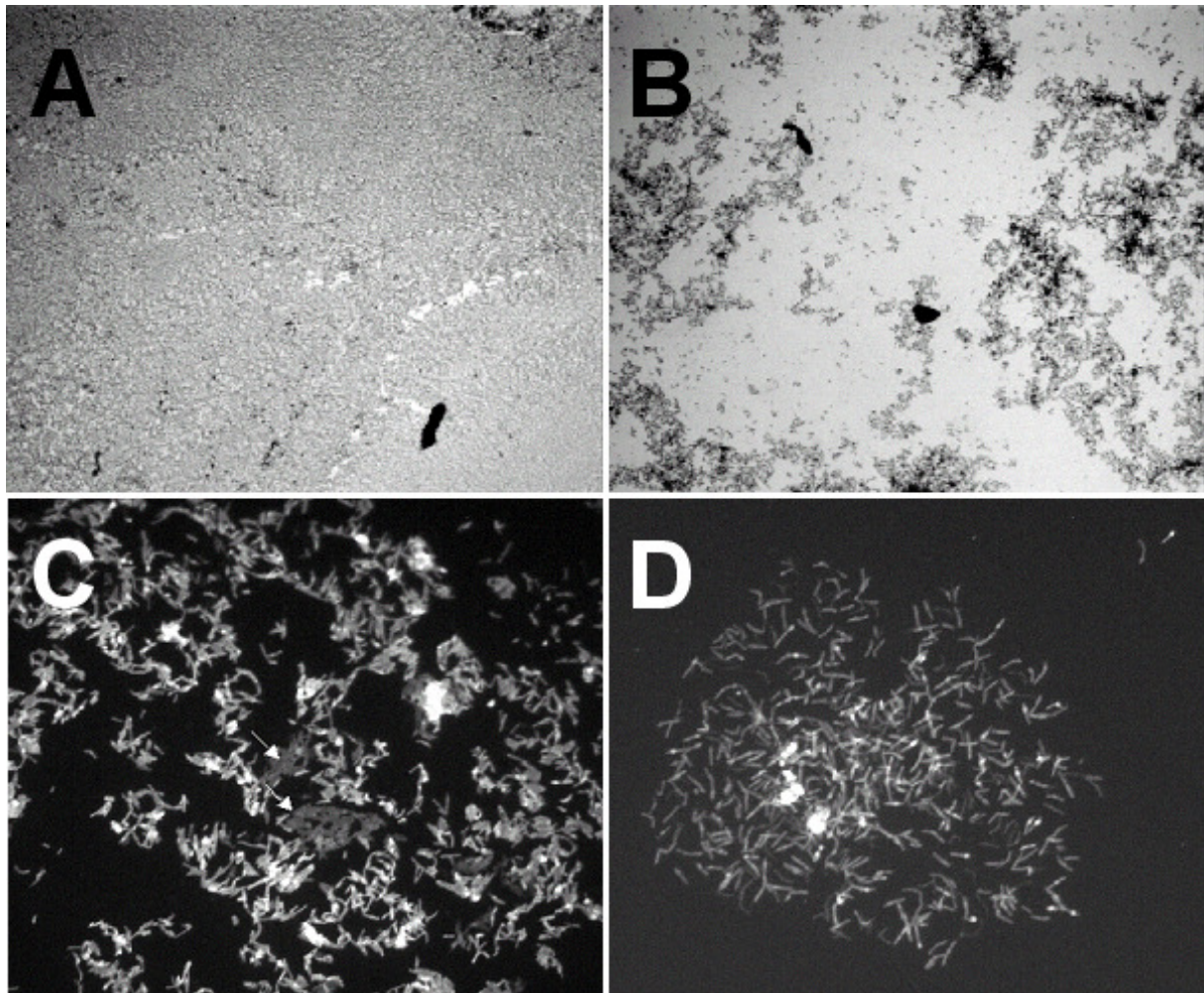Fig. 13 Differential biofilm formation. *M. smegmatis* mc^{2}155 (A, C) and *M. smegmatis* mc^{2}155Δ*upk* (B, D) were grown for 4 to 5 days at room temperature in biofilm medium and stained with crystal violet. The mutant exhibited impaired biofilm development. Rhodamine auramine staining (C, D) visualized even structures (highlighted by white arrows) only in wildtype biofilms.

Principally, an intact biofilm is characterized by a matrix consisting of extracellular polymer substances (EPS). Such a matrix was clearly visible for wildtype *M. smegmatis*, whereas the Δ*upk* mutant grew in separated single cells (Fig. 13).

Additional studies to follow *in vivo* biofilm development were performed. *M.*

smegmatis wildtype applied to a mouse penis induced smegma in 65 % of the

animals, whereas smegma development upon application of Δ*upk* deletion mutant

was observed for 42% only, which was about background level (Fig. 14A). Groups

consisted of 10 animals each.

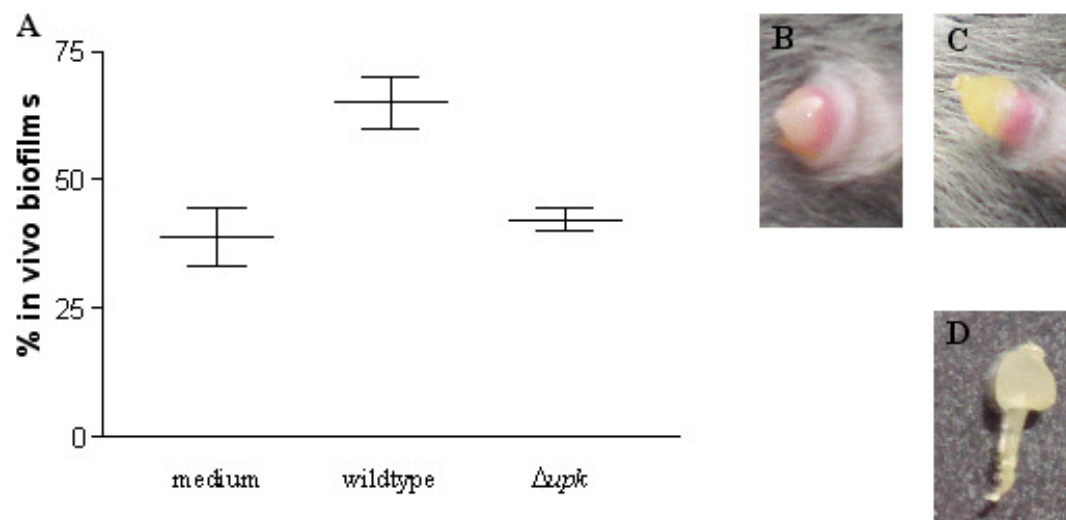Fig. 14A In vivo biofilm formation. Penises of C57BL/6 mice were exposed to medium, wildtype *M. smegmatis*, and Δ*upk* deletion mutant. The Figure shows combined results of 2 independent experiments with similar results. Before application of the *M. smegmatis* strains, mice had a clean penis (14B). A penis with an over night grown smegma is depicted in 14C. 14D shows a smegma plug removed from a penis.

3.1.7 Summary *M. smegmatis* **mc2155** Δ*upk*

The *M. smegmatis upk* gene was identified and an in-frame, unmarked deletion mutant was generated. The absence of Upk influenced bacitracin sensitivity, peptidoglycan synthesis, survival in macrophages, growth properties, and biofilm formation *in vitro* and *in vivo. In vitro* biofilms of *M. smegmatis* Δ*upk* mutant were characterized as scattered islands of bacteria compared to a completely covered surface observed for wildtype bacteria. The *M. smegmatis* Δ*upk* strain is the first to express a phenotype in a newly developed *in vivo* mouse model of biofilms.

3.2 *M. tuberculosis* Δ*upk* (and construction of *Mycobacterium bovis* BCG Δ*upk*)

3.2.1 Construction of Δ*upk* mutant strains of *M. tuberculosis* and *M. bovis* BCG

A temperature sensitive (ts) TM4 phage delivery system was used to generate hygromycin-marked knockout mutants in *M. tuberculosis* and *M. bovis* BCG. Flanking regions to the *M. tuberculosis upk* gene were cloned next to a hygromycin resistance cassette and fused to the phage genome. Recombinant ts phages were amplified at 30 °C using *M. smegmatis* growing in top agars as a host. At 37 °C, phages were impaired to become lytic and could be used to transduce *M. tuberculosis* H37Rv and *M. bovis* BCG. The recombinant phages transferred their DNA into the bacteria. Flanking regions induced double crossover events, thus exchanging the *upk* gene with a hygromycin resistance cassette, which subsequently was verified by Southern blot (Fig. 15). The mutant strains were named: *M. tuberculosis* Δ*upk* and *M. bovis* BCG Δ*upk*.
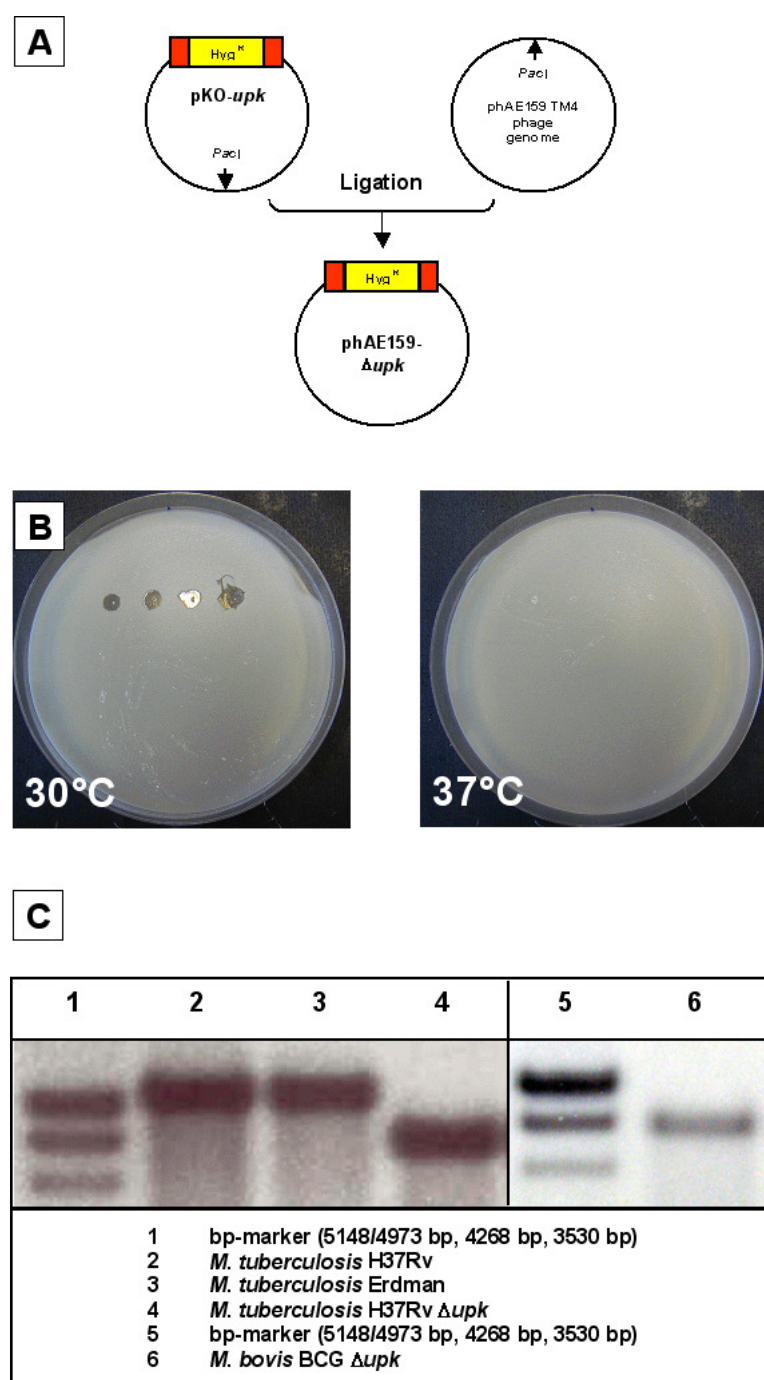
Fig. 15 Construction of *upk* knockout mutants in *M. tuberculosis* and *M. bovis* BCG. Knockout phage genome phAE159-Δ*upk* was generated by ligation of the plasmid pKO-*upk* and the phage genome phAE159 TM4 (A). Four phages were tested for temperature-sensitivity and revealed the expected phenotype- lysis at 30 °C but not at 37 °C (B). # 4 was picked, amplified and used for transduction of *M. tuberculosis* and *M. bovis* BCG. Lane 4 and 6 represent *upk* deletion mutants for *M. tuberculosis* H37Rv and *M. bovis* BCG, verified by Southern blot analysis (C).

A complementation strain of *M. tuberculosis* was constructed using pMV262-*rv2136c*, a multicopy plasmid expressing *upk* under control of the *groEL*2 (Hsp60) promoter of *M. bovis*. The parent plasmid, pMV262, is an episomal *E. coli*-mycobacteria shuttle-

plasmid. *M. tuberculosis* was difficult to transform by electroporation. In many cases, only the antibiotic resistance was transformed and other parts of the plasmid were lost. Thus, the appropriate size of the resistance cassette and the *rv2136c* gene (data not shown) was verified by PCR for kanamycin resistant colonies of *M. tuberculosis* H37Rv Δ*upk* mutants, transformed with pMV262-*rv2136c*. Additionally, whole DNA was prepared from a positive clone and used for transformation of *E. coli* DH5α. Subsequently, the plasmid was purified and compared to the original vector. *BamHI* digest, released the *rv2136c* insert. *SalI* digest was used to verify the correct orientation of the insert. The fragments were analyzed by gelelectrophoresis and appeared as the same size as the original vector. The recombinant *M. tuberculosis* Δ*upk* knockout clone carrying this vector was used as the complementation strain (Fig. 16). Transcription levels of *upk* were determined by RT-PCR in relation to *rv2946c*, a gene transcribed at the same level in the *M. tuberculosis* H37Rv Δ*upk* mutant and wildtype. Transcription of the *upk* gene under control of the *groEL2* promoter was 3.51 fold higher than *rv2946c*-transcription and 201.56 fold lower than transcription of *upk* in the wildtype strain under control of the natural promoter in late logarithmic growth phase.
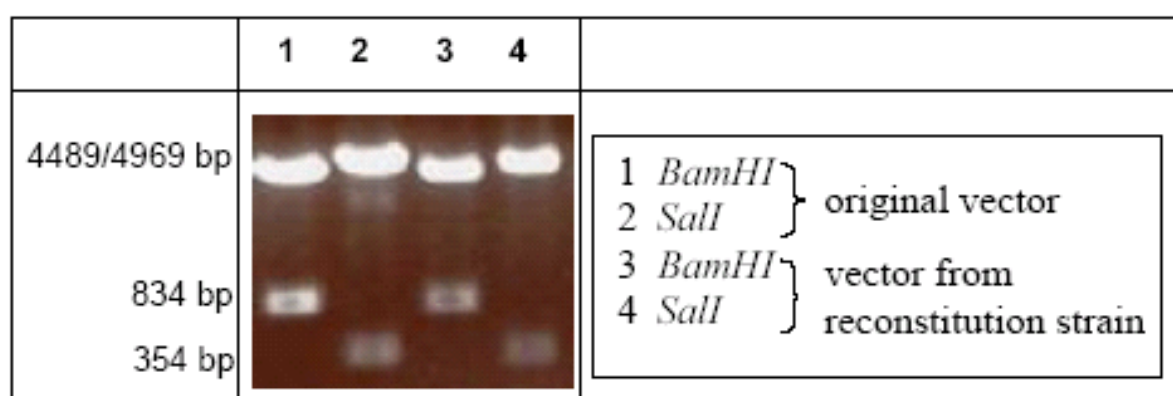

Fig. 16 Comparison of the original reconstitution vector pMV262-*rv2136c*, and the reconstitution vector purified from an electroporated Δ*upk* strain. Lanes # 1 and # 2 show the pattern of the original insert with accurate orientation. Lanes # 3 and # 4 confirm this pattern for the vector purified from the reconstitution strain.

3.2.2 Growth curve

Growth properties in 7H9 medium were examined for the 3 strains: wildtype, Δ*upk* mutant, and reconstitution. OD_{600} was measured once a day. The *M. tuberculosis* Δ*upk* mutant showed no differences in growth rate compared to wildtype whereas the complementation strain grew more slowly (Fig. 17).
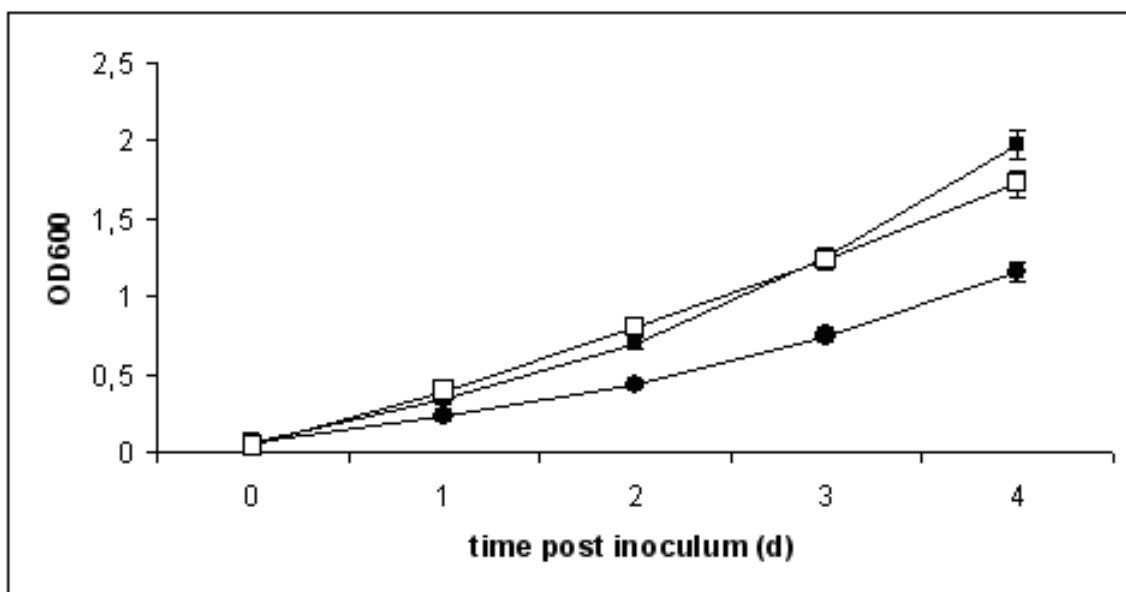

Fig. 17 Growth curves. *M. tuberculosis* H37Rv (■), *M. tuberculosis* H37Rv Δ*upk* (□), and *M. tuberculosis* H37Rv Δ*upk* + pMV262-*rv2136c* (•) were grown at 37 ℃ in 7H9 complete medium. The Figure shows 1 representative experiment of 2 with similar results.

3.2.3 In vitro assays

Colonies of *M. tuberculosis* wildtype, the *M. tuberculosis* Δ*upk* mutant and the reconstituted strain were of the same shape (data not shown). The attenuated strain *M. tuberculosis* H37Ra is known to behave differently compared to *M. tuberculosis* H37Rv in the following *in vitro* assays: Neutral red staining, cording assay, and pellicle culture. The H37Ra-strain is not stainable with neutral-red [61] (Fig. 18A). For virulent *M. tuberculosis* H37Rv, bacterial cord-factors e.g. trehalose dimycolate (TDM; [62] are necessary for growth in cords on a surface in non-shaking cultures [63].

After 2 to 3 weeks, cultures of *M. tuberculosis* grown without shaking in Sauton medium, form pellicles on top of the medium and bacteria push each other up the wall of the tube.

All *M. tuberculosis* strains were examined in these 3 assays:

The strains were treated with neutral red. Pellets of stained Δ*upk* knockout mutant and complementation strain exhibited red color like H37Rv wildtype did, thus revealing no phenotype-differences (Fig. 18A).

Also cording was not affected by loss of *upk*. All strains were stained with rhodamine auramine (Fig. 18B).

The *M. tuberculosis* strains revealed phenotype-differences in case of pellicle formation. The Δ*upk* mutant was hampered in pellicle formation and the

complementation strain developed a gapless, smooth pellicle in contrast to the rough
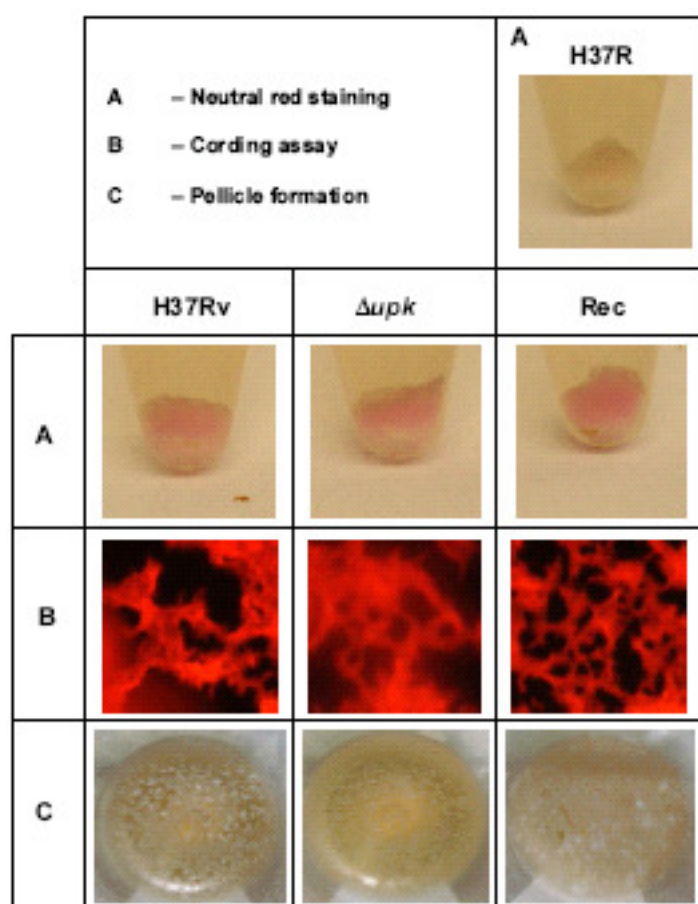
pellicle of *M. tuberculosis* wildtype (Fig. 18C).

Fig. 18 Assays on *M. tuberculosis* behavior under defined conditions. Neutral-red stained *M. tuberculosis* H37Rv, *M. tuberculosis* Δ*upk*, and the reconstitution strain but not *M. tuberculosis* H37Ra (A). Wildtype, mutant, and reconstitution strain grew in cords (B). *M. tuberculosis* wildtype formed a heterogeneous pellicle whereas *M. tuberculosis* Δ*upk* was retarded in pellicle formation, and the reconstituted mutant exhibited a smooth pellicle (C)

3.2.4 Proteome and transcriptome analysis

Cultures of *M. tuberculosis* H37Rv and the Δ*upk* mutant were grown to late log-phase

(OD$_{600}$ = 1.0) and whole cell lysates, as well as RNA were purified.

Proteome analysis was performed with 3 independent protein lysates of both strains,

M. tuberculosis wildtype and *M. tuberculosis* Δ*upk* mutant. Each sample was

analyzed on 2 gels. The comparative proteome analysis of 12 gels (6 wildtype and 6

mutant) revealed 45 spots of differential relative intensity. For the Δ*upk* mutant, 23

spots belonged to the group of higher intensity and 22 spots exhibited lower intensity

(Table 2) compared to *M. tuberculosis* wildtype. Representative examples are

depicted in Figure 19. The 2-DE gels were first evaluated visually. Subsequently, the

gels were re-evaluated by means of the image analysis program PDQuest. This

software allowed verification of significance of the results by t-test and offered the

possibility to quantify spot intensities.

In parallel to determine and compare gene expression profiles, RNA *of M.*

tuberculosis H37Rv and the Δ*upk* strain were purified and hybridized to a *M.*

tuberculosis array. Wildtype and mutant showed a high number of differentially

regulated genes. The 20 most significantly regulated genes of 2 independent

experiments are summarized in Figures 20 and 21.

Correlation of the results of proteome and transcriptome was limited. Comparing *M.*

tuberculosis Δ*upk* and *M. tuberculosis* wildtype, proteins of higher spot intensity, such

as Rv0341 and Rv2462 had a higher transcription rate, too. And proteins of lower

spot intensity, like Rv1912 and Rv0125 also had a lower transcription rate. However,

Rv2031c / HspX was a protein of high abundance in *M. tuberculosis* Δ*upk* whole cell

lysates, compared to *M. tuberculosis* wildtype, but gene expression did not differ

between both strains. HspX is of interest, because it is one of several proteins

produced during persistence of bacteria under low oxygen conditions and within

granulomas, but at a lower level during logarithmic growth phase [64,65]. The

examined bacterial cultures were harvested at late logarithmic growth phase (OD_{600} =

0.8 - 1).

Table 2a: *M. tuberculosis* H37Rv Δ*upk* protein spots of higher relative intensity

Spot number*	Identity	Functional category **	Fold change (mutant strain compared to wildtype)
⇑ 08	NADH dehydrogenase chain E (nuoE, **Rv3149**)	7	new spot
⇑ 09	Antigen 84 (wag31, **Rv2145c**)	3	new spot
⇑ 11	Hypothetical protein **Rv0341** and glu-tRNA-gln amidotransferase, subunit B (gatA, **Rv3011c**)	3, 2	new spot
⇑ 17	not identified		new spot
⇑ 18	not identified		new spot
⇑ 19	not identified		new spot
⇑ 20	not identified		new spot
⇑ 01	14 kDa antigen (hspX, **Rv2031c**)	0	12.0
⇑ 03	14 kDa antigen (hspX, **Rv2031c**)	0	8.0
⇑ 03b	14 kDa antigen (hspX, **Rv2031c**)	0	6.1
⇑ 12	[beta]-ketoacyl-ACP synthase (kasB, **Rv2246**)	1	3.7

Spot number*	Identity	Functional category **	Fold change (mutant strain compared to wildtype)
⇑ **03a**	14 kDa antigen (hspX, **Rv2031c**)	0	3.3
⇑ **05**	Hypothetical protein **Rv1284**	10	3.0
⇑ **17**	not identified		2.6
⇑ **04**	not identified		2.3
⇑ **12a**			2.3
⇑ **04**	not identified		2.3
⇑ **14**	not identified		2.2
new ⇑ **01**	Putative transcriptional regulator (**Rv1956**)	9	2.2
new⇑ **05**	Two-component response regulator (NarL, **Rv0844c**)	9	2.1
⇑ **13**	Chaperone protein, similar to trigger factor (tig, **Rv2462c**)	3	2.0
⇑ **07 left**	Hypothetical protein **Rv0207c**	10	2.0
⇑ **07 right**	Hypothetical protein **Rv0207c**	10	2.0

* Spot numbers are according to discovery order of spots of different intensity. "⇑" means higher spot intensity.

**see Table 4: tuberculist classification of functional categories

Table 2b: *M. tuberculosis* H37Rv Δ*upk* protein spots of lower relative intensity

Spot number*	Identity	Functional category **	Fold change (mutant strain compared to wildtype)
⇓ 06	Hypothetical protein **Rv0481c**	16	lost spot
⇓ 07	Hypothetical protein **Rv0968**	10	lost spot
⇓ 08	Hypothetical protein **Rv0968**	10	lost spot
⇓ 12	not identified		lost spot
⇓ 18	3-hydroxyacyl-CoA dehydrogenase (fadB5, **Rv1912c**)	1	lost spot
⇓ 04	not identified		10.3
⇓ 11	Hypothetical protein **Rv2302**	10	7.4
⇓ 24	Probable serine protease (pepA, **Rv0125**)	7	5.0
⇓ 02	Hypothetical protein **Rv3615c**	10	4.9
⇓ 03	Hypothetical protein **Rv3615c**	10	4.6
⇓ 09	Hypothetical protein **Rv0967**	10	3.7
⇓ 21	not identified		3.1
⇓ 13	possible Soj/para-related protein **Rv3213c**	3	2.9
⇓ 01	not identified		2.8
⇓ 23	Hypothetical protein **Rv3651**	10	2.8
⇓ 7a	Hypothetical protein **Rv0968**	10	2.4

Spot number*	Identity	Functional category **	Fold change (mutant strain compared to wildtype)
⇓ 05	Hypothetical protein **Rv3369**	10	2.1
⇓ 16	Possible haloalkane dehalogenase **Rv1833c**	7	2.1
⇓ 10	Hypothetical protein **Rv1558**	10	2.1
⇓ 22	Ribose-phosphate pyrophosphokinase (prsA, **Rv1017c**)	7	2.1
⇓ 06a	Hypothetical protein **Rv0481c**	16	2.0
⇓ 14	Possible ketoacyl reductase **Rv1544**	1	2.0

* Spot numbers are according to discovery order of spots of different intensity. "⇓" means lower spot intensity.
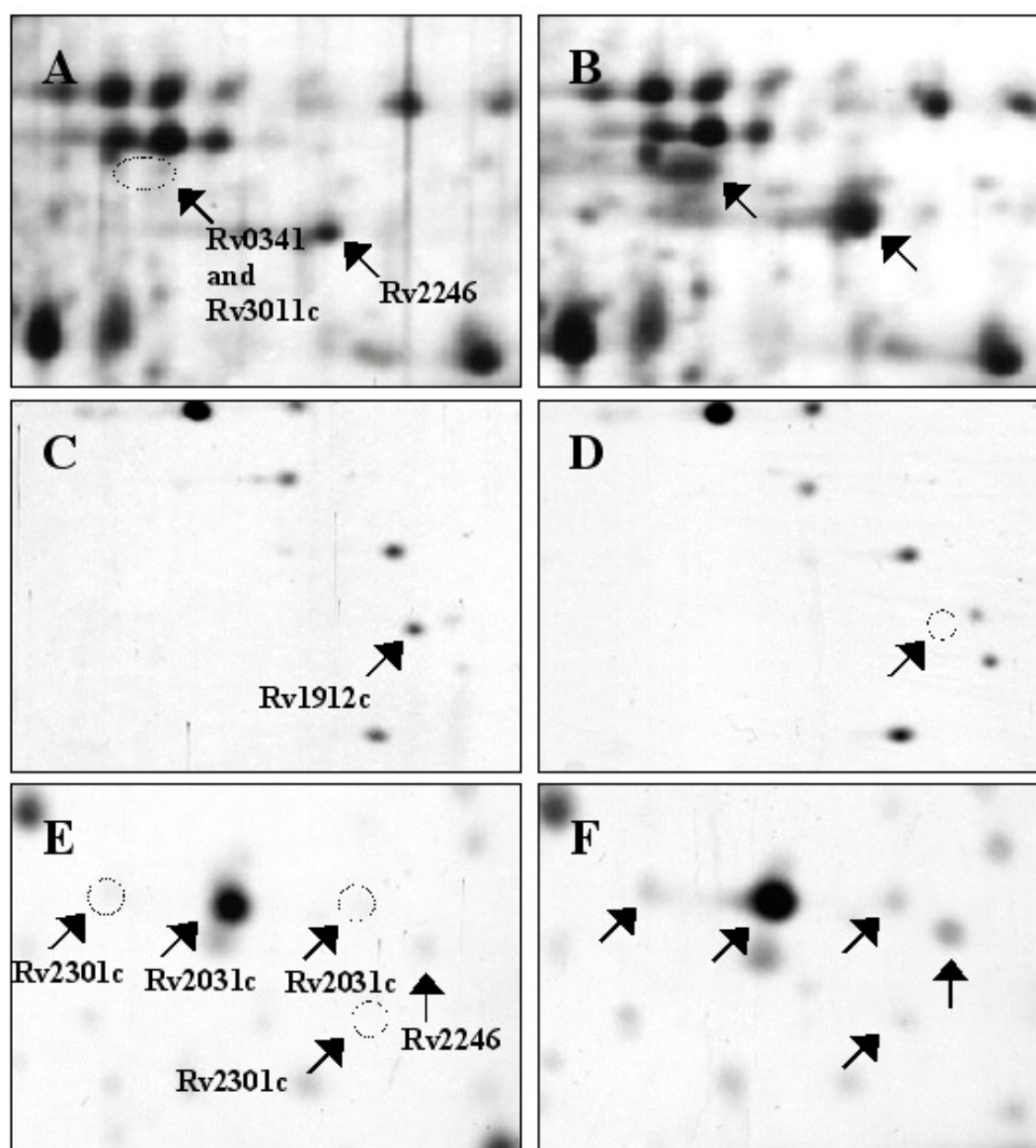**see Table 4: tuberculist classification of functional categories

Fig. 19 Examples of protein spots with differential relative intensity in 2-DE patterns of whole cell lysate proteins of the *upk* mutant strain (B, D, F) and the *M. tuberculosis* H37Rv control (A, C, E). The same protein can give rise to multiple spots as in the case of Rv2031c/HspX (picture E).

Table 3a: *M. tuberculosis* H37Rv Δ*upk* genes of higher transcription rate compared to wildtype

rv-number	Synonyms	Description	Functional category *
rv2243	*mtFabD*	malonyl CoA-Acyl carrier protein transacylase FabD (malonyl CoA:AcpM acyltransferase)	1
rv0873	*fadE10*	probable acyl-CoA dehydrogenase FadE10	1
rv3136	*PPE*	PPE family protein	6
rv3407		conserved hypothetical protein	10
rv2247	*accD6*	acetyl/propionyl-CoA carboxylase (beta subunit) AccD6	1
rv1871		conserved hypothetical protein	10
rv0702	*rplD*	probable 50s ribosomal protein L4 RplD	2
rv1103c		conserved hypothetical protein	10
rv2879c		conserved hypothetical protein	10
rv0874c		conserved hypothetical protein	10
rv3801c	*fadD32*	probable fatty-acid-CoA ligase FadD32 (fatty-acid-CoA synthetase) (fatty-acid-CoA synthase)	1
rv2245	*kasA*	3-oxoacyl-[acyl-carrier-protein] synthase 1 KasA (beta-ketoacyl-ACP synthase) (KAS I)	1
rv1094	*desA1*	probable acyl-[acyl-carrier-protein] desaturase DesA1 (acyl-[ACP] desaturase) (stearoyl-ACP desaturase) (protein Des)	1
rv1736c	*narX*	probable nitrate reductase NarX	7
rv0685	*tuf*	probable iron-regulated elongation factor Tu Tuf (Ef-Tu)	2
rv0313		conserved hypothetical protein	10

rv-number	Synonyms	Description	Functional category *
rv3548c		probable short-chain type dehydrogenase / reductase	7
rv3583c		possible transcription factor	9
rv1174c	*TB8.4*	low molecular weight T-cell antigen TB8.4	3
rv1821	*secA2*	possible preprotein translocase ATPase SecA2	3

*see Table 4: tuberculist classification of functional categories

Table 3b: *M. tuberculosis* H37Rv Δ*upk* genes of lower transcription rate compared to wildtype

rv-number	Synonyms	Description	Functional category *
rv2909c		probable 30s ribosomal protein s16 Rpsp	2
rv2649		probable transposase for insertion sequence element Is6110	5
rv2648		probable transposase for insertion sequence element Is6110	5
rv2278		probable transposase	5
rv1669		hypothetical protein	16
rv1276c		conserved hypothetical protein	10
rv3281		conserved hypothetical protein	10
rv1663	*pks17*	Probable polyketide synthase Pks17	1
rv2168c		probable transposase	5
rv1066		conserved hypothetical protein	10
rv3280	*accD5*	probable propionyl-CoA carboxylase beta chain 5 AccD5 (Pccase) (propanoyl-CoA:carbon dioxide ligase) key enzyme in the catabolic pathway of odd-chain-fatty acids	1
rv2666		probable transposase for insertion sequence element IS1081 (fragment)	5
rv0894		possible transcriptional regulatory protein (possibly LuxR-family)	9
rv1275	*lprC*	possible lipoprotein LprC	3
rv3824c	*papA1*	probable conserved polyketide synthase associated protein PapA1, thought to be involved in lipid metabolism	1
rv2717c		conserved hypothetical protein	10

rv-number	Synonyms	Description	Functional category *
rv2013		possible transposase	5
rv1047		probable transposase	5
rv2011		conserved hypothetical protein	10
rv2528c	*mrr*	probable restriction system protein Mrr	2

*see Table 4: tuberculist classification of functional categories

Table 4: functional categories

Tuberculist classification of functional categories	
# 0	virulence, detoxification, adaptation
# 1	lipid metabolism
# 2	information pathways
# 3	cell wall and cell processes
# 4	stable RNAs
# 5	insertion seqs and phages
# 6	PE/PPE
# 7	intermediary metabolism and respiration
# 8	unknown
# 9	regulatory proteins
# 10	conserved hypotheticals
# 16	conserved hypotheticals with an orthologue in *M. bovis*

Thirty percent of the genes with a higher transcription rate in *M. tuberculosis* ∆upk

mutant compared to *M. tuberculosis* wildtype encode for proteins involved in lipid

metabolism, additional 10 % were cell wall and cell-process related genes. Taken

together, 40 % of the most significantly up-regulated genes were involved in the cell

envelope complex. This corresponds to the observation that within the group of

higher intensity protein spots, 37 % belong to the cell envelope complex.

Twenty percent of the genes with a lower transcription rate in *M. tuberculosis Δupk*
encode for proteins which are related to the cell envelope complex. Again, this
corresponds to 21 % of the protein spots with lower intensity which are related to cell
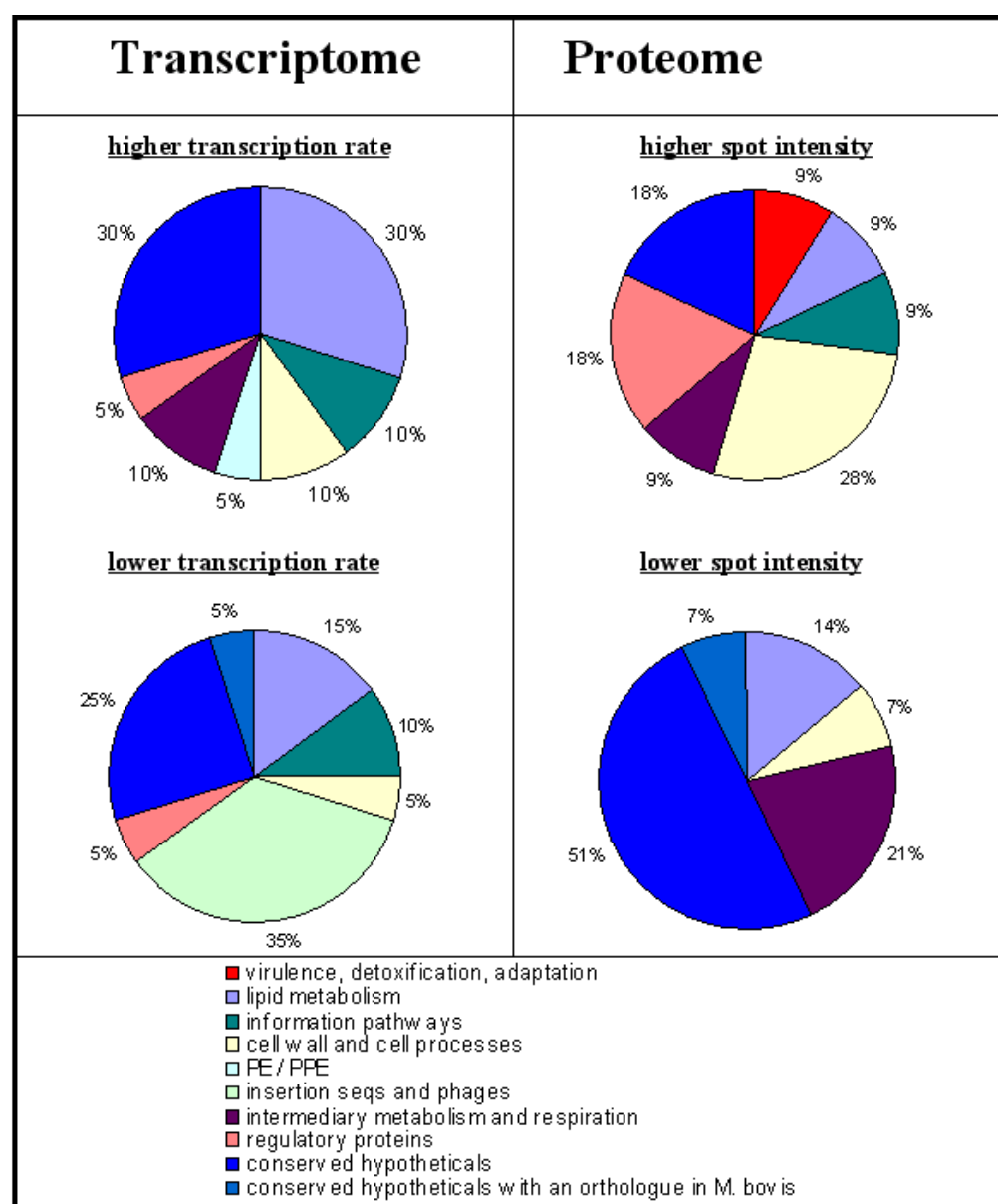envelope complex.

    Fig. 20 Percentage distribution of gene expression profiles and differential protein spot intensities
according to tuberculist classification of functional categories. Lipid metabolism was the most
prominent fraction within the group of up-regulated genes for the Δupk mutant (A) and insertion
sequences and phages protrude as a cluster of genes to be turned off (B).

Global analysis pointed to especially one significantly upregulated gene cluster of transcriptome analysis: *fabD* (*rv2243*), *kasA* (*rv2245*), and *accD6* (*rv2247*), and additionally from proteome analysis: KasB (Rv2246). This represents 4 members of a 5 gene operon (Fig. 21), consisting of FAS-II system encoding enzymes involved in biosynthetic pathway for long-chain fatty acids and precursors of mycolic acids which are part of MAPc. The higher transcription rate of a FAS-II system related operon in the case of the Δ*upk* deletion mutant may reflect a mechanism to overcome the *upk* deficiency. The *rv2244* gene and its geneproduct were inconspicuous concerning transcriptome and proteome analysis.
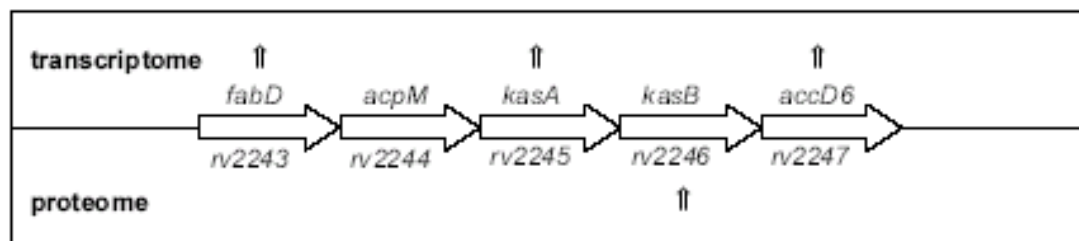

Fig. 21 Genomic organization of the Fas-II system related operon encoding enzymes involved in biosynthetic pathway for long-chain fatty acids. Genes / proteins with higher transcription rate / amount of protein in the *upk* deletion mutant are highlighted by arrows

3.2.5 Evaluation of sensitivity to antibiotics

The alamar blue assay was used to determine sensitivity to antibiotics in the same way as described for *M. smegmatis*. Since there was no access to an Elisa-reader under biosafety level 3 (BSL3) conditions, completed assays were documented with a digital camera and visual color change was the value of bacterial growth. Alamar blue turns from blue to red upon reduction, indicating growth. Based on observations with *M. smegmatis*, the Δ*upk* mutant was expected to be more sensitive to bacitracin. In contrast, no difference between *M. tuberculosis* H37Rv wildtype and Δ*upk* mutant was detectable. The reconstituted strain was slightly more susceptible to bacitracin at minute concentration differences of the antibiotic. *M. tuberculosis* H37Rv and *M. tuberculosis* Δ*upk* were resistant to bacitracin up to a concentration of 20 units / ml (Fig. 20A).

KasA and KasB which are over-expressed in the *M. tuberculosis* Δ*upk* mutant, had been proposed to contribute to Isoniazid-resistance [66,67]. Sensitivity of the Δ*upk* mutant to this antibiotic was therefore determined. All three examined *M. tuberculosis* strains were able to grow at concentrations of up to 20 μg Isoniazid / ml (Fig. 22) except for *M. tuberculosis* Δ*upk* mutant which was slightly more susceptible, rather contradicting profound contribution of KasA to Isoniazid resistance.
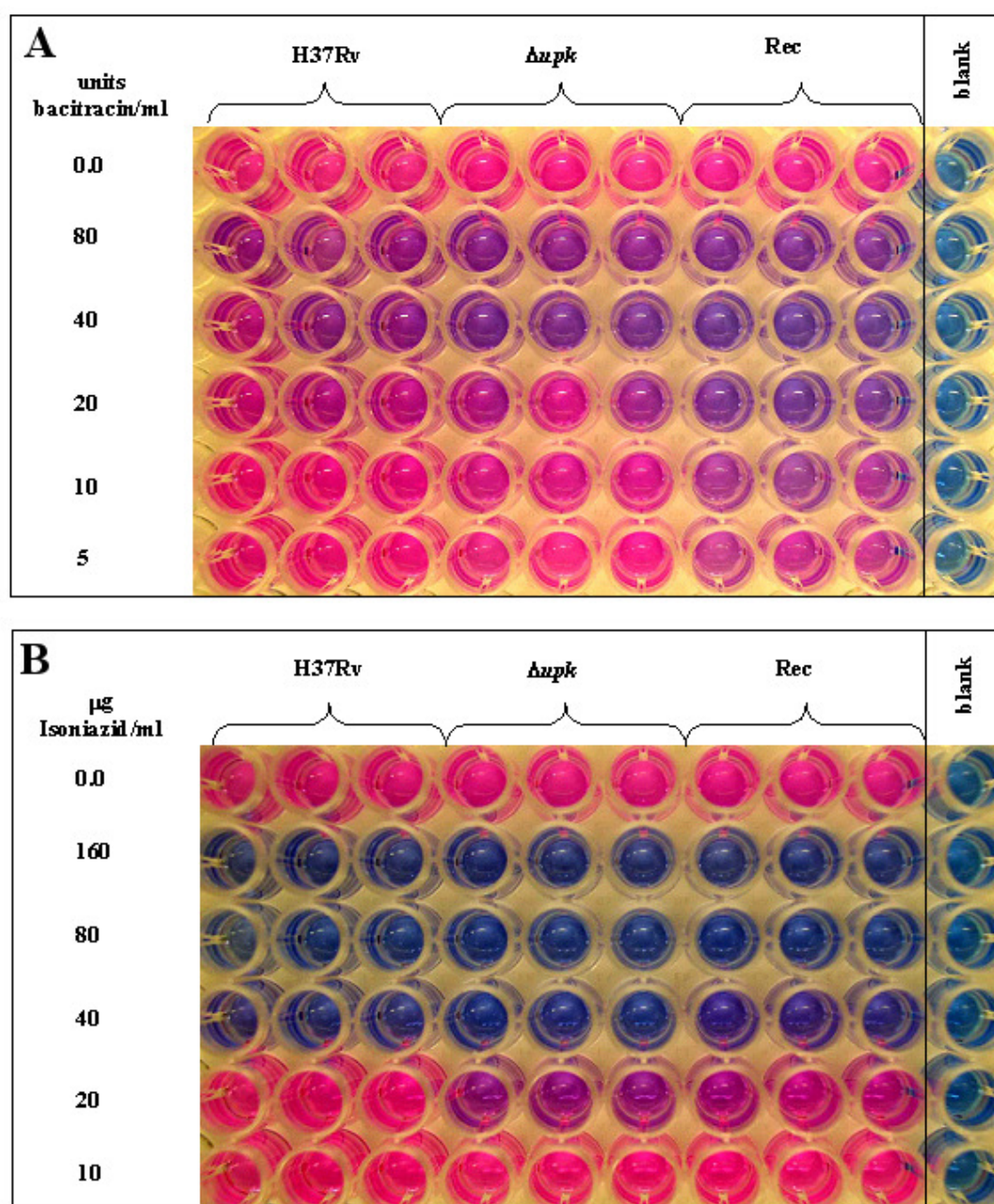
Fig. 22 Alamar blue assay. *M. tuberculosis* H37Rv wildtype (H37Rv), Δ*upk* mutant (Δ*upk*), and the reconstituted mutant (Rec) were tested for sensitivity against bacitracin (A) and Isoniazid (B). Red color indicates growth / resistance, blue indicates no growth / sensitivity. The Figure shows representative experiments of 4 with similar results.

3.2.6 Infection studies

To determine whether the *upk* deletion influenced growth of the mutant *in vivo*, C57BL/6 mice were infected intranasally with $1x10^3$ cfu. Five mice per group, infected with *M. tuberculosis* H37Rv, *M. tuberculosis* Δ*upk*, and *M. tuberculosis* Δ*upk* + pMV262-*upk*, were sacrificed at day 1 to precisely determine the concentration of the inoculum. At day 30, 60, and 90, bacterial load in lung and spleen were determined (Fig. 23). *M. tuberculosis* H37Rv showed a characteristic growth curve with a plateau in the lung at $1x10^7$ cfu. In contrast, cfu of the Δ*upk* mutant increased less than a log per lung during the first 30 days and remained at a level of about $1.4 x 10^4$ cfu / lung until day 90. The reconstituted strain reached an almost constant bacterial load of $1.8 x 10^3$ cfu / lung at day 90. Nevertheless, all 3 strains were able to disseminate and were detected in spleen and liver (data not shown). While the burden of wildtype bacteria in spleen rose up to $1 x 10^5$ cfu / organ by day 60, the burden of the *upk* mutant did exceed $4.1 x 10^3$ cfu / spleen at day 30 and decreased afterwards. The phenotype of the reconstituted strain was unexpected and exhibited a slightly lower bacterial load than the *M. tuberculosis* Δ*upk* strain in lung and spleen.
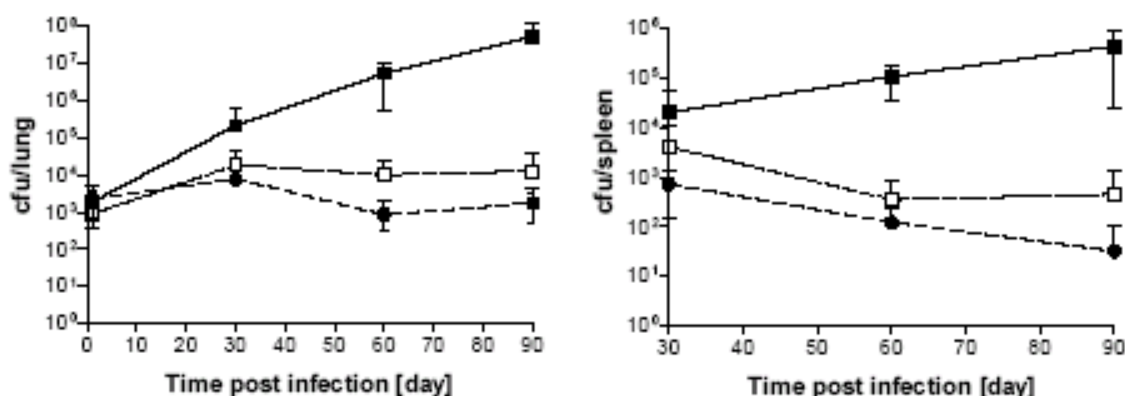

Fig. 23 Growth of *M. tuberculosis* wildtype, the *upk* deficient, and the reconstituted strain in lung and spleen. C57BL/6 mice were infected with $1x10^3$ cfu. Filled squares represent cfu of wildtype *M. tuberculosis,* open squares *M. tuberculosis* Δ*upk* deletion mutant, and filled reconstitution strain. The Figure shows 1 representative experiment of 2 with similar results.

According to Mann Whitney test, bacterial numbers of *M. tuberculosis* wildtype and *M. tuberculosis* Δ*upk* mutant were significantly different at day 60 and 90 in lung and spleen (P<0.0001).

3.2.7 Histology

Organs of infected animals, were removed for histological examinations. At day 90 post infection, lungs of *M. tuberculosis* wildtype and *M. tuberculosis Δupk* mutant infected mice revealed striking differences. Typically, animals infected with *M. tuberculosis* H37Rv showed severe pathology in the lung (Fig. 24). Granulomas were formed and a major part of the lung consisted of affected tissue. In the case of *upk* deficient *M. tuberculosis* (Fig. 25), granuloma and affected tissue were found but, in contrast to infection with *M. tuberculosis* wildtype, the majority of the lung appeared unaffected. The same observation was made for the reconstituted strain which failed to mimic the characteristics of the wildtype strain (Fig. 26).

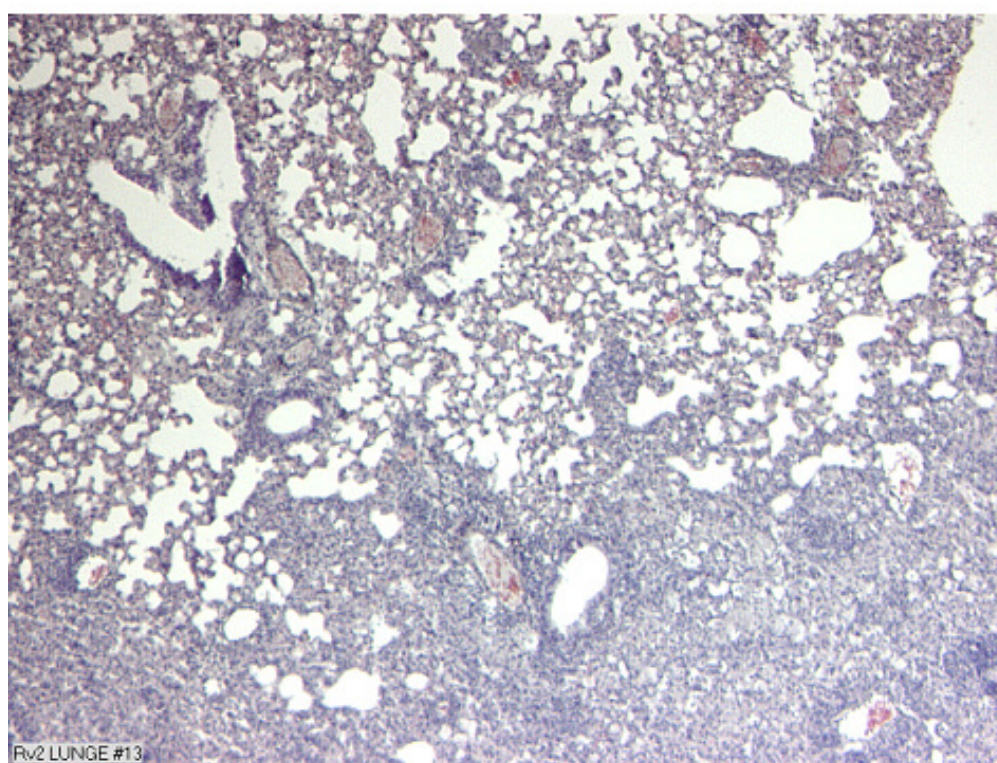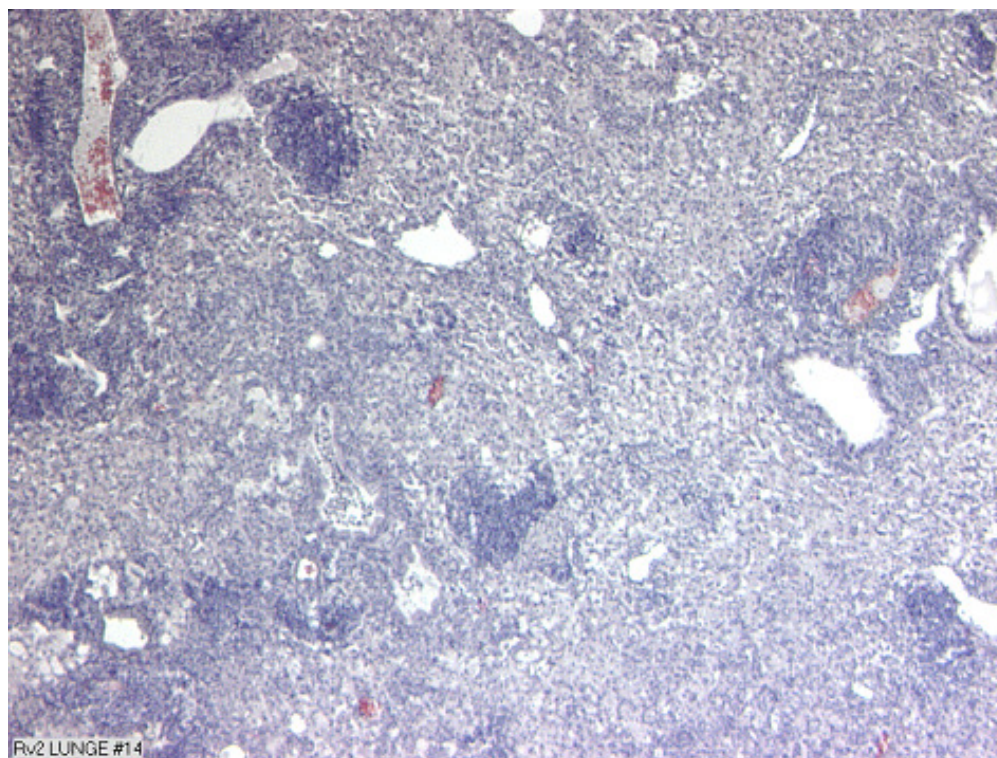Lung, 90 days post infection with *M. tuberculosis* H37Rv:

Fig. 24 Lungs of mice infected with *M. tuberculosis* H37Rv exhibited severe pathology 90 days post infection. Major part of the lung consisted of granulomatous, heavily infiltrated tissue. Only small regions with unaffected alveoli were found.

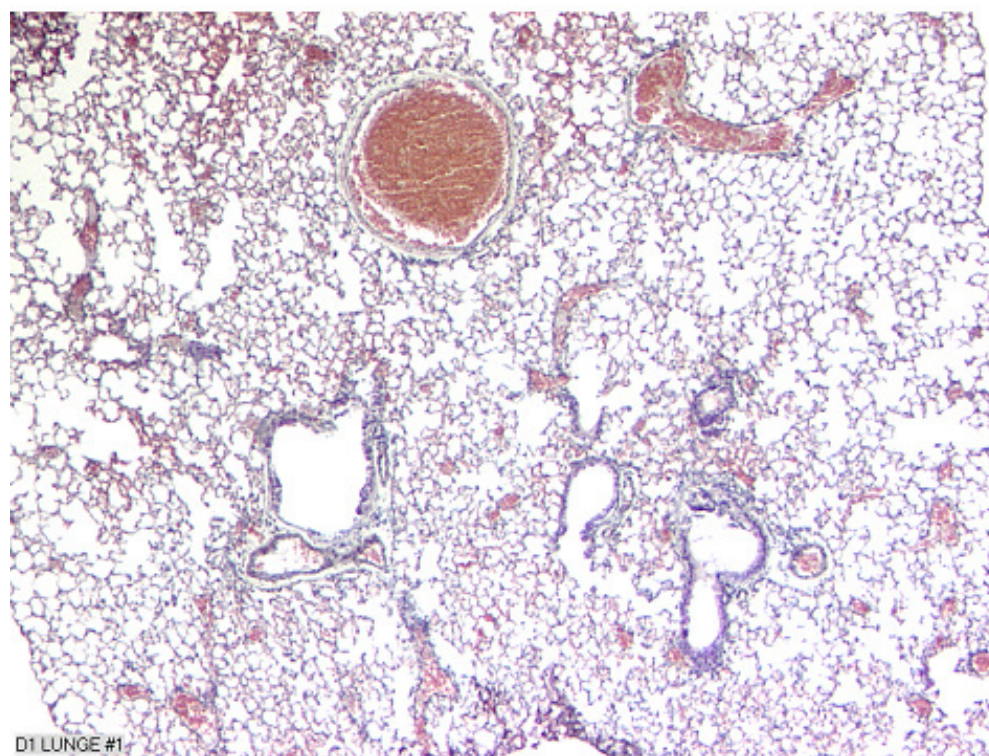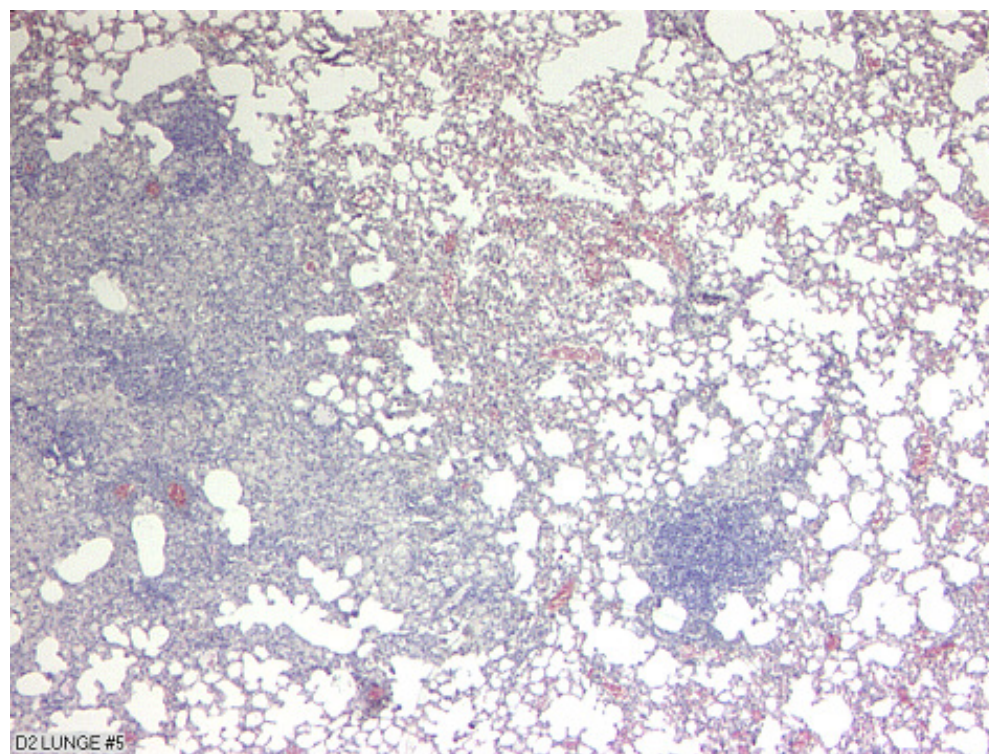Lung, 90 days post infection with *M. tuberculosis* H37Rv Δ*upk*:

Fig. 25 Lungs of mice infected with *M. tuberculosis* H37Rv Δ*upk* exhibited reduced pathology compared to *M. tuberculosis* wildtype 90 days post infection. Major part of the lung appeared non-infiltrated. Only small parts with granuloma could be detected.

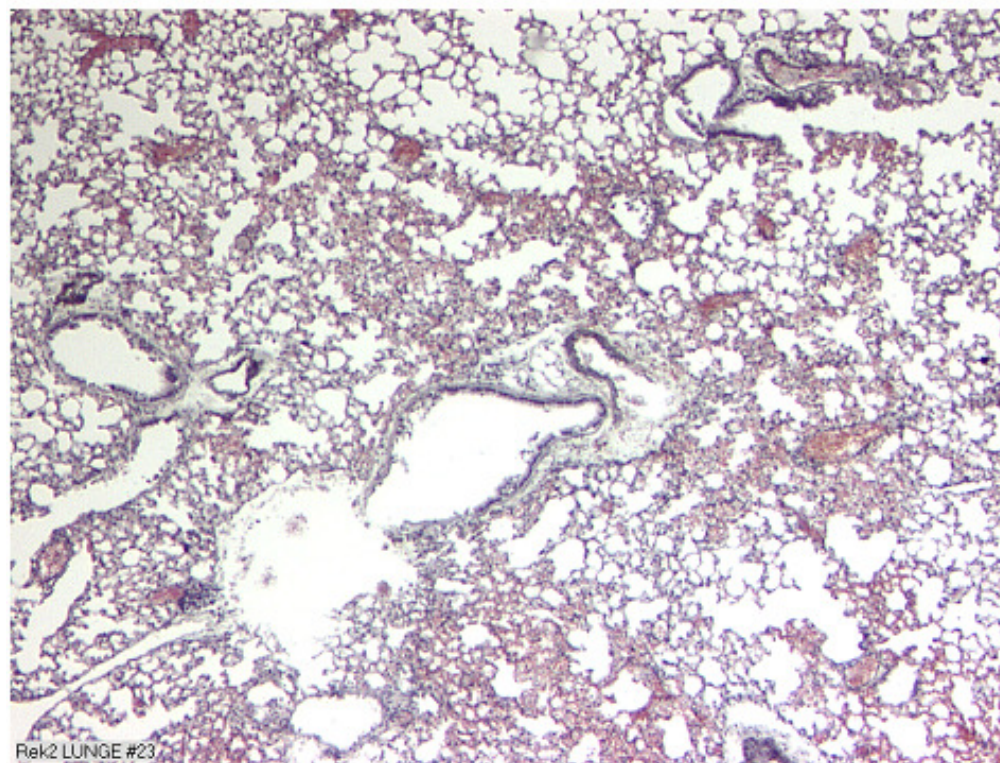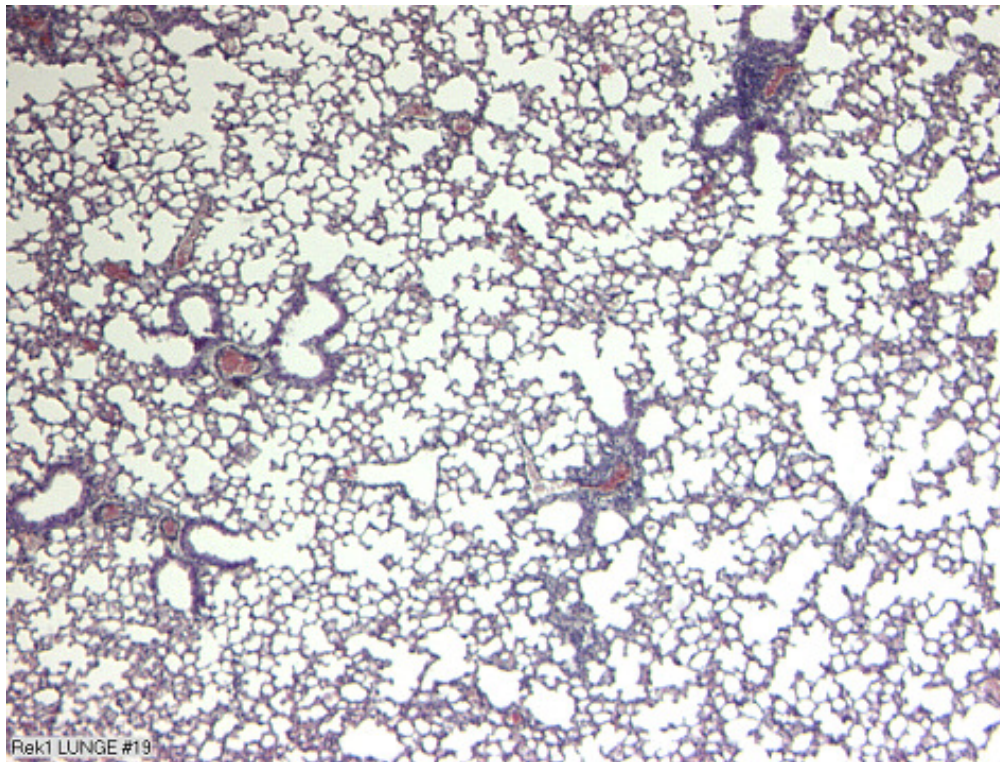Lung, 90 days post infection with *M. tuberculosis* H37Rv Δ*upk* + pMV262-*rv2136c*:

Fig. 26 Lungs of mice infected with the reconstitution strain of *M. tuberculosis* H37Rv Δ*upk* exhibited – like *M. tuberculosis* Δ*upk* - reduced pathology compared to *M. tuberculosis* wildtype 90 days post infection. Major part of the lung appeared non-infiltrated. Only small parts with granuloma could be detected.

3.2.8 Survival

Knowledge about virulence of a pathogen can be acquired by infection of immunocompromised mice which fail to control disease beyond a certain threshold. Commonly used immunocompromised animal models are i) highly susceptible Rag1^{-/-} mice which lack T and B cells and hence, fail to mount an adaptive immune response [68] and ii) IFNγ^{-/-} mice which are deficient in generating the central mediator of protection against tuberculosis. In this study, Rag1^{-/-} mice were infected with 1×10^6 cfu mycobacteria. *M. tuberculosis* wildtype infected mice survived 26 days in the median (range: d23 - d49). Mice infected with *M. tuberculosis* Δ*upk* survived 70 days in the median (range: d67 - d77) . Survival times of wildtype and mutant infected animals were significantly different according to logrank test (P<0.0001). The reconstituted strain killed mice after day 42 and about 50 % of the mice survived longer than those infected with the Δ*upk* strain (Fig. 27A).

Similar to Rag1^{-/-} mice, IFNγ^{-/-} animals were less susceptible to the Δ*upk* mutant strain than to *M. tuberculosis* H37Rv wildtype. The median survival time of wildtype infected animals was 30 days (range: d26 – d32), and for *M. tuberculosis* Δ*upk* mutant infected animals, 80 days (range: d63 – d126). Survival times of wildtype and mutant infected animals were significantly different according to logrank test (P<0.0001). Unexpectedly, the reconstituted strain was more attenuated than the mutant (Fig. 27B).

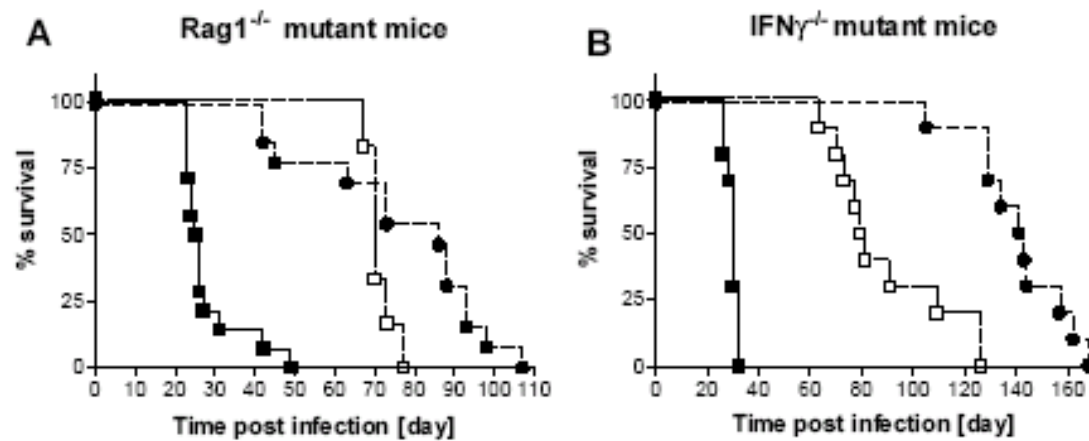Fig. 27 Survival of immunocompromised mice. Rag1^{-/-} (A) and IFNγ deficient animals (B) were infected with *M. tuberculosis* H37Rv(■), *upk* deficient *M. tuberculosis* (□), and the reconstituted strain (●), respectively. The experiments were performed with 10 mice per group. Survival of Rag1^{-/-} deficient animals was determined once. Figure B shows 1 representative experiment of 2 with similar results.

3.2.9   Summary *M. tuberculosis* **H37Rv** Δ*upk*

A *upk* deletion mutant (*M. tuberculosis* Δ*upk*) was generated on a *M. tuberculosis* H37Rv background. *In vitro* growth properties of the mutant in shaking culture in 7H9 complete medium, cording, and neutral red to staining of this strain were unaffected. In addition, standing cultures in Sauton medium exhibited impaired pellicle formation. Global analysis of proteome and transcriptome revealed a high number of genes associated with lipid metabolism upregulated in the mutant, especially an operon of the mycobacterial FAS-II system. Increased sensitivity to bacitracin, however, was not detected. The *upk* deficient *M. tuberculosis* strain exhibited markedly reduced growth and pathology *in vivo* as well as reduced virulence in Rag1$^{-/-}$ and IFNγ$^{-/-}$ KO mice infections.

3.3 *M. bovis* BCG Δ*upk*

3.3.1 Infection studies

Balb/c mice were infected with 5 x 10^5 cfu of the *M. bovis* BCG Δ*upk* strain and the *M. bovis* BCG wildtype strain i.v. and bacterial numbers were determined at days 15, 30, 60, and 90 post infection in lung and liver (Fig. 28). In the median, the bacterial burden in the lung of *M. bovis* BCG wildtype infected mice was about 2.17 times higher compared to mice infected with the *upk* deletion mutant, and 8.2 times higher in the liver. The small difference in bacterial load remained almost constant over the observed period of 90 days but was not significant according to "Mann Whitney" test (lung P = 0.5; liver P = 0.2).
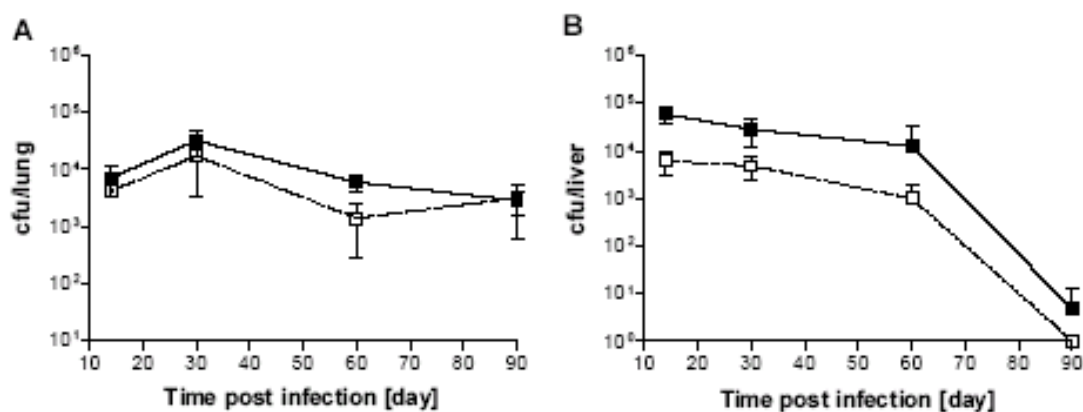

Fig. 28 Growth of wildtype and *upk*-deficient *M. bovis* BCG in lung and liver of Balb/C mice infected with 5 x 10^5 CFU. Filled squares represent cfu of wildtype *M. bovis* BCG, and open squares represent cfu of the *M. bovis* BCG *upk* deletion mutant. At each time-point 5 mice per group were sacrificed.

3.3.2 IFNγ production of stimulated spleen cells

IFNγ production by spleen cells of infected and of non infected mice was addressed by ELISA-assay (Fig. 29). Cells of whole spleens were either stimulated or left unstimulated with *M. tuberculosis* protein extracts. Spleen cells derived from naive mice failed to produce IFNγ, whilst cells of *M. bovis* BCG wildtype infected mice produced high levels of IFNγ at day 60 and day 90 post infection. Delayed IFNγ production of a comparably high level was measured at day 90 post infection in the case of spleen cells derived from mice infected with the BCG Δ*upk* deletion mutant.

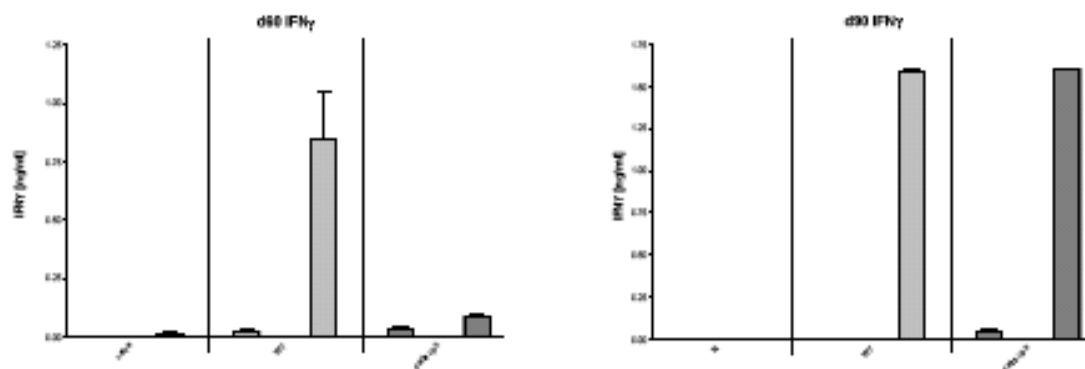Fig. 29 Measurement of IFNγ production by ELISA. Spleen cells of *M. bovis* BCG inoculated mice produced high levels of IFNγ upon stimulation at day 60 and 90 post infection. Within each group, left column displays unstimulated, right column displays stimulated samples. Spleen cells of mice vaccinated with *upk* deficient *M. bovis* BCG strain produced a delayed but also high response at day 90 post infection.

3.3.3 Vaccine trial

A major goal of studies with recombinant *M. bovis* BCG would be their utilization as improved vaccines. To exploit this possibility we compared vaccine efficacy of *M. bovis* BCG Δ*upk* to the existing vaccine M. bovis BCG. Balb/c mice were vaccinated i.v. with 5 x 105 cfu. After 120 days these animals and an unvaccinated control group were challenged with about 200 cfu *M. tuberculosis* H37Rv delivered as aerosol. At distinct time-points thereafter, bacterial loads in lung and spleen were determined (Fig. 30). *M. tuberculosis* cfu differences in the spleen were very small between the groups 30, 60, and 120 days post infection. The *M. tuberculosis* burden in the lung of both groups of vaccinated animals was about the same and 60 fold lower compared to unvaccinated animals at day 30 post infection. However, by day 120 post infection, the BCG Δupk mutant strain was able to induce a significantly superior protection (Δlog = 2.7 in relation to naive mice) compared to wildtype *M. bovis* BCG (Δlog = 0.9) in the lung.
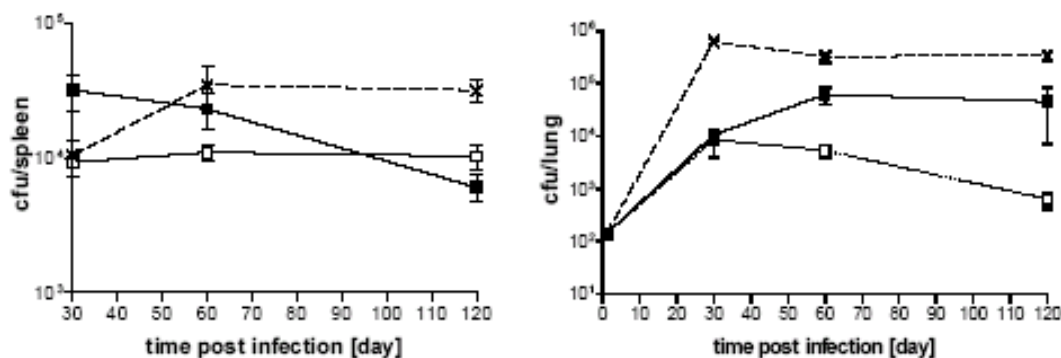
Fig. 30 Bacterial burden of Balb/c mice challenged with *M. tuberculosis* H37Rv via aerosol. Filled squares represent *M. tuberculosis* cfu of wildtype *M. bovis* BCG vaccinated animals, open squares represent *M. tuberculosis* cfu of the *M. bovis* BCG Δ*upk* vaccinated animals, crosses represent *M. tuberculosis* cfu of unvaccinated animals.

According to Mann Whitney test, bacterial numbers of *M. bovis* BCG and the *M. bovis* BCG Δ*upk* mutant were significantly different at day 60 and 120 in the lung (P<0.0001).

3.3.4 Summary *M. bovis* BCG Δ*upk*

Mice infected with the *M. bovis* BCG Δ*upk* strain exhibited lower bacterial load in lung and liver compared to mice infected with wildtype BCG. As a consequence, a delayed IFNγ response was observed. Protection against *M. tuberculosis* challenge induced by the BCG Δ*upk* mutant strain was highly improved in the lung of vaccinated animals at day 120 post infection compared to animals vaccinated with *M. bovis* BCG wildtype.

4 Discussion

BacA is responsible for phosphorylation of undecaprenyl in *E. coli* and other bacteria. This is an important step in peptidoglycan synthesis. Studies on homologues of *E. coli bacA* in *S. aureus* and *S. pneumoniae* revealed that gene deletion mutants were attenuated in mouse models of infection [39]. We identified homologues in the genomes of *M. smegmatis* and *M. tuberculosis* (Upk; Fig. 1), and investigated the role of the cognate Upk in mycobacteriae, *in vitro* and *in vivo*. In addition, downstream consequences of the gene deletion in *M. tuberculosis* were investigated globally on the transcriptome and proteome level.

4.1 Impact of *upk* deletion on cell wall attributes

S. aureus and *S. pneumoniae* Δ*bacA* mutants show no significant alterations in growth rate or morphology [39]. In contrast, the in-frame, unmarked deletion of *upk* (Fig. 3), in *M. smegmatis* revealed a distinct phenotype (Fig. 4). While the growth rate was almost unaltered, *M. smegmatis* Δ*upk* colonies did not display dome-like structures, like that of the wildtype strain. Rather, they showed caved-in structures indicating autolysis of the cells. Upk deletion must be responsible for the altered colony morphology since complementation resulted in a return to dome-like colonies. A comparable phenomenon did not appear for *M. tuberculosis* or *M. bovis* BCG. This suggests that Upk may play different roles, or at least have different physiological functions, in different mycobacteria.

An altered cell wall might exhibit visible changes when examined by electron microscopy, however, the *M. smegmatis* Δ*upk* cell wall appeared comparable to wildtype by electron microscopic examination (Fig. 8). More direct analyses of the cell

wall by immuno-gold staining revealed less, though still detectable, peptidoglycan in the mutant. Deletion of the *upk* gene, therefore, did not lead to complete loss of peptidoglycan in the cell wall. Although the effect observed was small, alternative, yet less efficient pathways for undecaprenyl-phosphorylation or transport of peptidoglycan precursors may exist, as indicated by the slightly slower growth of *M. smegmatis* Δ*upk* mutant *in vitro* (Fig. 9).

As described for *E. coli, S. aureus*, and *S. pneumoniae*, undecaprenyl phosphokinase deletion mutants exhibit higher sensitivity to bacitracin [38,39]. A knockout mutant strain of the mycobacterial homologue *upk* was expected to show the same susceptibility. This was verified unequivocally by the alamar blue assay for *M. smegmatis* (Fig. 10). Complementation with the *M. tuberculosis upk* homologue *rv2136c* partially reversed the susceptibility of *M. smegmatis*. Incomplete complementation may be due to constitutive gene expression of *upk* driven by the *groEL2* (Hsp60) promoter, which does not reflect the physiological regulation of the gene. Surprisingly, the *M. tuberculosis* mutant strain was the first described bacterial *upk* deletion mutant that did not exhibit altered sensitivity to bacitracin. This finding demonstrates the uniqueness of the *M. tuberculosis* cell envelope not only to other bacteria but also to fast growing non-pathogenic species of mycobacteria [24,69], and emphasizes that even highly conserved proteins can have a range of activities in different species. *M. tuberculosis* may possess an efficient alternative pathway to shuttle out peptidoglycan precursors or may preserve the integrity of its cell wall by overproduction of other components. However, growth properties of *M. tuberculosis* Δ*upk* in pellicle cultures were affected (Fig. 18) and this is likely due to altered surface features.

The reconstituted strains in this study were constructed on the knockout background by electroporation with the episomal multi copy plasmid pMV262-*upk*. In all cases, the *M. tuberculosis* H37Rv *upk* gene was under the control of the *M. bovis groEL2* (Hsp60) promoter. With regard to distinct properties, the reconstituted strain failed to display unilaterally a wildtype phenotype: *M. smegmatis* Δ*upk* + pMV262-*upk* grew in dome-like colonies and persisted in macrophages similar to wildtype *M. smegmatis*, whereas resistance to bacitracin was intermediate between wildtype and Δ*upk* mutant.

M. tuberculosis mouse infections never displayed a wildtype-like phenotype for *M. tuberculosis* Δ*upk* + pMV262-*upk*. This phenomenon is likely due to weak transcriptional activity. For various genes the *groEL2* promoter can provide the cell with more transcripts than the natural promoter, but for late log phase *in vitro* the *groEL2* promoter transcribed about 200 fold weaker than the *M. tuberculosis* wildtype promoter. This severe regulation problem provides the most likely explanation for the failure of the complementation strain to achieve a wildtype phenotype in infection. In the case of *M. tuberculosis* pellicle formation, an intermediate phenotype of the complementation strain compared to wildtype and Δ*upk* mutant was also observed.

4.2 Physiological balance

Upk is thought to be critical for mycobacterial cell envelope formation and it was, therefore, expected that the Δ*upk* mutant would attempt to compensate in some way. Global screening by proteome and transcriptome analysis was performed to identify putative compensatory mechanisms. One obvious response of the *M. tuberculosis* Δ*upk* mutant was the upregulation of a FASII-system related operon (*rv2243* –

rv2247; Fig. 21). The involvement of KasA / Rv2245, one gene product of this operon, in Isoniazid resistance, has been thoroughly investigated. A report by Mdluli et al. on Isoniazid-resistant patient isolates, which lacked other mutations associated with resistance to the drug, showed amino acid altering mutations in the KasA protein [70]. Additional studies further supported a role of KasA and KasB in Isoniazid resistance [67]. In contrast, other studies [71,72] reported that 3 of the 4 clinical isolates bearing mutated *kasA*-alleles were fully susceptible to Isoniazid. To date, gene transfer experiments determining whether any of these mutations confers Isoniazid resistance to susceptible strains of mycobacteria have not been performed. We show that the Δ*upk* deletion mutant of *M. tuberculosis* H37Rv, which overexpressed *kasA*, did not exhibit increased resistance to Isoniazid in the alamar blue assay (Fig. 22B), but rather had a slightly higher susceptebility. This finding supports a recent study which favors a gene distinct from *kasA*, namely *inhA*, as the major primary target for Isoniazid [66].

Mycobacterial FAS-II, unlike other bacterial type II FAS cognates, is incapable of *de-novo* fatty acid biosynthesis [73], however it appears able to elongate C_{14}-AcpM of mycobacteria and C_{16}-AcpM to preferentially long chain fatty acids ranging from 24 to 56 carbon atoms. Recent studies suggest that KasA (Rv2245) is part of FAS-II and participates in mycolic acid biosynthesis [74,75]. Mycolic acids are high molecular weight α-alkyl, β-hydroxy fatty acids with the general structure R-CH(OH)-CH(R')-COOH, where R is a meromycolate chain consisting of 50 – 56 carbons and R' is a shorter aliphatic branch possessing 22 – 26 carbons [24]. Mycolic acids are key components of the mycobacterial cell wall (Fig. 2) and play a role in producing an effective lipophilic barrier. Considering the importance of mycolic acids in bacterial survival and maintenance of cell wall integrity, the Δ*upk* deletion mutant may benefit

from overproduction of this cell wall component in order to overcome reduced peptidoglycan. In addition, increased mycolic acids may improve the blocking of phagosome-lysosome fusion and better allow the bacteria to escape degradation by the host. This strategy prevents exposure of the bacterium to the hostile environment of the lysosome while rendering it accesible to nutrients endocytosed by the cell. The underlying mechanism is not yet fully understood [76,77]. This function has been proposed and demonstrated for other cell envelope components, such as trehalose 6,6'-Dimycolate (TDM), a mycobacterial glycolipid cord factor. TDM has also been implicated in interfering with phagosome-lysosome fusion [78].

Infection of macrophages with *M. smegmatis* can be used as a model to analyze bacterial persistence in the host [30]. Lower persistence of the *M. smegmatis* Δ*upk* mutant in macrophages indicates a role of Upk in mycobacterial virulence/persistence. Indeed, the *M. smegmatis* Δ*upk* mutant was cleared more rapidly from the host cells. These findings indicate the importance of a robust cell envelope for persistence in the host. In this experiment complementation with the *M. tuberculosis upk* gene was sufficient to revert from mutant to wildtype phenotype. However, it is not valid to generalize knowledge gained from experiments with *M. smegmatis*. In certain aspects, *M. tuberculosis* is unique as was demonstrated in the case of resistance to bacitracin.

Biofilm formation

The term biofilm describes a population or community of bacteria living in organized structures at a liquid interface. Early confocal laser scanning microscopy (CLSM) of single species biofilms [79,80] revealed that biofilm bacteria live in cellular clusters or microcolonies that are encapsulated in a matrix composed of an extracellular polymeric substance (EPS), separated by open water channels which act as primitive circulatory system for the delivery of nutrients and removal of metabolic waste products. Within a biofilm, each bacterium occupies a specific microenvironment, which is defined by the surrounding cells, the proximity to a channel and the EPS matrix. The structuring of biofilms in microcolonies and fluid channels has been shown to be influenced by fluid flow, nutrient composition, and intracellular small messenger molecules, which are used for bacterial communication [81,82,83].

Various gram-negative and gram-positive bacteria, as well as fungi, grow in two forms: planktonic and, as a step of microbial development, in a biofilm [33]. *M. smegmatis* and other non-tuberculous mycobacteria such as *Mycobacterium fortuitum* and *Mycobacterium marinum* live and grow planktonicly or as a biofilm [34]. Biofilms support resistance to antimicrobial chemotherapy and play a role in contamination in clinical and industrial settings. Biofilm formation poses a major problem because they can increase drug resistance [36]. The reduced metabolic and growth rates shown by biofilm bacteria, particularly those deep within the biofilm, can render these microbes inherently less susceptible to antibiotics. The EPS matrix can act as an absorbent or reactant, thereby reducing the amount of drug available for action on biofilm cells. Moreover, biofilm bacteria are physiologically distinct from their planktonic cognates and express specific protective factors such as multidrug

efflux pumps and stress response regulons [84,85].

Biofilm growth of *M. smegmatis* was unaffected at Isoniazid concentrations that inhibited growth of planktonic bacilli [35]. Previously described deletion mutants of *M. smegmatis* lacking the capability of glycopeptidolipid acetylation, which affects the cell envelope, are defective in biofilm formation [60,86]. The in-frame, unmarked deletion mutant of the *M. smegmatis upk* gene is the first evidence for a role of Upk in biofilm formation. Upon adherence, the Δ*upk* mutant strain formed a scattered biofilm only. Adherence could have been reduced due to a missing extracellular matrix (Fig. 13) and to slightly inferior growth-properties in biofilm medium.

4.3 *In vivo*

The apathogenic environmental *M. smegmatis* owes its name from isolation from genital secretions (smegma): In November 1884, Lustgarten reported to the Royal Society of Medicine in Vienna that he had discovered a bacterium with staining characteristics of tubercle bacilli in syphilitic chancres and gummae [31]. Soon thereafter Alvarez and Tavel identified microorganisms similar to those in normal genital secretions (smegma) [32]. Smegma is associated with hygienic conditions and has been proposed as risk factor for penile cancer [87,88]. To determine whether Upk plays a role in genital smegma development by *M. smegmatis* we developed an *in vivo* model for *M. smegmatis* biofilm formation. In this *in vivo* mouse model of *M. smegmatis* biofilm formation the Δ*upk* deletion mutant was found to be deficient in induction of smegma development (Fig. 14), thus stressing the relevance of Upk in mycobacterial saprophytic life.

The giv phenotype

A direct consequence of the *upk* gene deletion in *M. tuberculosis* is the expression of a growth *in vivo* (*giv*) mutant phenotype. Studies on defined mutants of *M. tuberculosis* in the mouse model of infection have led to the classification of attenuated mutants in several phenotypic classes [89]. These mutants have been categorized by their growth characteristics, namely: i) severe growth *in vivo* (*sgiv*) mutants, which show a marked reduction in colony-forming units over time; ii) growth *in vivo* (*giv*) mutants, which grow less robustly than wildtype *M. tuberculosis* in the lungs of immunocompetent mice, yet still grow better than *sgiv* mutants; iii) persistence (*per*) mutants, which fail to grow or persist after the onset of acquired immunity, and iv) mutants with the same growth characteristics as *per* mutants, but show altered pathology (*pat*) compared with that of wildtype *M. tuberculosis*. Most mutants, including the Δ*upk* mutant, fall into the *giv* class, showing reduced growth (Fig. 23) and pathology (Fig. 25), resulting in an attenuated phenotype and increased survival of infected immunocompromised mice (Fig. 27). Examples for *giv* mutants of *M. tuberculosis* are the two component regulatory protein *phoP* [90], the accessory secretion factor *secA2* [91], the glutamine synthase *glnA1* [92], and *panCD* [93], which is involved in pantothenate synthesis. The gene encoding the exported repetitive protein (*erp*) in both *M. bovis* BCG and *M. tuberculosis* has no ascribed function and is specific for mycobacterial species [94]. Deletion of the *erp* gene results in impaired growth of bacilli in lungs and spleens of infected mice, as with the Δ*upk* mutant. Berthet et al. postulated that virulence depends on the ability of the bacilli to multiply [95]. The virulence reduced *M. tuberculosis* Δ*upk* mutant exhibited characteristics of a *giv* mutant, which could render it an interesting vaccine candidate, because it maintains replication and is more likely to result in a long-

lasting host immune response compared to a *sgiv* mutant. However, a potentially dangerous situation could arise if the mutant regains its rate of growth, as may happen in immunocompromised individuals (Fig. 27), resulting in disease. Thus, continued characterization of specific mutants of *M. tuberculosis* is required to develop strains which elicit a strong protective immune response, but fail to reactivate in immunodeficiet individuals.

The *giv* phenotype of the Δ*upk* mutant, which was related to reduced growth *in vivo*, is probably related to its altered cell envelope. Forty percent of the most significantly upregulated genes in the Δ*upk* mutant compared to wildtype were related to cell envelope processes and belonged to the tuberculist categories "lipid metabolism", and "cell wall and cell processes" (Fig. 20). Hence, impaired self protection of the tubercle bacilli, as consequence of the impaired cell wall, or improved accessibility of antigens, or upregulation of one or more antigens which resulted in better processing and recognition by T cells, and therefore a more potent immune response, could allow improved control by the host. Furthermore, the *M. tuberculosis* Δ*upk* mutant may switch prematurely to a dormancy program as may indicated by abundance of the HspX protein, a marker of *M. tuberculosis* latency [64,96].

In addition, host effector mechanisms may be more effective against the altered cell wall of *M. tuberculosis* Δ*upk* than against *M. tuberculosis* wildtype. Such mechanisms may include production of highly reactive low molecular weight molecules, in particular reactive oxygen intermediates (ROI) and reactive nitrogen intermediates (RNI) [97,98] (Fig. 1). ROI and RNI cause damage of cellular constituents by oxidation of cellular membranes and enzymes, DNA damage, mutagenesis, and inhibition of membrane transport processes [18,99,100].

The impaired cell wall structure of the *upk* deficient strain, could form a weaker barrier against these effector molecules with the possible consequence of enhanced killing of the pathogen by the host. A larger quantity of antigen that could be processed or a higher accessibility of antigens may further contribute to increased susceptibility *of M. tuberculosis* Δ*upk* to the adaptive immune response.

Vaccine

As discussed above, the *giv* mutant phenotype of *M. tuberculosis* Δ*upk* represents a promising phenotype for development of an attenuated *M. tuberculosis* mutant that could serve as a potential vaccine candidate. Nevertheless, a single gene deletion mutant in *M. tuberculosis* is unlikely to fulfill the safety standards required for a vaccine to be used in humans notably in immunocompromised individuals. Thus, a *giv* mutant like *M. tuberculosis* Δ*upk*, needs to be thoroughly characterized and subsequently refined in further steps of development before it could become a valid vaccine candidate.

The vaccine strain *M.* bovis BCG offers an impressive safety record but unsatisfactory protection [101]. In this study, we deleted the *upk* gene from *M. bovis* BCG. This is an alternative strategy that relies on the basic premise that *M. bovis* BCG could be re-engineered to enhance its efficacy. For example, recombinant *M. bovis* BCG expressing various cytokines have been shown to improve the response against *M. tuberculosis* antigens [102] and recombinant *M. bovis* BCG expressing listeriolysin of *Listeria monocytogenes* showed an enhanced capacity to stimulate CD8$^+$ T cells [103]. In addition, a recombinant *M. bovis* BCG strain that

overexpresses the 30 kDa Ag85 protein has been reported to provide an improved protection against *M. tuberculosis* infection [104].

The *upk* deletion which resulted in an even more attenuated strain, was not expected to cause safety problems and accordingly used in a vaccine trial. Considering the lower bacterial load of *M. bovis* BCG Δ*upk* upon vaccination (Fig. 28) and the delayed induction of the IFNγ response (Fig. 29) it was surprising that the modified vaccine strain was able to induce a significantly improved long-lasting protection *against M. tuberculosis* infection (Fig. 30). This phenotype is difficult to explain at present. Perhaps immunorelevant antigens were overexpressed to balance *upk* deficiency, or improved killing of *M. bovis* BCG Δ*upk* provides the immune system with a larger amount of antigens to be processed, resulting in an improved adaptive immune response.

4.4 Outlook

The mouse model of smegma was newly established and offers the opportunity for further development. The structure of smegmata can be investigated by microscopy and therefor allows the following questions to be addressed:

Is it possible to stain bacteria within the smegma?

Are the bacteria organized within the smegma?

As for biofilms, are channels existing for facilitated supply with nutrients?

Furthermore, the background growth which arose upon treatment, should be characterized to determine whether it contains other bacteria which induced genital secretions.

The reconstituted knockout strain of *M. tuberculosis* failed to exhibit the characteristics of a wildtype strain. Polar effects of the knockout construct may have disturbed transcription of downstream genes. It is also possible that the observed *M. tuberculosis Δupk* phenotype is due to disruption of the expression of an operon rather than a single gene. Transcription of putatively affected genes should be investigated by RT-PCR. And in the case of a disrupted operon, a reconstituted strain that complements all affected genes should be constructed.

It is still an unsolved problem why *M. tuberculosis Δupk* remains resistant to

bacitracin. Perhaps the antibiotic does not have access to its target in *M. tuberculosis*. Further tests to determine resistance/susceptibility to antibiotics other than bacitracin should be performed, as this may be an important question to consider for drug development against *M. tuberculosis*. Alternative functions of Upk should also be considered in regards to the mode of action of differentially active antibiotics.

The results derived from proteomic and transcriptomic analyses of *M. tuberculosis* Δ*upk* strongly suggest an altered cell wall composition. An obvious experiment to follow this would be to extract lipids and to compare the differences between wildtype and mutant *M. tuberculosis*.

The promising results of the vaccine trial with *M. bovis* BCG Δ*upk* advocate further development of the *M. tuberculosis* Δ*upk* mutant strain. A *M. tuberculosis* mutant might induce a better protection against *M. tuberculosis* wildtype infections because it would prime the immune system with the same antigens as the causative agent *M. tuberculosis*, including antigens that are missing in *M. bovis* BCG like the 129 antigens of the 16 regions of deletion which were lost when Calmette and Guérin generated the vaccine strain from *M. bovis*. Nevertheless, for safety reasons, a one gene deletion mutant of *M. tuberculosis* will never be considered as vaccine candidate. Another phase of development is needed to further attenuate the strain and keep its protective potential at the same time. Nevertheless, the promising results of the vaccine trial with *M. bovis* BCG Δ*upk* suggest this strain has potential for future development as a vaccine candidate. Survival experiments with immunocompromised animals would be necessary to demonstrate its safety. In order to further investigate whether optimal protection is due to persistence of the vaccine

strain, regulatory mechanisms of the immune system, or the timing/duration of IFNγ

response upon vaccination, additional modified vaccine trials need to be performed.

5

References

Literaturverzeichnis

[1] Falkinham, J. O., III (2002): Nontuberculous mycobacteria in the environment, Clin.Chest Med. 23 [3], Seite 529-551. URL: PM:12370991

[2] Rastogi, N.; Legrand, E. und Sola, C. (2001): The mycobacteria: an introduction to nomenclature and pathogenesis, Rev.Sci.Tech. 20 [1], Seite 21-54. URL: PM:11288513

[3] Koch, R. (1882):

[4] Ferlinz, R. (21995):

[5] Ehrlich, P (1882): Zur Färbung der Tuberkelbakterien, Deutsche Med Wochenschr 8, Seite 269-270.

[6] Ziehl, F (1882): Zur Färbung des Tuberkelbacillus, Deutsche Med Wochenschr 33, Seite 451.

[7] Neelsen, A (1883): Ein casuistischer Beitrag zu Lehre von der Tuberkulose, Centralblatt für die medizinischen Wissenschaften 28, Seite 497-501.

[8] Falkow, S. (1988): Molecular Koch's postulates applied to microbial pathogenicity, Rev.Infect.Dis. 10 Suppl 2, Seite S274-S276. URL: PM:3055197

[9] Bardarov, S.; Bardarov Jr S Jr; Pavelka, Jr MS, Jr.; Sambandamurthy, V.; Larsen, M.; Tufariello, J.; Chan, J.; Hatfull, G. und Jacobs, Jr WR, Jr. (2002): Specialized transduction: an efficient method for generating marked and unmarked targeted gene disruptions in *Mycobacterium tuberculosis*, *M. bovis* BCG and *M. smegmatis*, Microbiology 148 [Pt 10], Seite 3007-3017. URL: PM:12368434

[10] Bottiger, M.; Romanus, V.; de Verdier, C. und Boman, G. (1982): Osteitis and other complications caused by generalized BCG-itis. Experiences in Sweden, Acta Paediatr.Scand. 71 [3], Seite 471-478. URL: PM:6753476

[11] Fine, P. E. (1995): Variation in protection by BCG: implications of and for heterologous immunity, Lancet 346 [8986], Seite 1339-1345. URL: PM:7475776

[12] Kaufmann, S. H. und Hess, J. (1997): Rational design of antituberculosis vaccines: impact of antigen display and vaccine localization, Biologicals 25 [2], Seite 169-173. URL: PM:9236047

[13] Manabe, Y. C. und Bishai, W. R. (2000): Latent *Mycobacterium tuberculosis*-persistence, patience, and winning by waiting, Nat.Med. 6 [12], Seite 1327-1329. URL: PM:11100115

[14] Armstrong, J. A. und Hart, P. D. (1975): Phagosome-lysosome interactions in cultured macrophages infected with virulent tubercle bacilli. Reversal of the usual nonfusion pattern and observations on bacterial survival, J.Exp.Med. 142 [1], Seite 1-16. URL: PM:807671

[15] Russell, D. G.; Dant, J. und Sturgill-Koszycki, S. (1996): *Mycobacterium avium*-and *Mycobacterium tuberculosis*-containing vacuoles are dynamic, fusion-competent vesicles that are accessible to glycosphingolipids from the host cell plasmalemma,

J.Immunol. 156 [12], Seite 4764-4773. URL: PM:8648123

[16] Harth, G. und Horwitz, M. A. (1999): An inhibitor of exported *Mycobacterium tuberculosis* glutamine synthetase selectively blocks the growth of pathogenic mycobacteria in axenic culture and in human monocytes: extracellular proteins as potential novel drug targets, J.Exp.Med. 189 [9], Seite 1425-1436. URL: PM:10224282

[17] Ferrari, G.; Langen, H.; Naito, M. und Pieters, J. (1999): A coat protein on phagosomes involved in the intracellular survival of mycobacteria, Cell 97 [4], Seite 435-447. URL: PM:10338208

[18] Nathan, C. und Shiloh, M. U. (2000): Reactive oxygen and nitrogen intermediates in the relationship between mammalian hosts and microbial pathogens, Proc.Natl.Acad.Sci.U.S.A 97 [16], Seite 8841-8848. URL: PM:10922044

[19] Schaible, U. E.; Collins, H. L.; Priem, F. und Kaufmann, S. H. (2002): Correction of the iron overload defect in beta-2-microglobulin knockout mice by lactoferrin abolishes their increased susceptibility to tuberculosis, J.Exp.Med. 196 [11], Seite 1507-1513. URL: PM:12461085

[20] Kaufmann, S. H. (2001): How can immunology contribute to the control of tuberculosis?, Nat.Rev.Immunol. 1 [1], Seite 20-30. URL: PM:11905811

[21] Kaufmann, S. H. (2002): Protection against tuberculosis: cytokines, T cells, and macrophages, Ann.Rheum.Dis. 61 Suppl 2, Seite ii54-ii58. URL: PM:12379623

[22] Stenger, S.; Rosat, J. P.; Bloom, B. R.; Krensky, A. M. und Modlin, R. L. (1999): Granulysin: a lethal weapon of cytolytic T cells, Immunol.Today 20 [9], Seite 390-394. URL: PM:10462738

[23] Flynn, J. L. und Chan, J. (2001): Immunology of tuberculosis, Annu.Rev.Immunol. 19, Seite 93-129. URL: PM:11244032

[24] Brennan, P. J. und Nikaido, H. (1995): The envelope of mycobacteria, Annu.Rev.Biochem. 64, Seite 29-63. URL: PM:7574484

[25] Trias, J.; Jarlier, V. und Benz, R. (1992): Porins in the cell wall of mycobacteria, Science 258 [5087], Seite 1479-1481. URL: PM:1279810

[26] Heinz, C.; Roth, E. und Niederweis, M. (2003): Purification of porins from *Mycobacterium smegmatis*, Methods Mol.Biol. 228, Seite 139-150. URL: PM:12824550

[27] Niederweis, M. (2003): Mycobacterial porins--new channel proteins in unique outer membranes, Mol.Microbiol. 49 [5], Seite 1167-1177. URL: PM:12940978

[28] Trias, J. und Benz, R. (1994): Permeability of the cell wall of *Mycobacterium smegmatis*, Mol.Microbiol. 14 [2], Seite 283-290. URL: PM:7830572

[29] Navarre, W. W. und Schneewind, O. (1999): Surface proteins of gram-positive bacteria and mechanisms of their targeting to the cell wall envelope, Microbiol.Mol.Biol.Rev. 63 [1], Seite 174-229. URL: PM:10066836

[30] Miller, B. H. und Shinnick, T. M. (2000): Evaluation of *Mycobacterium tuberculosis* genes involved in resistance to killing by human macrophages, Infect.Immun. 68 [1], Seite 387-390. URL: PM:10603413

[31] Lustgarten, S. (1884): Ueber spezifische Bacillen in syphilitischen Krankheitsprodukten, Wiener medizinische Wochenschrift [47], Seite 1-1.

[32] Alvarez und Tavel (1885): Recherches sur le bacille de Lustgarten, Arch.Physiol.Normal Pathol., Seite 303-321.

[33] O'Toole, G.; Kaplan, H. B. und Kolter, R. (2000): Biofilm formation as microbial

development, Annu.Rev.Microbiol. 54, Seite 49-79. URL: PM:11018124

[34] Bardouniotis, E.; Ceri, H. und Olson, M. E. (2003): Biofilm formation and biocide susceptibility testing of *Mycobacterium fortuitum* and *Mycobacterium marinum*, Curr.Microbiol. 46 [1], Seite 28-32. URL: PM:12432460

[35] Teng, R. und Dick, T. (2003): Isoniazid resistance of exponentially growing *Mycobacterium smegmatis* biofilm culture, FEMS Microbiol.Lett. 227 [2], Seite 171-174. URL: PM:14592705

[36] Davies, D. (2003): Understanding biofilm resistance to antibacterial agents, Nat.Rev.Drug Discov. 2 [2], Seite 114-122. URL: PM:12563302

[37] Wallace, R. J., Jr.; Nash, D. R.; Tsukamura, M.; Blacklock, Z. M. und Silcox, V. A. (1988): Human disease due to *Mycobacterium smegmatis*, J.Infect.Dis. 158 [1], Seite 52-59. URL: PM:3392420

[38] Cain, B. D.; Norton, P. J.; Eubanks, W.; Nick, H. S. und Allen, C. M. (1993): Amplification of the *bacA* gene confers bacitracin resistance to *Escherichia coli*, J.Bacteriol. 175 [12], Seite 3784-3789. URL: PM:8389741

[39] Chalker, A. F.; Ingraham, K. A.; Lunsford, R. D.; Bryant, A. P.; Bryant, J.; Wallis, N. G.; Broskey, J. P.; Pearson, S. C. und Holmes, D. J. (2000): The *bacA* gene, which determines bacitracin susceptibility in *Streptococcus pneumoniae* and *Staphylococcus aureus*, is also required for virulence, Microbiology 146 (Pt 7), Seite 1547-1553. URL: PM:10878119

[40] Snapper, S. B.; Melton, R. E.; Mustafa, S.; Kieser, T. und Jacobs, W. R., Jr. (1990): Isolation and characterization of efficient plasmid transformation mutants of *Mycobacterium smegmatis*, Mol.Microbiol. 4 [11], Seite 1911-1919. URL: PM:2082148

[41] Schaible, U. E. und Kaufmann, S. H. (2002): Studying trafficking of intracellular pathogens in antigen-presenting cells, Methods in Microbiology 31, Seite 343-360.

[42] Klose, J. und Kobalz, U. (1995): Two-dimensional electrophoresis of proteins: an updated protocol and implications for a functional analysis of the genome, Electrophoresis 16 [6], Seite 1034-1059. URL: PM:7498127

[43] Jungblut, P. R. und Seifert, R. (1990): Analysis by high-resolution two-dimensional electrophoresis of differentiation-dependent alterations in cytosolic protein pattern of HL-60 leukemic cells, J.Biochem.Biophys.Methods 21 [1], Seite 47-58. URL: PM:1698848

[44] Doherty, N. S.; Littman, B. H.; Reilly, K.; Swindell, A. C.; Buss, J. M. und Anderson, N. L. (1998): Analysis of changes in acute-phase plasma proteins in an acute inflammatory response and in rheumatoid arthritis using two-dimensional gel electrophoresis, Electrophoresis 19 [2], Seite 355-363. URL: PM:9548303

[45] Aksu, S.; Scheler, C.; Focks, N.; Leenders, F.; Theuring, F.; Salnikow, J. und Jungblut, P. R. (2002): An iterative calibration method with prediction of post-translational modifications for the construction of a two-dimensional electrophoresis database of mouse mammary gland proteins, Proteomics. 2 [10], Seite 1452-1463. URL: PM:12422362

[46] Henzel, W. J.; Billeci, T. M.; Stults, J. T.; Wong, S. C.; Grimley, C. und Watanabe, C. (1993): Identifying proteins from two-dimensional gels by molecular mass searching of peptide fragments in protein sequence databases, Proc.Natl.Acad.Sci.U.S.A 90 [11], Seite 5011-5015. URL: PM:8506346

[47] James, P.; Quadroni, M.; Carafoli, E. und Gonnet, G. (1993): Protein identification by mass profile fingerprinting, Biochem.Biophys.Res.Commun. 195 [1],

Seite 58-64. URL: PM:8363627

[48] Mann, M.; Hojrup, P. und Roepstorff, P. (1993): Use of mass spectrometric molecular weight information to identify proteins in sequence databases, Biol.Mass Spectrom. 22 [6], Seite 338-345. URL: PM:8329463

[49] Mann, M. und Wilm, M. (1994): Error-tolerant identification of peptides in sequence databases by peptide sequence tags, Anal.Chem. 66 [24], Seite 4390-4399. URL: PM:7847635

[50] Peng, J. und Gygi, S. P. (2001): Proteomics: the move to mixtures, J.Mass Spectrom. 36 [10], Seite 1083-1091. URL: PM:11747101

[51] Jungblut, P. R.; Schaible, U. E.; Mollenkopf, H. J.; Zimny-Arndt, U.; Raupach, B.; Mattow, J.; Halada, P.; Lamer, S.; Hagens, K. und Kaufmann, S. H. (1999): Comparative proteome analysis of *Mycobacterium tuberculosis* and *Mycobacterium bovis* BCG strains: towards functional genomics of microbial pathogens, Mol.Microbiol. 33 [6], Seite 1103-1117. URL: PM:10510226

[52] Mollenkopf, H. J.; Mattow, J.; Schaible, U. E.; Grode, L.; Kaufmann, S. H. und Jungblut, P. R. (2002): Mycobacterial proteomes, Methods Enzymol. 358, Seite 242-256. URL: PM:12474391

[53] Mattow, J.; Jungblut, P. R.; Schaible, U. E.; Mollenkopf, H. J.; Lamer, S.; Zimny-Arndt, U.; Hagens, K.; Muller, E. C. und Kaufmann, S. H. (2001): Identification of proteins from *Mycobacterium tuberculosis* missing in attenuated *Mycobacterium bovis* BCG strains, Electrophoresis 22 [14], Seite 2936-2946. URL: PM:11565788

[54] Muller, E. C.; Schumann, M.; Rickers, A.; Bommert, K.; Wittmann-Liebold, B. und Otto, A. (1999): Study of Burkitt lymphoma cell line proteins by high resolution two-dimensional gel electrophoresis and nanoelectrospray mass spectrometry, Electrophoresis 20 [2], Seite 320-330. URL: PM:10197439

[55] Wilm, M.; Neubauer, G. und Mann, M. (1996): Parent ion scans of unseparated peptide mixtures, Anal.Chem. 68 [3], Seite 527-533. URL: PM:8712361

[56] Perkins, D. N.; Pappin, D. J.; Creasy, D. M. und Cottrell, J. S. (1999): Probability-based protein identification by searching sequence databases using mass spectrometry data, Electrophoresis 20 [18], Seite 3551-3567. URL: PM:10612281

[57] Rolph, M. S.; Raupach, B.; Kobernick, H. H.; Collins, H. L.; Perarnau, B.; Lemonnier, F. A. und Kaufmann, S. H. (2001): MHC class Ia-restricted T cells partially account for beta2-microglobulin-dependent resistance to *Mycobacterium tuberculosis*, Eur.J.Immunol. 31 [6], Seite 1944-1949. URL: PM:11433392

[58] Pavelka, M. S., Jr. und Jacobs, W. R., Jr. (1999): Comparison of the construction of unmarked deletion mutations in *Mycobacterium smegmatis*, *Mycobacterium bovis* bacillus Calmette-Guerin, and *Mycobacterium tuberculosis* H37Rv by allelic exchange, J.Bacteriol. 181 [16], Seite 4780-4789. URL: PM:10438745

[59] Collins, L. und Franzblau, S. G. (1997): Microplate alamar blue assay versus BACTEC 460 system for high-throughput screening of compounds against *Mycobacterium tuberculosis* and *Mycobacterium avium*, Antimicrob.Agents Chemother. 41 [5], Seite 1004-1009. URL: PM:9145860

[60] Recht, J. und Kolter, R. (2001): Glycopeptidolipid acetylation affects sliding motility and biofilm formation in *Mycobacterium smegmatis*, J.Bacteriol. 183 [19], Seite 5718-5724. URL: PM:11544235

[61] Soto, C. Y.; Andreu, N.; Gibert, I. und Luquin, M. (2002): Simple and rapid differentiation of *Mycobacterium tuberculosis* H37Ra from *M. tuberculosis* clinical isolates through two cytochemical tests using neutral red and nile blue stains,

J.Clin.Microbiol. 40 [8], Seite 3021-3024. URL: PM:12149369

[62] Ryll, R.; Kumazawa, Y. und Yano, I. (2001): Immunological properties of trehalose dimycolate (cord factor) and other mycolic acid-containing glycolipids--a review, Microbiol.Immunol. 45 [12], Seite 801-811. URL: PM:11838897

[63] Byrd, T. F.; Green, G. M.; Fowlston, S. E. und Lyons, C. R. (1998): Differential growth characteristics and streptomycin susceptibility of virulent and avirulent *Mycobacterium tuberculosis* strains in a novel fibroblast-mycobacterium microcolony assay, Infect.Immun. 66 [11], Seite 5132-5139. URL: PM:9784514

[64] Quinn, F. D.; Birkness K.A. und King J.K. (2002): Alpha-Crystallin as a Potential Marker of *Mycobacterium tuberculosis* Latency, ASM News.

[65] Sherman, D. R.; Voskuil, M.; Schnappinger, D.; Liao, R.; Harrell, M. I. und Schoolnik, G. K. (2001): Regulation of the *Mycobacterium tuberculosis* hypoxic response gene encoding alpha -crystallin, Proc.Natl.Acad.Sci.U.S.A 98 [13], Seite 7534-7539. URL: PM:11416222

[66] Kremer, L.; Dover, L. G.; Morbidoni, H. R.; Vilcheze, C.; Maughan, W. N.; Baulard, A.; Tu, S. C.; Honore, N.; Deretic, V.; Sacchettini, J. C.; Locht, C.; Jacobs, W. R., Jr. und Besra, G. S. (2003): Inhibition of InhA activity, but not KasA activity, induces formation of a KasA-containing complex in mycobacteria, J.Biol.Chem. 278 [23], Seite 20547-20554. URL: PM:12654922

[67] Slayden, R. A. und Barry, C. E., III (2002): The role of KasA and KasB in the biosynthesis of meromycolic acids and isoniazid resistance in *Mycobacterium tuberculosis*, Tuberculosis.(Edinb.) 82 [4-5], Seite 149-160. URL: PM:12464486

[68] Mombaerts, P.; Iacomini, J.; Johnson, R. S.; Herrup, K.; Tonegawa, S. und Papaioannou, V. E. (1992): RAG-1-deficient mice have no mature B and T lymphocytes, Cell 68 [5], Seite 869-877. URL: PM:1547488

[69] Lee, R. E.; Brennan, P. J. und Besra, G. S. (1996): *Mycobacterium tuberculosis* cell envelope, Curr.Top.Microbiol.Immunol. 215, Seite 1-27. URL: PM:8791707

[70] Mdluli, K.; Slayden, R. A.; Zhu, Y.; Ramaswamy, S.; Pan, X.; Mead, D.; Crane, D. D.; Musser, J. M. und Barry, C. E., III (1998): Inhibition of a *Mycobacterium tuberculosis* beta-ketoacyl ACP synthase by isoniazid, Science 280 [5369], Seite 1607-1610. URL: PM:9616124

[71] Lee, A. S.; Lim, I. H.; Tang, L. L.; Telenti, A. und Wong, S. Y. (1999): Contribution of *kasA* analysis to detection of isoniazid-resistant *Mycobacterium tuberculosis* in Singapore, Antimicrob.Agents Chemother. 43 [8], Seite 2087-2089. URL: PM:10428945

[72] Piatek, A. S.; Telenti, A.; Murray, M. R.; El Hajj, H.; Jacobs, W. R., Jr.; Kramer, F. R. und Alland, D. (2000): Genotypic analysis of *Mycobacterium tuberculosis* in two distinct populations using molecular beacons: implications for rapid susceptibility testing, Antimicrob.Agents Chemother. 44 [1], Seite 103-110. URL: PM:10602730

[73] Bloch, K. (1977): Control mechanisms for fatty acid synthesis in *Mycobacterium smegmatis*, Adv.Enzymol.Relat Areas Mol.Biol. 45, Seite 1-84. URL: PM:21523

[74] Kremer, L.; Douglas, J. D.; Baulard, A. R.; Morehouse, C.; Guy, M. R.; Alland, D.; Dover, L. G.; Lakey, J. H.; Jacobs, W. R., Jr.; Brennan, P. J.; Minnikin, D. E. und Besra, G. S. (2000): Thiolactomycin and related analogues as novel anti-mycobacterial agents targeting KasA and KasB condensing enzymes in *Mycobacterium tuberculosis*, J.Biol.Chem. 275 [22], Seite 16857-16864. URL: PM:10747933

[75] Kremer, L.; Dover, L. G.; Carrere, S.; Nampoothiri, K. M.; Lesjean, S.; Brown, A.

K.; Brennan, P. J.; Minnikin, D. E.; Locht, C. und Besra, G. S. (2002): Mycolic acid biosynthesis and enzymic characterization of the beta-ketoacyl-ACP synthase A-condensing enzyme from *Mycobacterium tuberculosis*, Biochem.J. 364 [Pt 2], Seite 423-430. URL: PM:12023885

[76] Russell, D. G. (2003): Phagosomes, fatty acids and tuberculosis, Nat.Cell Biol. 5 [9], Seite 776-778. URL: PM:12951608

[77] Fratti, R. A.; Vergne, I.; Chua, J.; Skidmore, J. und Deretic, V. (2000): Regulators of membrane trafficking and *Mycobacterium tuberculosis* phagosome maturation block, Electrophoresis 21 [16], Seite 3378-3385. URL: PM:11079558

[78] Fischer, K.; Chatterjee, D.; Torrelles, J.; Brennan, P. J.; Kaufmann, S. H. und Schaible, U. E. (2001): Mycobacterial lysocardiolipin is exported from phagosomes upon cleavage of cardiolipin by a macrophage-derived lysosomal phospholipase A2, J.Immunol. 167 [4], Seite 2187-2192. URL: PM:11490004

[79] Lawrence, J. R.; Korber, D. R.; Hoyle, B. D.; Costerton, J. W. und Caldwell, D. E. (1991): Optical sectioning of microbial biofilms, J.Bacteriol. 173 [20], Seite 6558-6567. URL: PM:1917879

[80] Lawrence, J. R. und Neu, T. R. (1999): Confocal laser scanning microscopy for analysis of microbial biofilms, Methods Enzymol. 310, Seite 131-144. URL: PM:10547787

[81] Davies, D. G.; Parsek, M. R.; Pearson, J. P.; Iglewski, B. H.; Costerton, J. W. und Greenberg, E. P. (1998): The involvement of cell-to-cell signals in the development of a bacterial biofilm, Science 280 [5361], Seite 295-298. URL: PM:9535661

[82] Martinelli, D.; Bachofen, R. und Brandl, H. (2002): Effect of medium composition, flow rate, and signaling compounds on the formation of soluble extracellular materials by biofilms of *Chromobacterium violaceum*, Appl.Microbiol.Biotechnol. 59 [2-3], Seite 278-283. URL: PM:12111158

[83] Huber, B.; Riedel, K.; Kothe, M.; Givskov, M.; Molin, S. und Eberl, L. (2002): Genetic analysis of functions involved in the late stages of biofilm development in *Burkholderia cepacia* H111, Mol.Microbiol. 46 [2], Seite 411-426. URL: PM:12406218

[84] Brown, M. R.; Allison, D. G. und Gilbert, P. (1988): Resistance of bacterial biofilms to antibiotics: a growth-rate related effect?, J.Antimicrob.Chemother. 22 [6], Seite 777-780. URL: PM:3072331

[85] Stewart, P. S. (2002): Mechanisms of antibiotic resistance in bacterial biofilms, Int.J.Med.Microbiol. 292 [2], Seite 107-113. URL: PM:12195733

[86] Recht, J.; Martinez, A.; Torello, S. und Kolter, R. (2000): Genetic analysis of sliding motility in *Mycobacterium smegmatis*, J.Bacteriol. 182 [15], Seite 4348-4351. URL: PM:10894747

[87] Brinton, L. A.; Li, J. Y.; Rong, S. D.; Huang, S.; Xiao, B. S.; Shi, B. G.; Zhu, Z. J.; Schiffman, M. H. und Dawsey, S. (1991): Risk factors for penile cancer: results from a case-control study in China, Int.J.Cancer 47 [4], Seite 504-509. URL: PM:1995481

[88] Chou, P. (1991): Review on risk factors of cervical cancer, Zhonghua Yi.Xue.Za Zhi.(Taipei) 48 [2], Seite 81-88. URL: PM:1654190

[89] Hingley-Wilson, S. M.; Sambandamurthy, V. K. und Jacobs, W. R., Jr. (2003): Survival perspectives from the world's most successful pathogen, *Mycobacterium tuberculosis*, Nat.Immunol. 4 [10], Seite 949-955. URL: PM:14515128

[90] Perez, E.; Samper, S.; Bordas, Y.; Guilhot, C.; Gicquel, B. und Martin, C. (2001): An essential role for *phoP* in *Mycobacterium tuberculosis* virulence, Mol.Microbiol. 41

[1], Seite 179-187. URL: PM:11454210

[91] Braunstein, M.; Espinosa, B. J.; Chan, J.; Belisle, J. T. und Jacobs, R. (2003): SecA2 functions in the secretion of superoxide dismutase A and in the virulence of *Mycobacterium tuberculosis*, Mol.Microbiol. 48 [2], Seite 453-464. URL: PM:12675804

[92] Tullius, M. V.; Harth, G. und Horwitz, M. A. (2003): Glutamine synthetase GlnA1 is essential for growth of *Mycobacterium tuberculosis* in human THP-1 macrophages and guinea pigs, Infect.Immun. 71 [7], Seite 3927-3936. URL: PM:12819079

[93] Sambandamurthy, V. K.; Wang, X.; Chen, B.; Russell, R. G.; Derrick, S.; Collins, F. M.; Morris, S. L. und Jacobs, W. R., Jr. (2002): A pantothenate auxotroph of *Mycobacterium tuberculosis* is highly attenuated and protects mice against tuberculosis, Nat.Med. 8 [10], Seite 1171-1174. URL: PM:12219086

[94] Mendonca-Lima, L.; Picardeau, M.; Raynaud, C.; Rauzier, J.; de la Salmoniere, Y. O.; Barker, L.; Bigi, F.; Cataldi, A.; Gicquel, B. und Reyrat, J. M. (2001): Erp, an extracellular protein family specific to mycobacteria, Microbiology 147 [Pt 8], Seite 2315-2320. URL: PM:11496008

[95] Berthet, F. X.; Lagranderie, M.; Gounon, P.; Laurent-Winter, C.; Ensergueix, D.; Chavarot, P.; Thouron, F.; Maranghi, E.; Pelicic, V.; Portnoi, D.; Marchal, G. und Gicquel, B. (1998): Attenuation of virulence by disruption of the *Mycobacterium tuberculosis erp* gene, Science 282 [5389], Seite 759-762. URL: PM:9784137

[96] Yuan, Y.; Crane, D. D.; Simpson, R. M.; Zhu, Y. Q.; Hickey, M. J.; Sherman, D. R. und Barry, C. E., III (1998): The 16-kDa alpha-crystallin (Acr) protein of Mycobacterium tuberculosis is required for growth in macrophages, Proc.Natl.Acad.Sci.U.S.A 95 [16], Seite 9578-9583. URL: PM:9689123

[97] MacMicking, J.; Xie, Q. W. und Nathan, C. (1997): Nitric oxide and macrophage function, Annu.Rev.Immunol. 15, Seite 323-350. URL: PM:9143691

[98] Miller, R. A. und Britigan, B. E. (1997): Role of oxidants in microbial pathophysiology, Clin.Microbiol.Rev. 10 [1], Seite 1-18. URL: PM:8993856

[99] Weiss, S. J. (1986): Oxygen, ischemia and inflammation, Acta Physiol Scand.Suppl 548, Seite 9-37. URL: PM:3019082

[100] Moncada, S. und Higgs, A. (1993): The L-arginine-nitric oxide pathway, N.Engl.J.Med. 329 [27], Seite 2002-2012. URL: PM:7504210

[101] Collins, H. L. und Kaufmann, S. H. (2001): Prospects for better tuberculosis vaccines, Lancet Infect.Dis. 1 [1], Seite 21-28. URL: PM:11871406

[102] Murray, P. J.; Aldovini, A. und Young, R. A. (1996): Manipulation and potentiation of antimycobacterial immunity using recombinant bacille Calmette-Guerin strains that secrete cytokines, Proc.Natl.Acad.Sci.U.S.A 93 [2], Seite 934-939. URL: PM:8570663

[103] Hess, J.; Miko, D.; Catic, A.; Lehmensiek, V.; Russell, D. G. und Kaufmann, S. H. (1998): Mycobacterium bovis Bacille Calmette-Guerin strains secreting listeriolysin of Listeria monocytogenes, Proc.Natl.Acad.Sci.U.S.A 95 [9], Seite 5299-5304. URL: PM:9560270

[104] Horwitz, M. A.; Harth, G.; Dillon, B. J. und Maslesa-Galic', S. (2000): Recombinant bacillus calmette-guerin (BCG) vaccines expressing the Mycobacterium tuberculosis 30-kDa major secretory protein induce greater protective immunity against tuberculosis than conventional BCG vaccines in a highly susceptible animal model, Proc.Natl.Acad.Sci.U.S.A 97 [25], Seite 13853-13858. URL: PM:11095745

Danksagung

Mein Dank gilt Herrn Prof. Dr. Stefan Kaufmann für die Vergabe des Themas, die hervorragenden Arbeitsbedingungen, seine Bereitschaft zur wissenschaftlichen Diskussion und die mir gewährte Forschungsfreiheit während der Promotionsarbeit.

Frau Dr. Sabine Daugelat und Herrn Dr. Peter Seiler danke ich besonders für die exzellente Betreuung meiner Doktorarbeit, für zahlreiche fruchtbare wissenschaftliche Diskussionen und für viele hilfreiche Hinweise bei der Laborarbeit.

Herrn Dr. Jens Mattow sowie Eva Müller und Frank Siejak danke ich für die hervorragende Hilfe bei der Proteom-Analyse und Herrn Dr. Helmy Rachman für die Kooperation bei der Transkriptom-Analyse. Herrn Dr. Volker Brinkmann sei für die praktische Hilfe bei der Elektronen Mikroskopie gedankt.

Herrn Prof. Dr. Erwin Schneider gilt mein besonderer Dank für die Vertretung meiner Dissertation am Institut für Biologie der Humboldt-Universität zu Berlin und die Begutachtung der Arbeit. Ebenso danke ich Herrn PD Dr. Ulrich Schaible für seine Bereitschaft, die Arbeit zu begutachten. Bei Herrn Prof. Dr. Richard Lucius möchte ich mich für die Leitung des Promotionsausschusses bedanken. Schließlich bedanke ich mich bei Herrn Prof. Dr. Rainer Borriss dafür, daß er als Mitglied des Promotionsausschusses zur Verfügung stand.

Allen jetzigen und ehemaligen Mitgliedern des Max-Planck-Instituts für Infektionsbiologie, Abteilung Immunologie, gilt ebenfalls mein Dank für viele wichtige Anregungen und die angenehme Atmosphäre – auch außerhalb des Labors.

Martin Beisiegel und Tracey Walker danke ich „for carefully reading the manuscript".

Meiner Freundin Nuran Özdugan danke ich für ihre liebevolle und geduldige Unterstützung. Schließlich möchte ich meinen Eltern für ihre ständige Zuneigung danken sowie dafür, daß Sie meine Ausbildung ermöglicht haben.

Selbständigkeitserklärung

Hiermit erkläre ich, daß ich die vorliegende Arbeit selbständig und nur mit den

angegebenen Hilfsmitteln erstellt habe.

Berlin, den

Appendix

Tables of strains, plasmids, and primers:

Table 4: Strains and plasmids used in this study

Strain or Plasmid	Descriptiona	Source or Reference
Strains		
E. coli DH5α	standard cloning strain.	Invitrogen
E. coli HB101	cloning strain for resolvase instable plasmids	
M. smegmatis mc^{2}155	wildtype, ept-1	[40]
M. smegmatis mc^{2}155 pYUB657-Δ*upk*	single crossover strain, Hyg^R, Suc^S	This study
M. smegmatis mc^{2}155 Δ*upk*	deletion mutant of the *upk* gene, Hyg^S, Suc^R	This study
M. smegmatis mc^{2}155 Δ*upk* + pMV262-*rv2136c*	reconstitution of the *upk* deletion mutant, Hyg^S, Suc^R, Kan^R	This study
M. tuberculosis H37Rv	wildtype, standard laboratory strain	
M. tuberculosis H37Rv Δ*upk*	deletion mutant of *upk* gene, Hyg^R	This study
M. tuberculosis H37Rv Δ*upk* + pMV262-*rv2136c*	reconstitution of the *upk* deletion mutant, Hyg^R, Kan^R	This study
M. bovis BCG	standard vaccine strain	
M. bovis BCG Δ*upk*	deletion mutant of *upk* gene, Hyg^R	This study
Plasmids		
pPCR-Script Amp	Cloning vector, Amp^R	Stratagene

pYUB657	suicide plasmid, bearing *groEL2* (Hsp60) promoter and *sacB,* Hyg[R], Amp[R]	[58]
pYUB657-Δ*upk*	suicide plasmid carrying *upk*-deletion template	This study
pMV262-*rv2136c*	pMV262-Kan containing the *M. tuberculosis rv2136c* gene	This study
pMV262-Kan	*E. coli*-mycobacteria shuttle vector, *groEL2* (hsp60) promoter, Kan[R], ColE1, OriM	W.R. Jacobs Jr.
pJSC284	starting plasmid for construction of a knockout template, Hyg[R]	W.R. Jacobs Jr.
pKO-*upk*	pJSC284, containing flanking regions, Hyg[R]	This study

[a] Amp[R], ampicillin resistance; Kan[R], kanamycin resistance; Hyg[R], hygromycin resistance

Table 5: List of primers

Amplified DNA fragment	Primer[a]	Template DNA
M. smegmatis		
flanking region 1	P1: 5'-GATATCcttttcgagcacgaccga-3' P2: 5'- AAGCTTcttggcaccggggtactg -3'	*M. smegmatis* mc[2]155
flanking region 2	P3: 5'-AAGCTTcatcgcaggaacgtcagt-3' P4: 5'-GATATCaggtcgacacggaagtagcca-3'	*M. smegmatis* mc[2]155
M. tuberculosis		
flanking region 1	P1: 5'-GGATCCcgtcatcgaagaccatga-3' P2: 5'-GGATCCgacttgccaccaagacat-3'	*M. tuberculosis* H37Rv
flanking region 2	P3: 5'-ACCGGTctcgtgctgctggctacc-3' P4: 5'-ACCGGTcacctccaaaataccgcg-3'	*M. tuberculosis* H37Rv
rv2136c	rv2136c-START: 5'-GGATCCatgctgtggcacgcaatg-3' rv2136c-END: 5'-GGATCCccagtcgtcctcttcgtc-3'	*M. tuberculosis* H37Rv
RealTime		
rv2136c	*rv2136c*-fw: 5'-atcctgagcgcttggttg-3' *rv2136c*-rev: 5'-gggtttgggcaataccaac-3'	*M. tuberculosis* H37Rv wildtype, Δ*upk* mutant, reconstitution
rv3627c	*rv3627c*-fw: 5'-ccacagtcaaggcgggagtggt-3' *rv3527c*-rev: 5'-acacgacaggtccctgggggtt-3'	*M. tuberculosis* H37Rv wildtype, Δ*upk* mutant, reconstitution
rv2946c	*rv2946c*-fw: 5'-aactcgagtctgccggtg-3' rv2946c-rev: 5'-tagcaccgaggcatccac-3'	*M. tuberculosis* H37Rv wildtype, Δ*upk* mutant, reconstitution

[a] capital letters indicate the added restriction sites

5 Publications

Terness, P., Bauer, T. M., Röse, L., Dufter, C., Watzlik, A., Simon, H., and Opelz, G.

(2002)

Inhibition of allogeneic T cell proliferation by indoleamine 2,3-dioxygenase-

expressing dendritic cells: mediation of suppression by tryptophan metabolites.

J.Exp.Med. **196**, 447-457

Röse, L., Kaufmann, SHE., Daugelat, S

(2003)

Involvement of *Mycobacterium smegmatis* undecaprenyl phosphokinase in biofilm

and smegma formation

manuscript status: submitted

Presentation of the poster:

Deletion of *rv2136c* in *Mycobacterium tuberculosis*.

on the Keystone symposium "Tuberculosis: Integrating Host and Pathogen Biology"

was supported by the "Keystone Symposia Scholarship" (2003).